1990

Receptor Specific Radiotracers For Imaging Dopamine And Estrogen Receptors

Lou Anne Strickland

RECEPTOR SPECIFIC RADIOTRACERS FOR IMAGING DOPAMINE AND ESTROGEN RECEPTORS

by

Lou Anne Strickland

Department of Chemistry

Submitted in partial fulfilment
of the requirements for the degree of
Doctor of Philosophy

Faculty of Graduate Studies
The University of Western Ontario
London, Ontario
July, 1990

ISBN 0-315-59121-8

ABSTRACT

The preparation and evaluation of potential dopamine receptor imaging agents and an estrogen receptor imaging agent is the topic of this thesis. The dopamine (D-2) receptor imaging agent could be employed as a diagnosis tool for several neurological diseases and the estrogen receptor agent could be used to detect estrogen receptor positive tumors.

Three different monoiodinated derivatives of the haloperidol were synthesised as potential D-2 agents. The results of an *in vitro* competitive binding assay showed one derivative to have much higher affinity than the other two for D-2 receptors. This derivative was labelled with 131-iodine and biodistribution studies in rats were done to determine if selective uptake by D-2 receptors could be seen. However, over forty-eight hours no selectivity was observed.

A radioiodinating procedure based on the iododediazotization reaction was developed for preparing E and Z-[^{131}I]-iodotamoxifen (estrogen receptor agent) from the isolated diazonium salt. Presented are the results of a series of experiments in which variour catalysts, diazonium salt counter ions, solvents and reaction conditions were tried. From these results a procedure was developed which allowed the preparation of 0.1 to 2.0 mCi (3.7 to 74 MBq) of [^{131}I]-iodotamoxifen in a 40 to 60 per cent radiochemical yield. The relative binding affinities of both the E and Z

iodinated derivative and E and Z aminotamoxifen for estrogen receptors were determined *in vitro*. All four compounds showed some ability to bind, with Z-iodotamoxifen having the highest affinity and E-iodotamoxifen the lowest. The biological distributions of E and Z [^{131}I]-iodotamoxifen were determined in tumor-bearing mice. Selective uptake by both isomers was observed in the uterus and the tumors. *In vivo*, receptors binding was shown by a washout experiment with estradiol in mice. Also described are the results of a preclinical trial to determine E and Z-[^{131}I]-iodotamoxifen's potential as tumor imaging agents. Unfortunately no uptake in known estrogen receptor positive tumors was observed.

ACKNOWLEDGEMENTS

I find myself indebted to many people for their help with this work. To Dr. Y. Zea Ponce, I am grateful for the aminotamoxifen sample. To Dr. P. Seeman, I thankful for measuring the D-2 receptor binding affinities. To Mr. K. Barr, I am grateful for the estrogen receptor cytosol and for his guidance in performing the assay. To Dr. M. Hyland, I am thankful for the XPS analysis. To Dr. C. Hansch, I am grateful for the Log P's values. To Dr. R. Flanagan, I am grateful for his helpful advise and for the joint financial support his employer, Merk Frosst Canada and NSERC. To the staff and faculty of the Chemistry Department I am thankful for their assistance in aspect of my studies.

I will always be indebted to the Radiopharmaceutical Development Group for providing me with this opportunity and for their support. To Ms. P. Zabel, Dr. M. Chamberlain, Dr. A. Dreidger, Dr. J. Powe, Mr G. Morrissey and Mr. A. Wearing I am very grateful for their patient instruction on the biological aspects of this work.

To my fellow chemists Paul, Yolanda, Vince, Vinod, Mahejabeen and Alok; I am grateful for your patience, expertise and especially their friendship. To my family and Harold, I will always be grateful for their support and encouragement.

To Duncan Hunter, supervisor as well as friend, above all, I am indebted for his quidance, encouragement and enthusiasm.

TABLE OF CONTENTS

LIST OF FIGURES

LIST OF SCHEMES

LIST OF TABLES

APPENDIX

Chapter 1: Introduction

Imaging small quantities of radioactivity, *in vivo*, provides information which is used by clinicians for diagnosis. This noninvasive technique has been proven to be very powerful and is now the major focus of Nuclear Medicine. Key to the success of radionuclide imaging is the radiopharmaceutical. The research described in this thesis is directed towards the development of two different receptor specific radiopharmaceuticals; one for dopamine receptors and one for estrogen receptors. The clinical application of these types of agents will be described in the following sections. This chapter is a general introduction to topics common to both projects. More detailed Introductions are given at the beginning of each of the two sections (Chapter 2 and 6).

1.1) Radiopharmaceuticals

A radiopharmaceutical consists of two components; the carrier and the radionuclide. In a very few cases the radionuclide does not have a carrier. The function of the carrier is to distribute the radionuclide throughout the body so a particular organ or process may be observed. The carrier can be a pharmaceutical, a chelate or a naturally occurring substance. Therefore the carrier is chosen for its *in vivo* properties. To say radiopharmaceutical implies a biological effect occurs. However, this is misleading.

Radiopharmaceuticals for imaging are not intended to have a biologically response and they do not at the low concentration they are administered. It is important, in fact, that they do not modify or interfere with the biological system being observed. One type of radiopharmaceutical has a known pharmaceutical as the carrier. The mechanism by which the pharmaceutical acts, such as binding to a receptor or an enzyme, can also be used to concentrate the radiopharmaceutical.

Another type of radiopharmaceutical distributes simply by its lipophilicity. For example, damage in cell membranes, which leads to a breakdown in the blood-brain barrier, can be imaged with sodium [^{99m}Tc]-pertechnetate by observing it crossing into the brain.[1] The intact blood-brain barrier does not allow perfusion of pertechnetate or any other inorganic anion to enter the brain due to their low lipophilicity.

A third category of radiopharmaceuticals is labelled, naturally occurring molecules or proteins. [^{99m}Tc]-Technetium labelled red blood cells have been used to trace red blood cells.[2] They are used to measure total red cell volume, identify gastrointestinal bleeding as well as image the blood pool in the heart. This is possible since the labelled cell acts identically to the nonlabelled cells.

1.1.1) Receptor Specific Radiopharmaceuticals

We have attempted to use the high selectivity some

corpour ·; have for biological receptors as a mechanism for localizing the radiopharmaceutical. Receptor specific radiopharmaceuticals are usually developed to measure the concentration and distribution of the receptor. Changes in the concentration of many receptors have been related to disease conditions.[3] Also, receptor bound radiopharmaceuticals can be used to concentrate the pharmaceutical in tissue which has a high receptor concentration for the purpose of visualizing the tissue.[4]

1.1.2) Receptors

Presented in this section are some of the basic principles of receptors. The concept of a receptor was developed to explain the way in which hormones, neurotransmitters and drugs can quickly elicit a biological effect at low concentrations.[5] The interaction between these compounds (ligands) and the receptor is described as being analogous to a lock and key. The lock is the receptor which is usually a large protein and the key is the ligand which fits in to it. In most cases, the ligand binds noncovalently and reversibly to the receptor by a combination of van der Waals forces, hydrogen bonding and hydrophobic interactions.

The efficiency with which the molecule can bind to receptor is called its affinity. A molecule which binds to a receptor and causes an observable response is an agonist.[6] The higher the affinity the agonist has for the receptor, the lower the concentration required to achieve a response. Therefore a low affinity agonist requires a higher

concentration to elicit the same response.

An antagonist is a molecule that binds to the receptor but does not elicit a response.[6] If it is a competitive antagonist, it binds directly to the receptor and blocks the agonist from binding. Noncompetitive antagonists block the agonist activity by binding to another site which, by some mechanism, distorts the receptor therefore lowering its affinity for agonist.

The binding of a molecule with a protein is not necessarily a receptor mediated event. An operational definition using properties which are determined *in vitro* in assays similar to those described in Appendix I, has been given and the criteria are expanded on below.[7]

i) The ligand must bind saturably to the receptor. A given amount of tissue has a finite number of receptors therefore once they are all bound, no more ligand can bind. Receptors are generally present in homogenized tissue at 10^{-7} to 10^{-10} M concentrations

ii) The ligand must have a high affinity and specificity for the receptor. That is, the ligand binds much more strongly to the receptor than to other proteins with which it might interact. Receptors often bind ligands stereospecifically. One stereoisomer of a d,l pair binds with much higher affinity than the other. Receptor affinity as described above is very closely related to receptor selectivity.

iii) The final criterion is that the receptor ligand

interaction is related to the physiological response. This is often shown by demonstrating a correlation between the affinity of different agonists for the receptor and the size of the *in vivo* biological effect.

1.2) Imaging and Radionuclides

Deciding which radionuclide to use as the label is partially governed by the type of imaging to be done. Therefore, prior to discussing the properties of the radionuclides commonly used, a brief discussion of the imaging techniques available is presented.

There are two types of imaging systems used for receptor imaging. The most commonly used techniques are based on the detection of gamma emitting nuclides using a gamma camera with or without tomography. For determining receptor concentration with a gamma emitting radiopharmaceutical, single photon emission computed tomography (SPECT) is employed. The second type of imaging is done by detecting annihilation photons from positron emitting isotopes. This imaging technique is known as positron emission tomography (PET). The facilities available to us are for SPECT imaging so my discussion will focus on this technique.

1.2.1) Gamma Cameras

The gamma camera was developed by Anger in 1958[8]. The camera's purpose is to detect gamma rays being emitted from in the body and determine the location from where the

ray was emitted. A schematic diagram of the detector is given in Figure 1.1.[9]

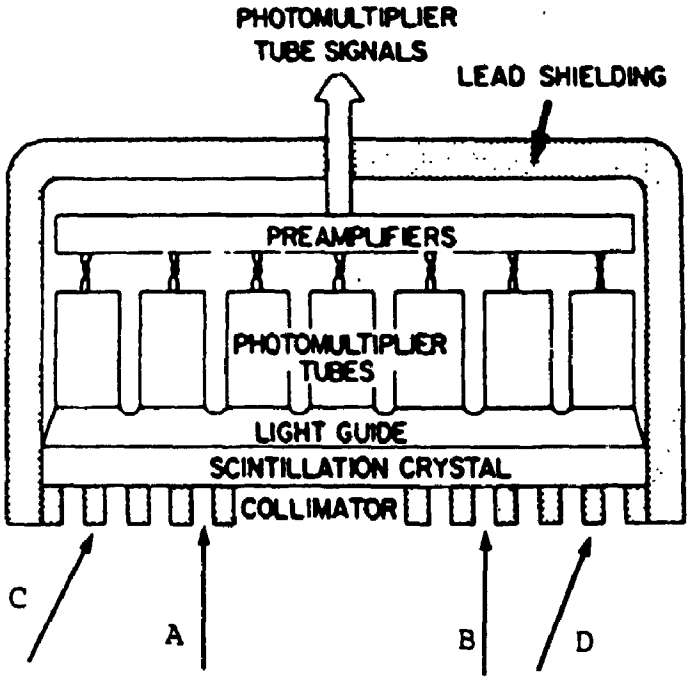

Figure 1.1: Cross-Section of a Gamma Camera Detector

Gamma rays are emitted isotropically. Therefore, it is impossible to determine the point of origin of the ray from the position it interacts with the camera. To solve this problem, collimators are used. A collimator is a lead plate with many holes. The parallel hole collimator is the most commonly used. As illustrated in Figure 1.1 only rays (A,B) which are travelling at an angle which will permit them to pass through the holes can be detected. The others (C,D) are absorbed. Other collimators, such as pin hole and converging collimators have holes on an angle allowing better imaging of small areas.

The gamma rays are detected by a scintillation detector. Gamma rays, when interacting with matter cause the formation of excited or ionized atoms or molecules. When these ionized or excited products recombine or deexcite they give off energy. This energy is generally released as molecular vibrations. Some materials release a small portion of this energy as visible light. These materials are scintillators.

The most commonly used scintillator for a gamma camera detector is thallium activated solid sodium iodide. Sodium iodide is only a scintillator when in its crystalline form. The pure sodium iodide crystal, however, only scintillates at liquid nitrogen temperatures. If the crystal is formed containing an impurity, in this case thallium, the crystal lattice is disturbed which results in a scintillator. Other commonly used crystal scintillators are silver-activated cadmium sulphide and zinc sulphide.

Very little light is emitted from the scintillator. To enhance its detection, photomultiplier tubes are used. They produce an electric current when stimulated with light at very low levels. The signals produced by the photomultiplier tubes are amplified and position logic circuits determine the X and Y positions and a pulse-height analyser determines the Z position.

1.2.2) Tomography

Initially, imaging was done by simply obtaining a two dimensional image from the signal produced by determining

its spacial origin from the location it hit the scintillation crystal. The drawback of this technique stems from obtaining a two dimensional projection from a three dimension source. Structures at one depth in a patient are obscured by over and under lying structures. Tomographic techniques have since been developed which handle the data in a way that two dimensional images from a selected plane can be obtained.

There are two types of tomography; longitudinal and transverse.[10] With longitudinal tomography, images of a single plane are formed by keeping the details of that plane in focus while blurring the details from other plains. The more commonly used method for SPECT is transverse tomography. For this method the data are collected from a single plane at several different angles and reconstructed by mathematical techniques using a computer. The most common method of obtaining this information is with a rotating gamma camera and a parallel hole collimator. The detector is moved in a circle around the patient to obtain data.

PET is the other frequently used imaging technique. Though not of specific interest to us, I will briefly describe it. Certain isotopes decay by emitting a positron. The positron then travels until it annihilates with an electron resulting in the release of photons which are emitted at 180 degrees from each other. Coincident detection by a pair of detectors establishes the line on which the annihilation has occurred. Therefore a collimator is not

necessary to determine the angle at which the photon is detected. PET cameras are a circular array of detectors which feed information to a computer which reconstructs images layer by layer.

A discussion of the advanages and disadvantages of each method could itself be a chapter. There are, however, a few major differences between PET and SPECT worth noting. The difference in resolution between the two techniques changes with each technicological advance made in camera design. PET is more quantitatively accurate. For this reason the development of receptor binding radiopharmaceuticals is at present more advanced for PET than SPECT. The drawbacks for PET come from the set up cost which include a multi-detector camera and a cyclotron for synthesizing isotopes. Positron emitting isotopes are short lived. Therefore it is necessary to have their source of production very close to the location where they are used. For this reason most nuclear medicine departments, including the department we are associated with, have gamma cameras.

1.2.3) Radionuclides

The radionuclides routinely used for imaging are chosen for several reasons. One of the most important considerations is the isotope must emit photons at a detectable level while minimizing the radiation dose to the patient.

Technetium-99m is, at present, the ideal gamma emitting isotope.[11] It decays almost completely at an energy level of

140 keV. Approximately ninety per cent of the photons emitted are at this level. This minimizes difficulties in detection. Gamma rays at less than 30 keV are absorbed by tissue and gamma rays greater than 300 keV are difficult to collimate and are inefficiently detected due to incomplete absorption by the scintillation crystal.[12]

The half life of technetium-99m is six hours. This is long enough to obtain images before emissions are too low. Also it is short enough that lower total amounts of radiation may be used resulting in a lower radiation exposure to the patient. Though technetium-99m has ideal properties for imaging, it has not been successfully used for receptor specific agents. The nuclide is usually used directly as a pertechnetate salt or chelated to an organic ligand. The purpose of the ligand is to modify its distribution by changing the lipophilicity of the radionuclide. Receptor binding pharmaceuticals are usually small organic molecules which would likely not retain their binding ability if a chelated technetium was added. The shape and size of the molecule would be sufficiently changed that extrapolation of its distribution from the parent pharmaceutical would be unreliable.

Table 1.1 lists the isotopes which are commonly used for receptor specific agents for both SPECT and PET. Listed also in Table 1.1 are the half-life, the energies and the mode of decay.[13]

Carbon-11 is a commonly used isotope whose decay is 100

per cent positron (β^+) emission. Positron emission is due to a proton in the nucleus being transformed into a neutron and a positively charged electron (positron). The positron is ejected from the nucleus and collides with an electron in an annihilation reaction which results in two photons being emitted in opposite directions at 511 keV. The major advantage to carbon-11 is that a known pharmaceutical can be isotopically labelled without changing its molecular structure. However carbon-11 has a half life of 20 minutes which makes handling difficult and allows only the simplest and quickest chemical manipulations.

Table 1.1: Isotopes Commonly Used for Receptor Specific Radiopharmaceuticals

Radionuclide	$T_{1/2}$	Mode of Decay	Photon Energy Level (keV)
^{11}C	20 min	β^+	511 (100%)[a]
^{18}F	1.8 h	β^+	511 (97%)
^{123}I	13 h	EC, γ	159 (97%)
^{131}I	8.06 d	β^-, γ	364 (82%)

a) percentage of disintegrations which are at this level

The other commonly used positron emitting isotope for receptor compounds is fluorine-18. Ninety-seven percent of its decay is by positron emission. Fluorine is more attractive than carbon due to its longer half life however

introduction of fluorine almost always means a change in molecular structure. Many examples have been reported where a fluorine has been substituted for a hydrogen in a receptor binding compound without significantly changing its ability to bind.

Of more importance to this project are the gamma emitting isotopes which have been used for receptor specific compounds. Iodine-131 is by far the most popular gamma emmitting isotope for receptor specific compounds. It decays by electron capture (EC). That is, an orbiting electron is captured by the nucleus and combines with a proton to form a neutron. The neutron is emitted from the nucleus. The daughter nucleus is in an excited state and decays by emitting a gamma ray at 159 keV. This is the ideal energy for imaging.[12] Also emitted from the daughter nucleus are Auger electrons and X-rays. The product of this decay is tellurium-123. The half life is thirteen hours which is long enough for most imaging procedures and short enough that low levels of radiation may be used.

Iodine-131 is also used for imaging. This isotope of iodine decays by β^- decay to an excited daughter nuclide which emits a gamma ray at 364 keV. The high energy gamma rays make imaging difficult. The collimator must be much thicker than for iodine-123 and the efficiency of scintillation is lower. Both of these contribute to fewer photons being detected. Therefore a higher dose is required. The longer half life means a higher dose is required to

obtain a comparable level of photon flux as iodine-123. However the β^- emissions limit the allowable dose. A longer half-life is advantageous at the experimental stage. 131-Iodine decays to xenon-131.

A β^- particle is simply an electron. The electron along with a proton and a neutrino are formed from neutron in this mode of decay. This process occurs in the nucleus and subsequently, the electron and the neutrino are ejected from the nucleus. A neutrino is a "particle" having no mass or electrical charge which undergoes virtually no interaction with matter and is therefore undetectable. Ideally, radiopharmaceuticals should not be labelled with particle emitting isotopes. The interaction of particles with molecules in tissue can cause ionization of atoms and molecules which may cause much greater damage than gamma rays.

1.3) Characteristics Required for a Receptor Specific Radiopharmaceutical

There are several characteristics one must design into a proposed receptor specific radiopharmaceuticals. Listed below are a few of the factors which must be considered.

1.3.1) Metabolism

The design of a radiopharmaceutical must be such that the radioisotope will not be metabolized off of the compound. Depending on the radionuclide used, certain precautions can be taken. For iodine, substitution on an sp^2

carbon prevents nucleophilic substitution which occurs more readily at sp^3 carbons. This, of course, in not fail-safe so all potential radioiodinated compounds must be tested for deiodination. The simplest method is by monitoring thyroid uptake during biodistribution studies since free iodide naturally concentrates there.[14]

1.3.2) Specific Activity

Specific activity (SA) is defined as the activity (in millicuries or megabequerals) per mass (in moles or grams). The maximum specific activity is proportional to the half life of the isotope and can be calculated from the foll ıg equation.

$$SA_{max} \text{ in mCi/mmol} = 1.308 \times 10^8/T_{1/2}(\text{days})$$

The maximum specific activity for the two radioactive isotopes of iodine used for receptor specific agents are given in Table 1.2. Also given is the isotopic abundance which can purchased. Due to the process used to manufacture iodine-131 it is contaminated with iodide-127.[15] Estimates range from 5 to 20 % of the iodide content being the 131 isotope. On the other hand iodide-123 is produced in a manner that leaves it fairly isotopically pure.

Since receptors are present in a low concentration (10^{-7} to 10^{-10} M), it is important that the specific activity be as high as possible since so little of the radiotracer will be bound. The low concentration of receptors is easily saturated with cold agent if the specific activity is low. For this reason imaging receptors is more easily done with

iodine-123 than iodine-131. Also, one does not wish to flood the receptors with nonradioactive compounds present from the labelling procedure. To avoid this, labelling procedures involve careful purification with HPLC to remove any contaminant which also might have affinity to the receptor.

Table 1.2: Specific Activity of the Two Radioisotopes of Iodine used for Imaging

Isotope	Maximum Specific Activity (mmol/mCi)	Isotope Abundance Commercially Available (%)
^{131}I	6.25×10^{-5}	5 to 20
^{123}I	4.17×10^{-6}	99

Since nonradioactive isotope may quite easily be inadvertently added, it is difficult to know the specific activity without measuring it independently. Unintentional contamination with small amounts of iodide is difficult to avoid. This is particularly true with iodine due to its presence in every organic laboratory and its volatile nature. The term "no carrier added" is used to describe a procedure in which no nonradioactive isotope of the label has been intentionally added. However the term carries no real assurance with it since unintentional addition of cold iodine is suspected to be likely.

1.3.3) Target to Background Ratio

To image successfully the uptake of a radiotracer by a

receptor there must be a significant difference between the amount of receptor bound tracer and tracer in the background. The background is often made up of activity in the blood or muscle. It also could be due to nonspecific unsaturable binding to proteins or binding to other saturable binding sites. In investigating a potential receptor specific radiopharmaceutical, one must determine an organ tissue which can be taken as representative of specific uptake and one which can be representative of nonspecific uptake.

The remainder of this thesis is composed of two separate and independent parts due to the diversity of the two topics. Chapters 2 to 5 describe the synthesis and evaluation of a dopamine receptor imaging agent. The topic is introduced in Chapter 2. The results and discussion are divided into Chemistry, Chapter 3 and Biology, Chapter 4. Chapter 5 is the Experimental for the dopamine receptor agent project. The references for Chapters 2 to 5 follow Chapter 5. Chapters 6 to 9 describe efforts made towards the development of an estrogen receptor imaging agent. It is set up in the same manner as the first project. The references for these chapters follow Chapter 9. It also should be noted that the compounds are numbered separately for each project.

References

1. Ell, P.J.; Williams, E.S. Nuclear Medicine: *An Introductory Text*; Blackwell Scientific Publications: Oxford, 1981; p 28.

2. *ibid*, pp. 73 and 175.

3. Eckelman, W.C. In *Radiopharmaceuticals: Progress and Clinical Perspectives*; Friztberg, A.R. Ed.; CRC Press: Boca Raton, Florida, 1986; p 94.

4. Katzenellenbogen, J.A.; Heiman, D.F.; Carlson, K.E.; Lloyd, J.E. In *Receptor-Binding Radiotracers* Eckelman, W.C. ed.; CRC Press, Inc.: Boca Raton, Florida, 1982; pp 93-126.

5. Nogrady, T. *Medicinal Chemistry*; Oxford University Press: New York, 1985; 56.

6. *ibid*, p 59.

7. Eckelman, W.C. In *Radiopharmaceuticals: Progress and Clinical Perspectives*; Friztberg, A.R. Ed.; CRC Press: Boca Raton, Florida, 1986; p. 91.

8. Sharp, P.F.; Dendy, P.P.; Keyes, W.I. *Radionuclide Imaging Techniques*; Academic Press, Inc.: Orlando, 1985; 50.

9. *ibid*, p. 62.

10. *ibid*, p. 92.

11. Burns, H.D. In *The Chemistry of Radiopharmaceuticals*; Heindel, N.D.; Burns, H.D.; Honda, T.; Brady, L.W. Eds.; Masson Publishing USA, Inc.: New York, 1978; p 38.

12. Saha, G.B. *Fundamentals of Nuclear Pharmacy, 2nd Ed.*; Springer-Verlag: New York, 1984; p 70.

13. Burns, H.D. In *The Chemistry of Radiopharmaceuticals*; Heindel, N.D.; Burns, H.D.; Honda, T.; Brady, L.W. Eds.; Masson Publishing USA, Inc.: New York, 1978; pp. 38-39.

14. Saha, G.B. *Fundamentals of Nuclear Pharmacy, 2nd Ed.*; Springer-Verlag: New York, 1984; p. 203.

15. Bolton, A.E. *Radioiodination Techniques*; Printarium Ltd: England, 1977, p 10.

Chapter 2: Introduction to the Dopamine Receptor Imaging Agent Project

The synthesis and evaluation of a series of potential dopamine (D-2) receptor imaging agents is the topic of the following four chapters. Before discussing D-2 receptor imaging agents and our efforts in this area, a brief biological background is given. This discussion is not meant to review dopamine receptor pharmacology or biochemistry but to describe and define concepts which are important to the design of a D-2 imaging agent.

In the first part of this section, I describe the dopaminergic system in the brain. In the second part, I have outlined the relationship between a class of pharmaceuticals called neuroleptics and dopamine receptors. This focuses on the evidence which led to the conclusion that neuroleptics are dopamine receptor antagonists. In the third part, I describe the relationship between certain neurological diseases and dopamine receptor concentration. The purpose of arranging the information in this fashion is to allow the reader to understand the rationale for using labelled neuroleptics as imaging agents for these neurological diseases. Section 2 is a review of labelled neuroleptics which have already been prepared and evaluated as D-2 imaging agents. The final section of this chapter is our proposal for a labelled neuroleptic imaging agent.

2.1) Biological Background

2.1.1) Dopamine Receptors

Dopamine is likely the most studied neurotransmitter. Its structure and that of its biosynthetic precursor is given in Figure 2.1 Dopamine itself cannot cross the blood-brain barrier. l-Dopa, the precursor to dopamine, has been used as a medicinal source of dopamine due to its ability to cross the blood-brain barrier. It is metabolised *in vivo* to dopamine.

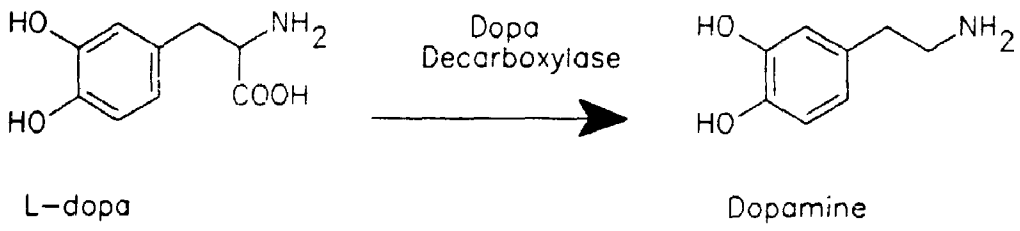

Figure 2.1: Dopamine and its Biosynthetic Precursor

Neurotransmitters are the chemical messengers responsible for communication between neurons. Figure 2.2 shows the presynaptic bulb of one neuron and the postsynaptic membrane of another neuron. The space between them is the synaptic gap or cleft. Neurotransmitters are synthesized and stored in the presynaptic bulb of a neuron. Stimulation of the nerve causes release of the neurotransmitter into synaptic cleft between two nerve cells. The neurotransmitter is then free to bind to a receptor on the dendrite of the next neuron. The action of the neurotransmitter binding with the receptor stimulates

neuronal activity.

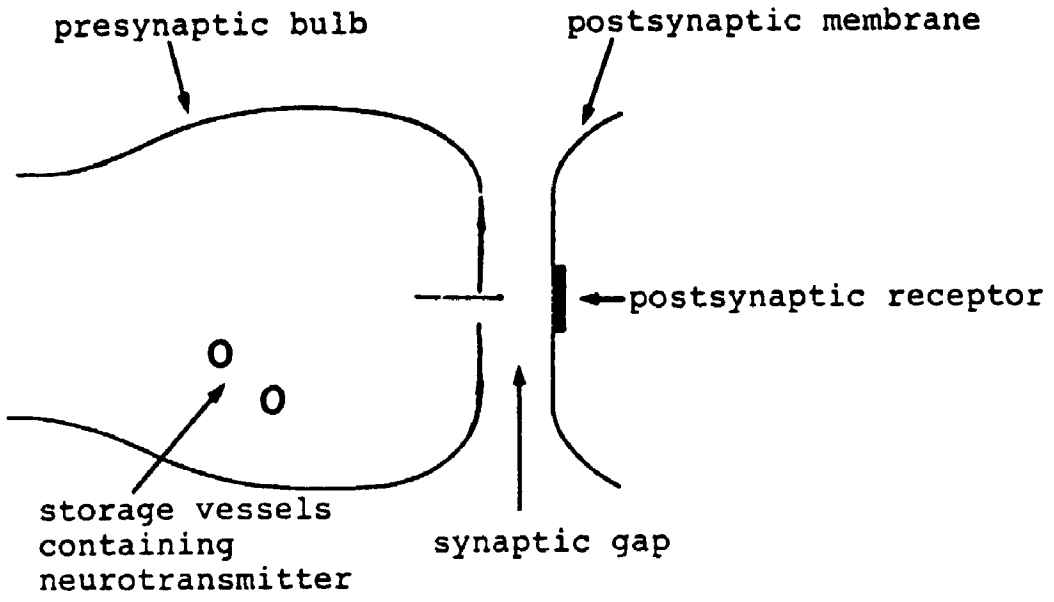

Figure 2.2: Site of Interaction Between Nerve Cells

Dopamine interacts with two different subpopulations of postsynaptic receptors (D-1 and D-2).[1] They have been classified by their differing biochemical and pharmacological characteristics. Interaction of dopamine with the D-1 receptor activates adenylate cyclase, an enzyme which catalyses the conversion of ATP to cyclic-AMP. Cyclic-AMP initiates many different events which result in neuronal activity. The D-2 receptor is biochemically differentiated as not being linked with the adenylate cyclase enzyme.

Pharmacological evidence for the existence of two subpopulations is derived from the binding affinities of different D-2 receptor agonists and antagonists. The two subpopulations, D-1 and D-2, each have a high and low

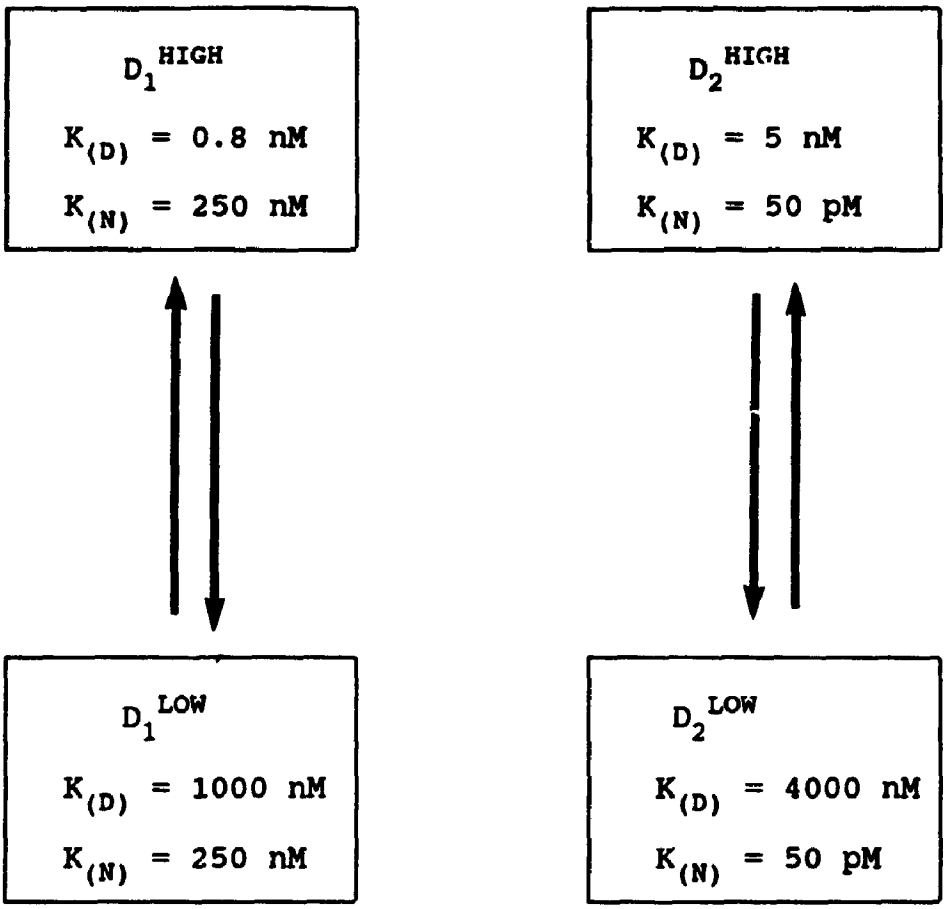

Figure 2.3: Dopamine Receptor Subpopulations and Affinity States

The dissociation constants (K_D, K_N) are for dopamine (D) and a neuroleptic (N), spiperone.

affinity state. This is illustrated in Figure 2.3.[2] The ability of an agonist and an antagonist to bind to each subpopulation and affinity state is shown in Figure 2.3 The antagonists (N) are neuroleptics which are discussed in the following section. The agonist (D) is dopamine. The affinity is given as dissociation constant which are defined in Appendix I. A lower K_D indicates a higher affinity for the receptor. The low affinity D-1 site is characterized by being sensitive to dopamine at micromolar concentrations as well as antagonized by neuroleptics at micromolar concentrations. The low affinity D-2 receptor is also sensitive to dopamine at micromolar concentration but is antagonized by neuroleptics at nanomolar concentrations. That is, D-2 receptors bind neuroleptics much more effectively than D-1. The high affinity states of D-1 and D-2 receptors are sensitive to lower concentration of dopamine (nM) but have the same affinity as the corresponding low affinity state for neuroleptics.

Dopamine is mainly present in three systems in the rat brain. Figure 2.4 is a diagram of the nerve pathways in the brain where dopamine is found.[3] The first is the nigrostriatal pathway with the cell bodies in the substantia nigra projecting into the striatum. The striatum is made up of the caudate nucleus and the putamen. The second system has cell bodies in the interpeduncular nucleus projecting to the mesolimbic forebrain. The mesolimbic forebrain contains the nucleus accumbens and the olfactory tubercle. The third

pathway is the tuberoinfundibular system which has its cell bodies in the arcuate nucleus of the hypothalamus extending to the median eminence.

The areas of high dopamine receptor concentration correlate well with the nerve terminals of the dopaminergic pathways. D-2 dopamine receptors in a rat brain are found in highest concentrations in the caudate putamen of the striatum and the intermediate lobe of the pituitary. The concentration in the caudate membranes is 40 pmol/g wet tissue. The concentration in humans determined by the same method is approximately 15 pmol/g and 20 in the caudate of a calf.[4] The method used to determine receptor concentration is described in Appendix I.

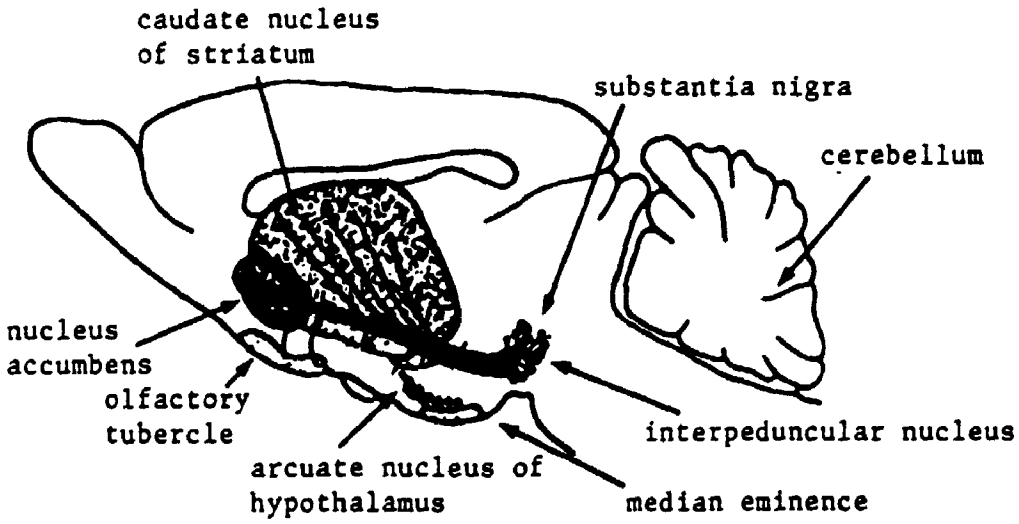

Figure 2.4: Distribution of Dopamine Receptors in the Rat Brain

2.1.2) Neuroleptics and Dopamine Receptors

Neuroleptics are a group of structurally diverse compounds whose biological activity is due to blocking D-2 receptors. As with most drugs, the pharmacological effect of neuroleptics was discovered long before the biochemical mechanism for their action was known. The first compound to be recognized as a neuroleptic was discovered in 1952 by Delay and Daniker who synthesized chlorpromazine, **1**.[5] Chlorpromazine was accidently discovered while searching for antihistaminic compounds and found to have a sedative effect on agitated schizophrenics. Many structurally related compounds, the phenothiazenes, and structurally unrelated compounds, the butyrophenones and benzamides, have since been discovered and classified as neuroleptics due to their antipsychotic action. The structures of a few neuroleptics are given in Figure 2.5.[6] I will focus my discussion on the butyrophenones and benzamides since D-2 imaging agent research has primarily involved these types of compounds.

The first butyrophenone was synthesised in 1957 by P.A.J. Janssen and was found to have chlorpromazine-like biological activity.[7] Various analogues were synthesized and the structural requirements for their activity was defined. The examples given, haloperidol, **2**, spiperone, **3**, and benperidol, **4**, are the most clinically important compounds from this group. It should be noted that spiperone is also called spiroperidol. The most active members of this group have in common a 4-fluorobutyrophenone moiety and a

Phenothiazenes

Chlorpromazine, **1**

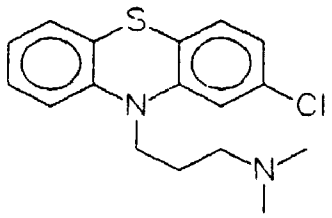

Butyrophenones

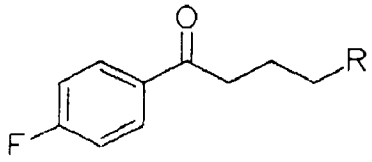

R

Haloperidol, **2**

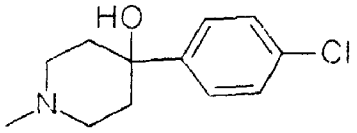

Spiperone, **3**

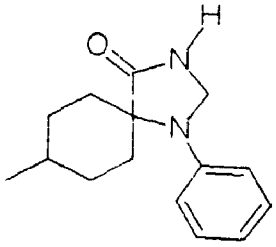

Benperidol, **4**

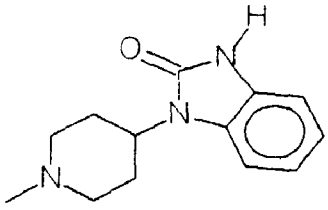

Benzamides

Procainamide, **5**

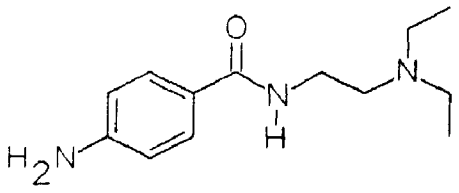

Sulpiride, **6**

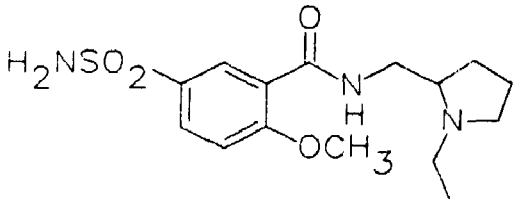

Figure 2.5: Structures of Selected Neuroleptics

piperidine ring.

The benzamides, a quite structurally different group of neuroleptics, were developed from Procainamide, **5**. In 1942 Procainamine was synthesized and reported to have antiarrythmic activity.[8] After a series of structural changes, mostly ring substitutions, sulpiride, **6**, was developed. Sulpiride is presently used in the treatment of schizophrenia. The structural features which all benzamides have in common is an acetanilide ring usually substituted ortho with a methoxy group. The methylene of the amide is substituted with a group containing a tertiary amine.

Prior to the development of *in vitro* receptor binding assays only indirect evidence for the binding of neuroleptics to D-2 receptors was available.[9] These were either biochemical or pharmacological observations made after neuroleptic administration. For example, increased dopamine turnover was observed suggesting that neuroleptics were blocking dopamine receptors and by a feedback mechanism dopamine synthesis was increased. Neuroleptics decrease the activity of dopamine receptor agonists. Also, neuroleptics cause catalepsy in animals and Parkinsonian-like symptoms in humans. Parkinson's disease and the association between it and dopamine will be discussed later. Evidence such as this indicated that neuroleptics block dopamine receptors.

In the mid 1970's, high specific activity radiolabelled neurotransmitters became available. This, along with the refinement of *in vitro* assay techniques, allowed the actual

measurement of the affinity of neuroleptics for receptors. The assay employed is described in Appendix I. The affinity of neuroleptics for D-2 receptors has been shown to correlate linearly to their clinical potency.[10] This establishes that their action is primarily due to D-2 receptor blocking. The inhibitor affinity constants (K_i) of neuroleptics used as D-2 imaging agents are given in Table 2.1.

2.1.3) Dopamine Receptors and Disease

The density of D-2 receptors has been studied most extensively in Parkinson's disease, schizophrenia, tardive dyskinesia, and Huntington's disease.[11] Prior to the development of the receptor binding assay, the association between these neurological diseases and the dopamine system was developed from indirect evidence. Once *in vitro* receptor binding techniques were developed, a more direct means of quantifying this relationship was available. Of the parameters which may be determined by this method, it is the concentration of D-2 receptors which has been found to correlate with different disease states. Receptor concentration in tissue is usually determined by saturation analysis.[12] This assay is very similar to that used to determine the affinity of a neuroleptic for the receptor and is also described in Appendix I. In the following pages I have described the indirect and direct evidence which has been reported.

Parkinson's disease, first described by James Parkinson in 1817, is prevalent in the United Kingdom in 0.1 % of the population. This disease causes tremors, rigidity and often posteurial deformity. It can shorten life-expectancy and be responsible for secondary psychiatric disorders. The first reported association between the dopaminergic system and this disease was in 1960 by Ehringer and Hornykiewicz, who found a deficiency of dopamine and its metabolites in the brain tissue of patients who had died of Parkinson's disease.[13] This eventually led to the current use of l-DOPA (see Figure 1.1), the biosynthetic precursor of dopamine for the treatment of Parkinson's disease. Later, the D-2 receptor concentration was measured in post-mortem brain tissue from early stages of untreated patients who had died from Parkinson's disease. The concentration was shown to be elevated. Tissue from patients which had been treated with l-DOPA showed normal D-2 levels.[14]

Schizophrenia is a complex disease in which the patients have a number of different symptoms, including auditory hallucinations and disturbances in their train of thought.[15] The association between dopamine receptors and schizophrenia was established from l-DOPA treatment of Parkinson's disease. It was observed that high doses of l-DOPA can precipitate the symptoms of schizophrenia and elicit hallucinations. This led to the hypothesis that certain dopaminergic pathways are overactive in schizophrenics.[16] Further evidence arises from the

successful use of neuroleptics in the treatment of schizophrenics. The concentration of D-2 receptors in the striatum and nucleus accumbens has been shown to be elevated in post-mortem tissue from schizophrenics.[17] The increase varies from 20 to 110 percent. Concern that this increase was due to prolonged neuroleptic use led to studies of patients who were known to be drug free. However, it was found that they also had elevated D-2 receptor concentrations.

The involuntary muscle movements which develop in patients who have taken neuroleptics for long periods of time is known as tardive dyskinesia. Even after the neuroleptic is no longer being taken, the symptoms often persist.[18] These phenomena have been attributed to overstimulation of the dopamine mechanism in the brain. Many different clinical observations support this hypothesis. Symptoms of tardive dyskinesia can be reduced by drugs which suppress dopamine synthesis and storage. The symptoms can be brought on by abruptly stopping neuroleptic intake. Dopamine agonists exacerbate these symptoms.[19] It had been proposed that over-stimulation is a result of an increase in dopamine receptors in the brain.

Numerous studies have since addressed the question of long-term neuroleptic use causing increased D-2 receptor concentrations. Rats which had been injected with a high dose of neuroleptics for 4 weeks had doubled the number of D-2 receptors. However, in Alzheimer's disease and

Huntington's chorea, post-mortem analysis of tissue from patients who were on neuroleptics showed no major effect on the D-2 receptor concentration compared to tissue from patients with the same disease but who were not on neuroleptics.[20]

This question was also examined in Parkinson's patients who had been on neuroleptics. They reported an increase in D-2 concentration of 150 percent. However, the neuroleptics could possibly have been given to alleviate the schizophrenic-like symptoms caused by prolonged l-DOPA treatment. It is therefore difficult to determine if the increase in receptors was due to prolonged l-DOPA treatment or neuroleptic treatment. It appears that the symptoms of tardive dyskinesia cannot be attributed entirely to a change in D-2 receptor concentration.

Huntington's chorea is a rare inherited disease which progresses from symptoms of unsteadiness and clumsiness to involuntary jerky movements and eventually into a generalized dementia. The evidence for a connection between the dopaminergic system and this disease is indirect and has not been convincing.[21] A decrease in dopamine and its metabolites has been inconsistently reported in brain tissue obtained for post-mortem analysis. This disease causes the basal ganglia to atrophy and this physical change complicates the analysis of different biochemical observations. However, receptor assays show Huntington's chorea to cause a reduction in D-1 and D-2 concentration in

both the caudate nucleus and the putamen.[22] The decrease is approximately fifty percent compared to normal levels.

From the study of D-2 concentrations in postmortem brain tissue it is apparent that the relationship between receptor level and disease is not straight forward.[23] The methodology itself can be problematic as was demonstrated by the differing results reported. Also most tissue for postmortem analysis is obtained from patients who are in the advanced stages of the disease. Less is known about changes in receptor concentrations at early stages of the disease and over its time course. Complications in interpretation of data also occur from the patient's use of neuroleptics and l-DOPA.

2.2) D-2 Receptor Imaging Agents

2.2.1) Characteristics Required for a D-2 Imaging Agent

The noninvasive nature of nuclear medicine makes it an ideal tool for the measurement of D-2 receptors levels at any stage of the disease. Successful imaging of D-2 receptors would not only benefit research efforts in this area but would be a useful diagnostic tool. Listed below are the characteristics required of the radiopharmaceutical to image D-2 receptors:

i) The agent must be an antagonist, not an agonist, of dopamine (D-2) receptors. Antagonists bind to both affinity states of the D-2 receptor with the same high affinity. An agonist binds more weakly to the low affinity state of the

D-2 receptor.

ii) The agent must have a high affinity for D-2 receptors. The K_i (see Appendix I) must be at least nanomolar or less.

iii) The agent must bind selectively to D-2 receptors. Many neuroleptics also bind well to serotonin S-2 receptors which are present in the striatum.

iv) The agent must have either initially low nonspecific binding or the nonspecific binding must clear over time to give a good target to background ratio. For D-2 receptors this is determined by comparing the concentration of agent in the striatum with that in the cerebellum. The striatum has a high concentration of D-2 receptors and the cerebellum has a very low concentration.

v) The agent must have a high enough absolute uptake in the brain to allow good counting statistics for imaging. Since the higher the absolute uptake the lower the total dose to which the patient will have to be exposed.

vi) The agent must have the characteristics described in the introduction to the thesis. That is, it must be produced in high specific activity. It must be metabolically stable and the radioisotope must be bonded to an sp^2 carbon for chemical stability.

Over the past ten years many radiopharmaceuticals have been proposed for this purpose. As is often the case with radiopharmaceutical research, these efforts were initially focused on imaging agents for PET. Lately, however, there

has been more attention to SPECT imaging agents and in particular radioiodinated agents. The majority of these compounds are either radiolabelled derivatives of benzamides or butyrophenones.

Tables 2.1 and 2.2 summarize investigations into selected D-2 receptor imaging agent. These Tables include the structure of the radiopharmaceutical and the radioisotope used. The first step in evaluating a new radiopharmaceutical is to determine its ability to bind to D-2 receptors, if not already known. This value is given in Table 2.1 as the K_i. The lower this value is the greater its ability to bind to the receptor. The next step is to synthesize the labelled compound and determine its biodistribution in the specific parts of the brain and other organs. This is usually done in rats or mice which are injected with the radiopharmaceutical, sacrificed at various time points and then dissected. The percent injected dose per gram of tissue is then determined.

Another method often employed is to measure the amount of radioactivity in the different regions of the primate brain by PET. By either method the ratio of the uptake in the striatum to the cerebellum is reported. This value is also reported in Table 2.1 along with the animal in which it was determined. This is important for making comparison since rats and mice have a higher concentration of D-2 receptors in the striatum than do primates. Also include in Table 2.1 is the absolute amount of uptake in the striatum.

Table 2.1: Butyrophenone Imaging Agents

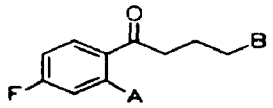

Compounds	A	B	K_i (nM)	Uptake (Striatum/cerebellum)	%ID/g
[^{18}F]-haloperidol, 2	H	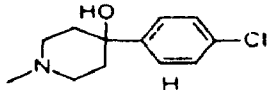	1.17[24]	1.5/baboon image[25]	.07
[^{18}F]-spiperone, 3	H	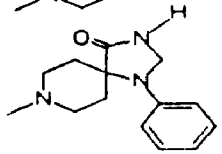	0.26[24]	4.0/baboon image[25]	.02
[^{18}F]-benperidol, 4	H	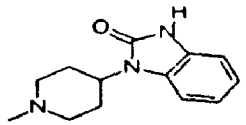	0.24[24]	6.7/baboon image[25]	.02
[$^{77/75}$Br]-bromoperidol, 7	H	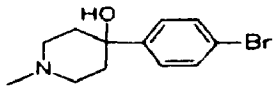	1.4a	1.0/rat dissection[26]	1.1
[$^{77/75}$Br]-bromspiperone, 8	H	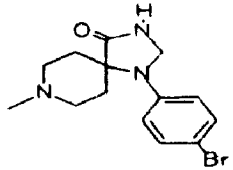	0.29[a]	5.0/rat dissection[26]	0.5
[$^{77/75}$Br] -Bromobenperidol, 9	H	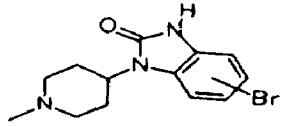	o.65[a]	3.0/rat dissection[26]	0.6

a) These values were calculated from IC_{50}'s given in reference 26 assuming K_D =0.26 for spiperone. See Appendix I for details on the calculation.

Table 2.1 Continued: Butyrophenone Imaging Agents

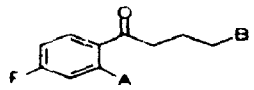

Compounds	A	B	K_i (nM)	Uptake (Striatum/cerebellum)	%ID/g
[^{18}F]-2-fluoroethyl-spiperone, 10	H	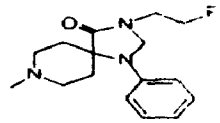	0.38[27]	8.7/baboon image[28]	4.6[29] (mice)
[^{18}F]-fluoropropyl spiperone, 11	H	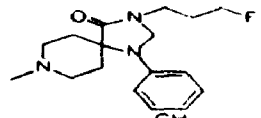	0.18[27]	9.1/baboon image[28]	4.1[29] (mice)
[^{11}C/^{18}F]-N-methyl-spiperone, 12	H	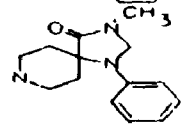	0.25[30]	20/mouse dissection[30]	1.3
2'-iodohalperidol, 13	I	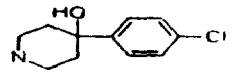	27.8[32]		
2'-iodotrifluoroperidol 14	I	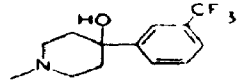	41.0[32]		
2-'iodospiperone, 15	I	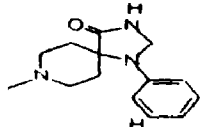	1.0[32]	13.6/mouse dissection[33]	1.0
p-iodospiperone, 16	H	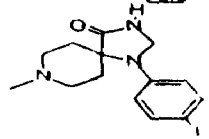	0.3[34]		
[$^{123/122}$I]-iodo-haloperidol, 17	H	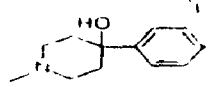			0.8[36] (rat)

2.2.2) Labelled Butyrophenones

The first to be investigated were labelled butyrophenones. These investigations have centred around haloperidol, **2**, spiperone, **3**, benperidol, **4** and their derivatives. Table 2.1 summarizes the results of studies employing these compounds as potential D-2 imaging agents.

Compounds which were considered to be worth further investigation gave inhibitor affinity constants (K_i) in the nanomolar or less range. All the butyrophenones in this range have a 4-fluorobutyrophenone moiety. This made them attractive targets for labelling with the positron emitting isotope fluorine-18. Labelled spiperone, haloperidol and benperidol were synthesized.[24] The initial uptake of all butyrophenones in the brain is quite fast. Of these three, haloperidol had the highest initial uptake which was three times greater than that of the other two.[25] However, the ratio of striatum to cerebellum uptake was only 1.5. This data was obtained from PET images of baboons at four hours. Benperidol, **4**, provided the highest ratio of striatum to cerebellum uptake. Spiperone, **3**, had the second highest at four to one. Some evidence for defluorination of benperidol was given making it a less attractive imaging agent.

Brominated butyrophenones were also synthesized and extensively investigated.[26] Potentially these compounds would provide imaging agents for both SPECT and PET since isotopes of bromine are available which have suitable emission properties for both types of imaging. The chlorine

of haloperidol was replaced with bromine to give bromperidol, 7. This compound was previously investigated as a neuroleptic and determined to have a binding affinity similar to that of haloperidol. Also bromo substitution on spiperone, 8, and benperidol, 9, did not reduce their ability to bind to receptors. Of these three compounds, 8 gave the highest striatum to cerebellum ratio of five to one at two hours as determined by a rat dissection experiment. Though, bromperidol, 7, had the highest absolute striatal uptake (1.1 % injected dose per gram), it showed no selectivity at two hours for the striatum over the cerebellum. Bromobenperidol, 9, showed an intermediate level of cerebral uptake and of selective distribution. PET imaging experiments in baboons showed similar results with 8 appearing to be the most promising of these agent.

In an attempt to simplify the labelling of spiperone with short-lived positron emitting isotopes, analogues alkylated at the secondary amide nitrogen were synthesized and their binding affinities determined. The 2-fluoroethyl, 10, and 3-fluoropropyl, 11, derivatives were found to be potent D-2 antagonists *in vitro*.[27] They were labelled and their biodistribution determined by PET imaging in baboons.[28] At four hours they both showed high specific uptake in the striatum. The 2-fluoroethyl derivative however had a higher absolute uptake.[29] N-Methylspiperone, 12, was also synthesized and labelled with both fluorine-18 and carbon-11.[30] It was labelled with a ^{11}C-methyl on the amide

which was conveniently added in the last step of the synthesis. N-Methylspiperone binds well to D-2 receptors and it gave a ratio of uptake in striatum over the cerebellum of twenty. This was determined in a mouse biodistribution at one hour after injection. However, PET imaging studies in a rhesus monkey at one hour after injection showed a ratio of only 1.73 greater times uptake in the striatum as in the cerebellum.[31]

Of more direct relevance to this project, iodinated butyrophenones have been synthesized and evaluated for use in the SPECT imaging. A series of butyrophenones iodinated ortho to the butanone moiety have been synthesized and their *in vitro* binding affinity determined.[32] The highest affinity was found for 2-iodospiperone, **15**. The others, **13** and **14**, were less potent antagonists of D-2 receptors. 2-Iodohaloperidol, **13**, is one order of magnitude less potent than Haloperidol itself. Labelling and biodistribution studies were performed on **15**.[33] Biodistribution studies in mice showed 13.6 times more activity in the striatum than in the cerebellum at two hours.

Also prepared was p-iodospiperone, **16**, by electrophilic iodination of the aniline ring. The ability of **16** to bind to D-2 receptors was not affected by iodine substitution when measured *in vivo*.[34] However *in vitro* studies also showed poor selectivity for the receptors.[35] The other iodinated butyrophenone synthesized was iodoperidol, **17**.[36] Its biodistribution was determined in rats and total brain

uptake of 0.8 %ID/g at two hours was reported. No attempt was made to demonstrate selectivity for D-2 receptors. PET images in a dog demonstrated good cerebral uptake of the [^{122}I]-**17**.

Of these compounds both fluorine-18 and carbon-11 labelled N-methyl spiperone, **12**, have been most extensively studied in humans. The D-2 receptor density in the caudate nucleus of normal volunteers by *in vivo* PET was reported to be similar to that as determine by **12** in postmortem brain homogenate measured *in vitro*.[37] Studies on patients diagnosed with Parkinson's Disease, Huntington's chorea, pituitary tumours and schizophrenia have also been published.[38] Radiobrominated **8** was also studied in humans. PET studies employing [^{76}Br]-**8** has been used to access receptor concentration in patients taking neuroleptics. Fluorine-18 labelled spiperone, **3**, was studied in healthy humans for the assessment of image processing and in unhealthy patient.[39] Less success has been reported for SPECT imaging employing a butyrophenone agent. The [^{77}Br]-**7** was used for SPECT imaging in a limited study of normal volunteers and schizophrenic patients.[40] Though the studies were successful the high energy emissions of bromine-77 resulted in too high a radiation dose for the patient.

2.2.3) Labelled Benzamides

The second group of compounds which more recently have been investigated as D-2 imaging agent are the benzamides. Table 2.2 shows the structure and the results of initial

studies of compounds from this group.

Raclopride, **18**, labelled withcarbon-11 is the most thoroughly investigated compound for PET imaging.[41] Initial biodistribution studies in rats showed a 5.75 times greater uptake in the striatum over the cerebellum. Subsequent PET studies in a monkey showed a 10-fold difference in the caudate compared to cerebellum uptake.[42] Iodopride, **19**, was purposed as a potential SPECT imaging agent. *In vitro* binding studies on **19** showed a high affinity for D-2 receptors. By rat biodistribution study they showed a 7.2 to 1 ratio of uptake in the striatum over the cerebellum by one hour.[43] Iodobenzamide (IBZM), **20**, a compound very similar to **19** has also been studied. It also has a high binding affinity and selectivity for D-2 receptors.[44] A ten to one ratio of uptake in the striatum over the cerebellum was observed in a rat.[45]

PET studies employing [^{11}C]-raclopride, **18**, have been reported in healthy and schizophrenic subjects.[46] Human images of D-2 receptors have also been reported for [^{123}I]-IBZM employing SPECT imaging. To date this is likely the most successful D-2 agent for SPECT. Studies employing IBMZ which were successful in measuring D-2 receptor levels in healthy and diseased patients were recently reported at the latest meeting of the Society of Nuclear Medicine.[47]

Table 2.2: Benzamide Imaging Agents

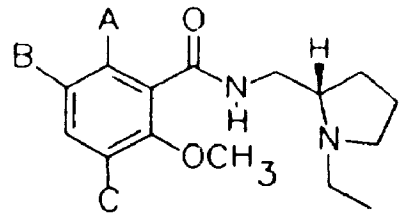

Compound	A	B	C	K_i (nM)	Uptake (striatum/cerebellum)	%ID/g
[^{11}C]-Raclopride, 18	OH	Cl	Cl	4.0[41]	5.75/rat dissection[41]	NA
[^{125}I]-Iodopride, 19	H	I	H	1.2[43]	7.2/rat dissection[43]	0.9
[^{123}I]-Iodobenzamide, (IBZM) 20	OH	I	H	0.56[44]	10.3/rat dissection[44]	0.5

2.3) Strategy for D-2 SPECT Imaging Agent Design

At the initiation of this project the available data was surveyed and potential D-2 imaging agents for SPECT were proposed. We attempted to incorporate the desired characteristics and proposed an iodinated derivative of Haloperidol would have potential as a SPECT D-2 imaging agent. Haloperidol was chosen over spiperone since it was reported to have a higher selectivity for D-2 receptors[48] and a lower affinity for serotonin S-2 receptors. In rat striatum, approximately twenty per cent of spiperone's binding is to S-2 receptors.[49] Our concern in labelling a butyrophenone with iodine lies in the potential for high nonspecific binding due to increased lipophilicity. This would lower the target to background ratio.

One advantage SPECT imaging has over PET is the availability of longer lived isotopes which are suitable for imaging. A PET imaging agent must reach the desired target to background ratio within a few hours of injection because the isotopes used have half lives which are measured in minutes. By using iodine-123 as the label which has a half life of thirteen hours the image could be taken between twenty-four and forty-eight hours, after injection. By taking advantage of this, we hoped to overcome the high nonspecific binding in the brain characteristic of lipophilic compounds.

The three compartment model has been employed for analysis of data from PET images of receptor bound

radiopharmaceuticals in the brain.[50] The schematic representation for this model, shown in Figure 2.6, describes the distribution of a receptors binding agent in the brain. I have borrowed this Scheme to explain our strategy. The first stage, after intervenous injection of the agent is clearance from the plasma and uptake in the brain. To perfuse freely across the blood-brain barrier the compound must be quite lipophilic. In this model a lipophilic compound would have a large k_1. Usually lipophilic compounds also have high nonspecific binding in the brain. Haloperidol, **2**, bromperidol, **7**, and iodoperidol, **17**, all showed high initial uptake in the brain and low plasma levels. Compounds **2** and **7** also showed initially high nonspecific binding. This information was not reported for Iodoperidol. However, it is likely that the nonspecific binding would be high since it is more lipophilic than bromperidol. The nonspecific binding for haloperidol and bromperidol was determine within four hours of injection.

The amount of nonspecific binding in Figure 2.6 is represented by M_{rev}. Therefore, if an agent had a large k_1 which is consistent with lipophilic compounds it will likely have a large M_{rev} initially. The nonspecific binding is in rapid equilibrium with M_{free} which is in an exchangeable pool of agent which is free to clear from the brain, bind to the receptor and bind to the nonspecific sites. Which it does will depend on the relative values of k_2, k_3 and k_5. For our purposes it is desirable for the association

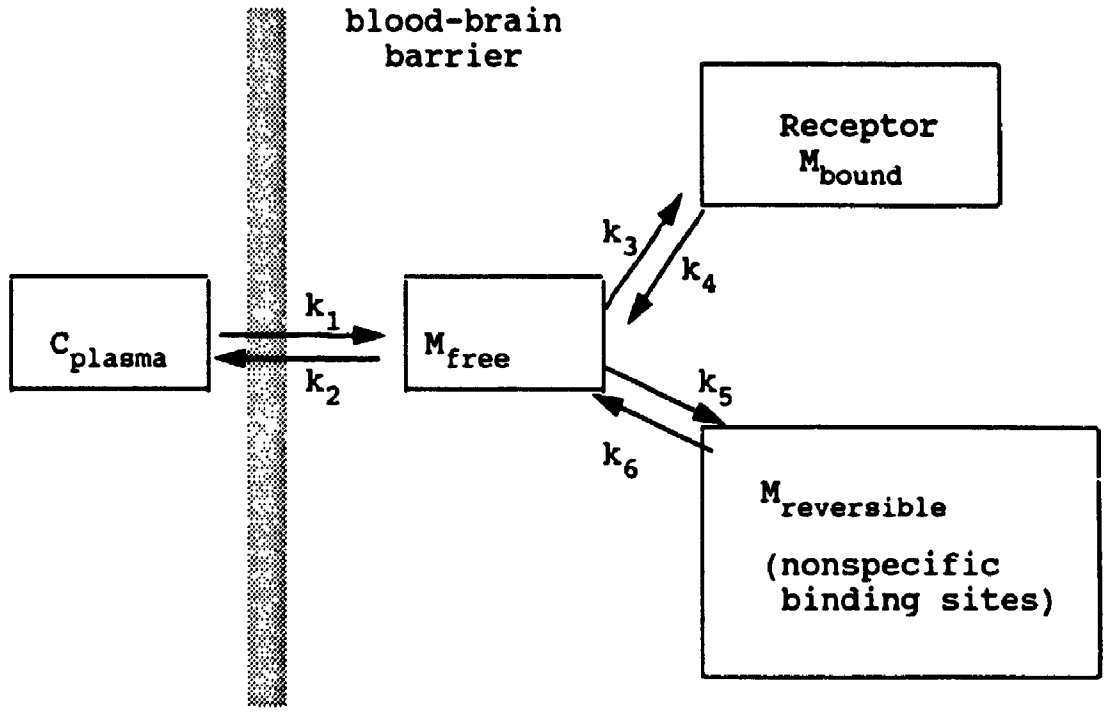

C_{plasma} = concentration of agent in blood

M_{free} = amount of agent in exchangeable pool in the tissue

M_{bound} = amount of agent bound to the receptor

$M_{reversible}$ = amount of agent nonspecificly bound

k_1 and k_2 = rate constants for crossing the blood-brain barrier

k_3 and k_4 = rate constants for binding to receptor

k_5 and k_6 = rate constants for binding to nonspecific binding site

Figure 2.6: Model Binding Kinetics of Brain Receptor Imaging Agent

constant for the receptor binding (k_3) to be greater than that for nonspecific binding (k_5). This is true for a compound which has a high affinity for the receptor. The rate of clearance from the brain (k_2) must be fast enough that the compund will eventually clear from the brain but not so fast that receptor binding cannot compete. It is also important that the rate of dissociation from the receptor be slow. If all these factors were true the initial uptake of the compound would be largely nonspecific and over time $M_{reversible}$ would act as a reservoir for M_{free} which in turn would act as a reservoir for M_{bound} and brain clearance. Hopefully $M_{bound}/M_{reversible}$ would than increase to a point that imaging would be possible.

We proposed that an iodinated derivative of haloperidol could fulfil the requirements described as long as it had similar binding affinity as haloperidol. Structure activity relationships suggested that para substitution on the butyrophenone ring is essential for optimal potency. The unsubstituted compound is much less potent.[51] Other substitution on this ring usually leads to a loss in potency. The known exception to this being ortho amino substitution. The substitution of an iodine in place of the fluorine or meta to the fluorine has not to our knowledge been reported, though it might be predicted that meta substitution would reduce its potency. The ortho iodocompound, **13**, was reported to have ten times less affinity for D-2 receptors than Haloperidol itself. The

other phenyl group appears to be less sensitive to substitution. Optimum potency is obtained when the ring is in the same plane as the nitrogen and c_4 of the piperidine ring.

With this in mind we proposed to synthesize five different iodo-haloperidol derivatives which are shown in Figure 2.7. As mentioned earlier only derivatives substituted on a sp^2 carbon are likely to be stable *in vivo*. This list includes iodoperidol, **17**, since we wished to determine if it shows selective uptake.

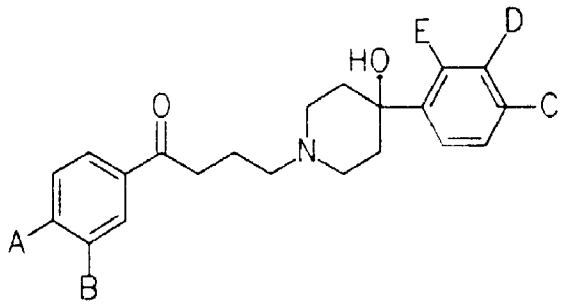

Compounds	A	B	C	D	E
Haloperidol, **2**	F	H	Cl	H	H
21	I	H	Cl	H	H
22	F	I	Cl	H	H
17	F	H	I	H	H
23	F	H	Cl	I	H
24	F	H	Cl	H	I

Figure 2.7: Structures of Proposed Iodohaloperidol Derivatives and Haloperidol, **2**

Reported in the following chapters of this section is the synthesis and receptor binding affinities for three of the five 127-iodinated derivatives **21**, **22**, **17**. Also I will report on the synthesis of radioiodinated **17** and its biodistribution in rats with particular attention paid to its distribution in D-2 receptor rich areas of the brain. To our knowledge **21** and **22** have not been previously synthesized.

Chapter 3: Results and Discussion - Chemistry

3.1) Synthetic Strategy

The strategy employed to synthesize the iodohaloperidols, **17**, **21** and **22** was somewhat analogous to that described by Janssen for the synthesis of Haloperidol[52]. This utilizes the coupling of 4-aryl-4-piperidols, with 4-halogenated butyrophenones. When appropriately substituted, the desired iodinated Haloperidol derivatives **17**, **21**, **22** could be synthesized by this route. The three substituted butyrophenones, A, B and **25** and the two substituted arylpiperidols C and **26** required for the synthesis of **17**, **21** and **22** are shown in Figure 3.1. I have used A, B and C to describe a type of compound that would be functionalized appropriately to allow the synthesis of radioactive and nonradioactive **17**, **21** and **22**. Compounds **25** and **26** are fragments that will also be needed.

Often two different routes are employed to synthesize the iodine-127 and the iodine-131 or 123 analogues. Not all reactions used in the synthesis of nonradioactive aryl iodides can be employed in the synthesis of no-carrier-added radioiodinated aryl compounds. Also it is desirable, to introduce the radioiodine during the last stages of the synthesis since this minimizes the handling of radioactive compounds.

Butyrophenones

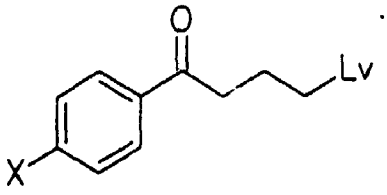

Compound A

	X
28	NH_2
31	I
25	F

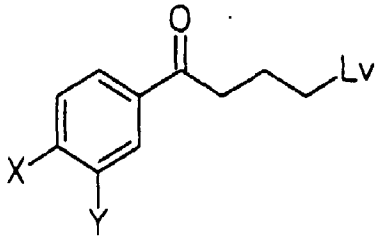

Compound B

	X	Y
27	F	NH_2
30	F	I

Lv = leaving group

Aryl Piperidols

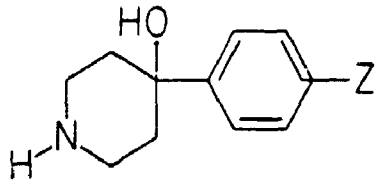

Compound C

	Z
29	NH_2
32	I
26	Cl

Figure 3.1: Functionalized Butyrophenones and Aryl Piperidols Required for the Synthesis of 17, 21 and 22

The two approaches to the desired substituted arylpiperidols and butyrophenones are shown in Scheme 3.1.

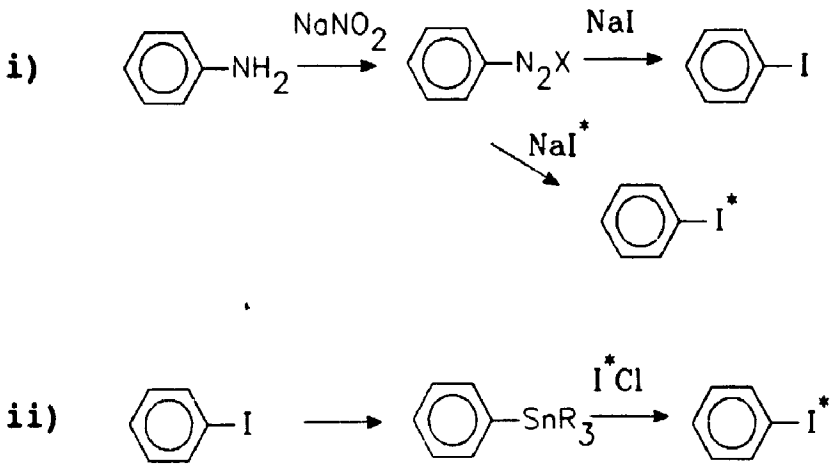

Scheme 3.1: Two Approaches to the Synthesis of Radioactive and Nonradioactive Iodohaloperidol Derivatives

The first approach was to synthesize anilino derivatives, **27**, **28** and **29** from which the iodinated compounds could be obtained by means of a Sandmeyer reaction[53]. As well, by following the "no carrier added" labelling procedure developed for iodotamoxifen[54] (see Chapter 7), the radioiodinated derivative could also be obtained. The second strategy, which proved to be successful, was to synthesize the iodinated derivatives **30**, **31** and **32** by directly incorporating the iodine at any convenient stage in the synthesis. The [^{127}I]-iodohaloperidol derivatives would then be converted to the trialkyl tin derivative and in the last step, these would be converted to the radioiodinated compounds. Aryltrialkyl tin

compounds have been used before as precursors to "no-carrier-added" aryl iodides.[55]

3.2) Substituted Butyrophenones

3.2.1) Synthesis of Anilino Derivatives

3.2.1.1) Amino Butyrophenone 27

The synthesis of **27** was initially attempted by nitration of 4'-fluoro-4-chlorobutyrophenone. If successful, the nitro group could be reduced to give **27**. Standard nitration conditions[56] employing nitric acid and sulphuric acid however failed to nitrate the ring. The major product, by ^{1}H and ^{13}C NMR spectra, was 4-fluorobenzoic acid formed by oxidative degradation. Nitration using nitronium tetrafluoroborate, an active nitrating agent but milder oxidizing agent, was attempted.[57] At room temperature, the reaction was very slow. After three hours, it appeared by ^{1}H NMR that less than 50% of the starting material had reacted. Heating the mixture led to degradation of the side chain.

In an attempt to make the aromatic ring less deactivated, the ketone was reduced with sodium borohydride to give an alcohol, **33**. Subsequent reoxidation should allow conversion back to a ketone. Nitration of **33** with nitronium tetrafluoroborate gave 1-(4'-fluoro-3'-nitrophenyl)-4-chloro-1-butylnitrate, **34**, in a 62% yield after purification by column chromatography. This product resulted from aromatic nitration as well as O-nitration to give the organonitrate. It appeared that the organonitrate partially

decomposed during chromatography. Vacuum distillation decomposed most of this product. Unpurified nitrate was used in the described attempts to convert the nitrate to the ketone described. The crude product was shown by ^{1}H and ^{13}C NMR to be approximately 90% **34** and the minor impurities to be starting material, **33**, and possibly the product of aromatic nitration meta to the fluorine, **35**.

The nitration of **33** with nitronium tetrafluoroborate in acetonitrile was run under argon at -23°C. If the reaction mixture was allowed to warm above this temperature, a second product **36** was formed. The structure and proposed mechanism for its formation is given in Scheme 3.2. The formation of this product can be rationalized by a reaction similar to the Pinner synthesis which converts an alcohol and a nitrile to an imino hydrochloride and eventually to a carboxylic ester.[58] The alcohol attacks an activated carbon of acetonitrile to form the imino compound. The imino salt can be readily hydrolysed during workup in aqueous acid to the carboxylic ester.

Hydrolytic decomposition of alkyl nitrates has been described in a series of papers by J.W. Baker in the early 1950's.[59] They found three products were formed from the treatment of alkyl nitrates with potassium hydroxide. An organonitrate can under go bimolecular substitution (S_N2) to give the alcohol, elimination ($E_{CO}2$) to form the carbonyl or elimination (E2) to give the olefin. The distribution of products varies depending on structure of the organonitrate.

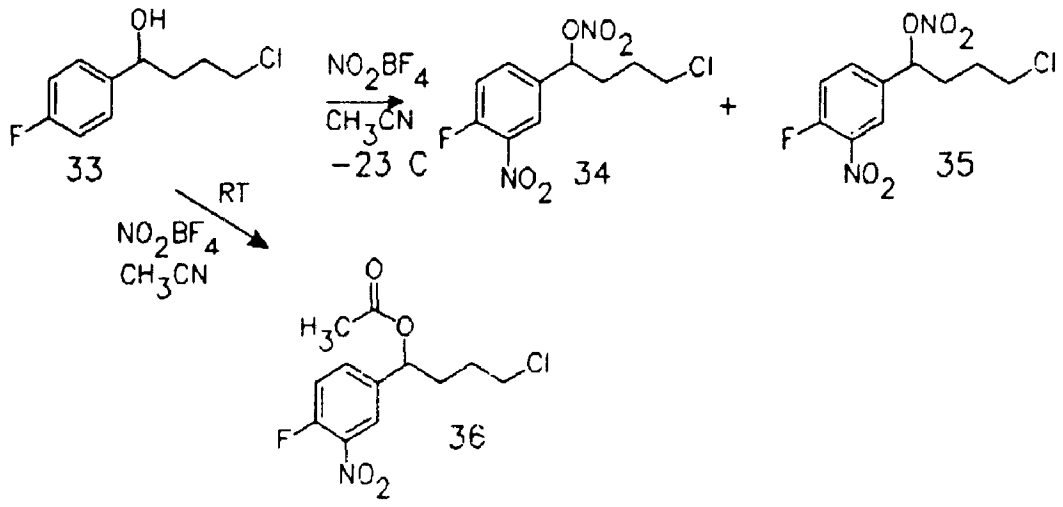

Pinner Synthesis

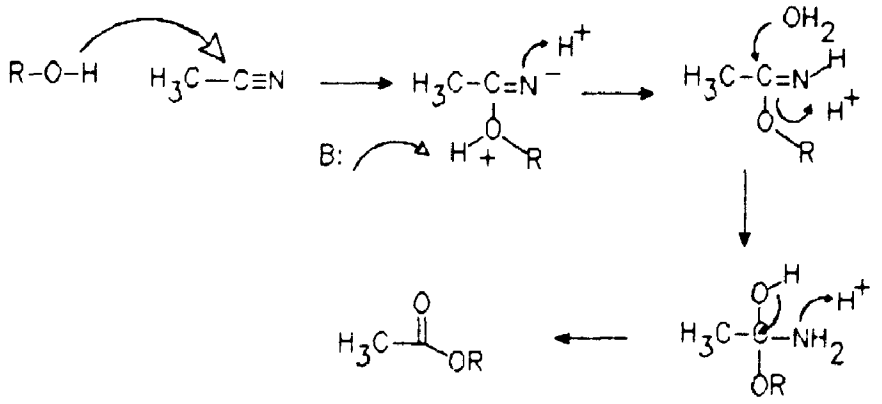

Scheme 3.2: Products From the Nitration of 33 and the Mechanism for the Pinner Synthesis

Benzyl nitrates were studied and it was found that electron withdrawing groups on the phenyl increase the rate of the $E_{CO}2$ reaction while they decrease the rate of the S_N2 reaction.

This prompted us to attempt regeneration of the ketone by $E_{CO}2$ elimination on **34**. The results of these attempts employing several different bases are described in Table 3.1.

Table 3.1: The Results of Elimination Attempts with Various Bases on Organonitrate **34**

Base	Products
NaOEt/EtOH	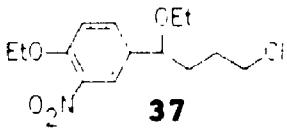 **37** 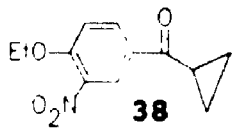 **38**
DBN, Et_3N LDA	**34**
NaH	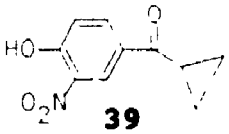 **39** **34**
NaOtBu/tBuOH	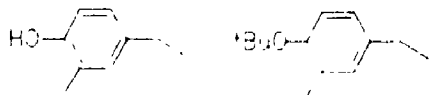

Treatment of the crude organonitrate, **34**, with anhydrous sodium ethoxide in ethanol gave two major products in approximately equal amounts: 1-(4'-ethoxy-3'-nitrophenyl)-4-chloro-1-ethoxybutane, **37**, which was apparently formed by nucleophilic substitution of the

nitrate as well as aromatic nucleophilic substitution of the aryl fluoride by ethoxide ion. The second product was 4-ethoxide-3-nitrophenyl cyclopropyl ketone, **38**. It was formed by ethoxide substitution of the aryl fluoride, $E_{CO}2$ elimination to give the carbonyl, and subsequent base catalysed cyclization to give the cyclopropyl ketone. The formation of the ketone would increase the reactivity of the fluoride towards substitution.

The formation of cyclopropyl ketone from 4-chlorobutyrophenones reappears as an undesirable side product and possibly appeared in reactions run under both acidic and alkaline conditions. A mechanism for its formation is given in Scheme 3.3. In the presence of base the enolate is formed and it readily cyclizes to give the cyclopropyl ketone. The reverse reaction is difficult since it requires a good nucleophile to attack and open the cyclopropyl ring. In aqueous acid, the enol is formed and may also cyclize to the cyclopropyl ketone. However, the carbonyl is protonated and ring opens. The functional group in the 4-position of the butanone chain is then replaced with the nucleophile in greatest abundance.

In an attempt to reduce the side reaction of aromatic substitution, less nucleophilic bases: DBN, triethylamine, sodium hydride, sodium butoxide and lithium diisopropyl diamine (LDA) were tried. DBN, triethylamine and LDA failed to react significantly with **34** under the conditions employed.

Base Catalysed

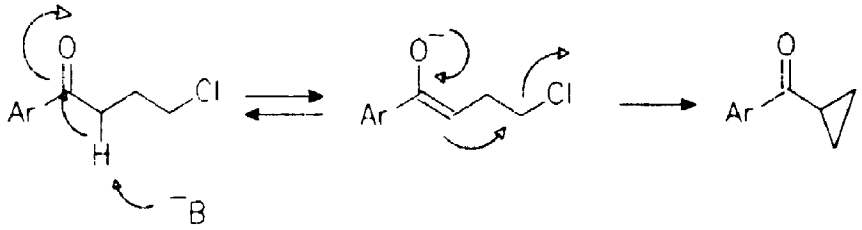

Acid Catalysed

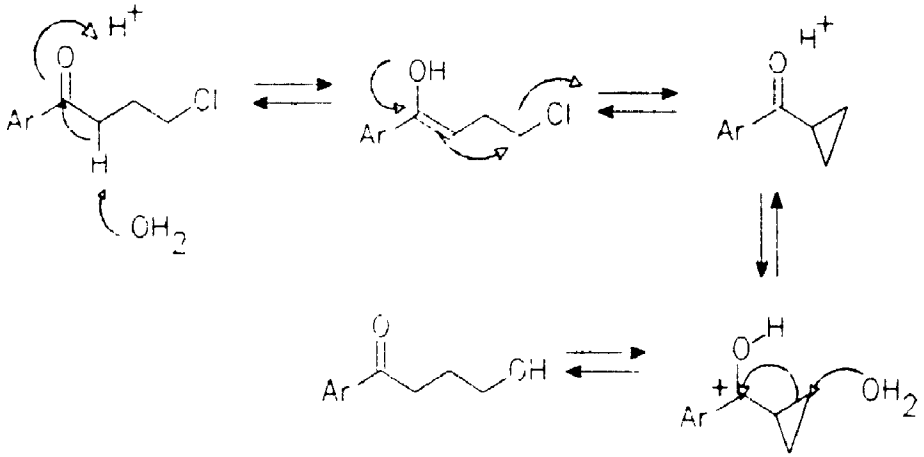

Scheme 3.3: Cyclization Mechanisms of 4-Chlorobutanones

The reaction of **34** with sodium hydride overnight at room temperature gave 4-hydroxy-3-nitrophenyl cyclopropyl ketone, **39** and **34**. Dry solvent (% H_2O in tetrahydrofuran = 0.01 by Karl Fischer titration) and inert atmosphere had been employed. If moisture had been eliminated from the reaction, the phenol must have from hydroxide present in the sodium hydride or less likely formed during work-up with aqueous acid. It is interesting to note that formation of the phenol with the nitrate intact was not observed. Water may be sufficiently nucleophilic to replace the fluoride

when both a carbonyl and nitro group are present but not with just a nitro group.

Treatment of organonitrate **34** with sodium t-butoxide gave three products in all of which the fluorine had been displaced to give either the phenol or the t-butyl ether. This was evident by the lack of fluorine coupling in the ^{1}H NMR spectrum. These products were not separated or characterized further.

The possibility of regenerating the ketone by a radical mechanism seemed feasible due to the stability of NO_2 which would be formed, though a literature precedent was not found. However, attempts to initiate the process with AIBN, and benzoyl peroxide with and without N-bromosuccinimide failed to give any reaction with NMR analysis showing only **34**.

The results of the elimination attempts suggested that the desired 4-fluoro-3-nitro-butanone or 4-fluoro-3-nitrophenyl cyclopropyl ketone may well be too sensitive to be viable synthetic intermediates. Since organonitrates can be reduced to the corresponding alcohol,[60] attempts were made to simultaneously reduce both the nitro and the nitrate to give the corresponding amino alcohol. Low pressure hydrogenation over palladium on carbon and reduction with hydrazine or cyclohexene also catalysed by palladium on carbon all produced too many products to make the procedure of any preparative use. This route was then abandoned.

3.2.1.2) Amino Butyrophenone **28**

In an attempt to synthesize amino derivative, **28**, butyrophenone **40** was synthesized by Friedel Crafts acylation of acetanilide with 4-chlorobutyryl chloride as shown in Scheme 3.4. Hydrolysis with aqueous acid gave 4'-amino-4-hydroxybutyrophenone, **41**. This facile substitution of a primary chloride by the hydroxyl likely occurred via the cyclopropyl intermediate as shown in Scheme 3.3 with water providing the nucleophile. Base catalysed hydrolysis of **40** and concurrent cyclization gave 4'-anilino cyclopropyl ketone **42**.

Treatment of the **41** with concentrated hydrochloric acid gave mostly 4'-amino-4-chlorobutyrophenone, **28**. This substitution is again likely via a cyclopropyl intermediate. This compound was difficult to purify presumably due to the ease with which it could polymerize and its use was abandoned. No attempts were made to take this compound any further.

3.2.2) Synthesis of Iodinated Derivatives

It became apparent that the aromatic nitro compounds were not viable intermediates on the route to both cold and hot iodo compounds.

The second approach was to produce the hot iodo compounds from the cold iodo compounds via the trialkyltin intermediate. The synthetic route to nonradioactive iodinated butyrophenones is shown in Scheme 3.4. Iodine could be incorporated at almost any point in the synthesis. The ease at which the 4-substituted butyrophenone rearranged

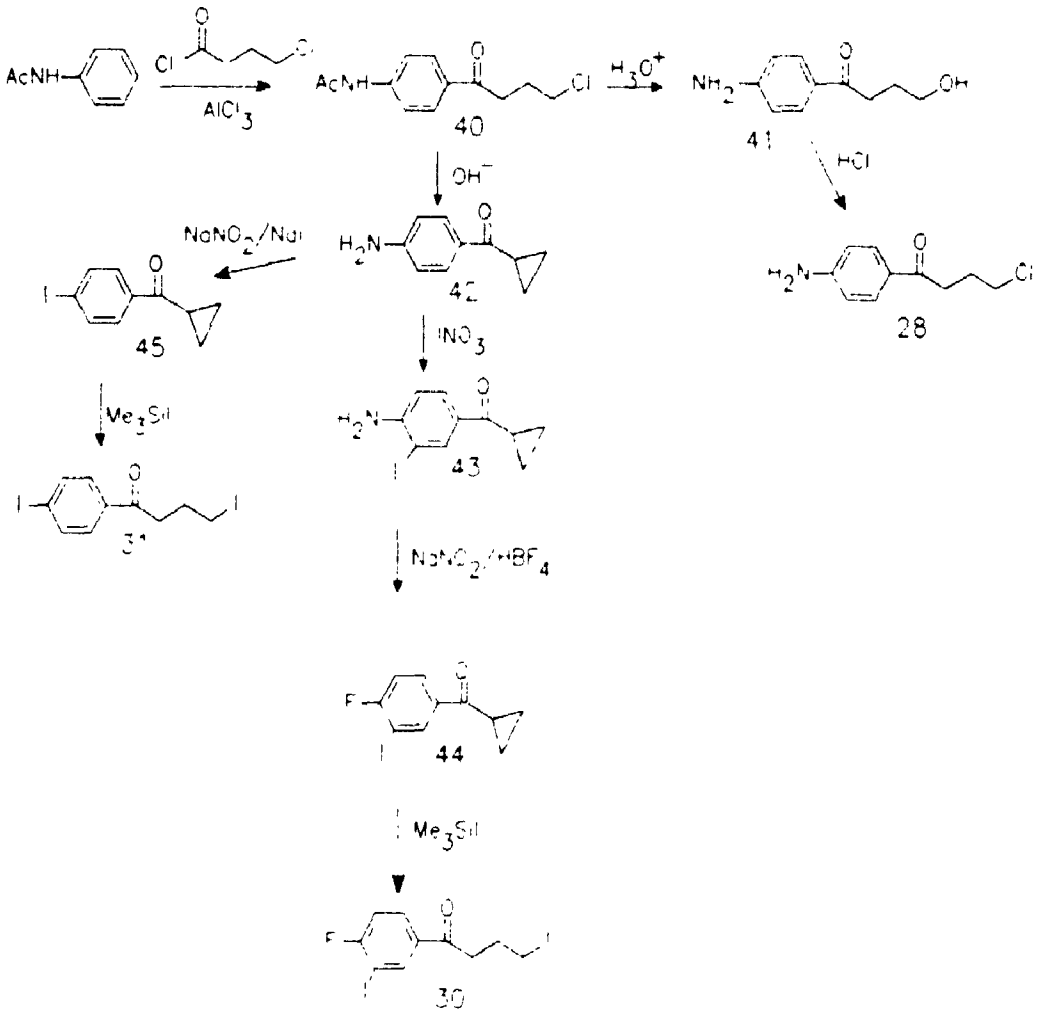

Scheme 3.4: Synthetic Pathway for Butyrophenone Fragments, 30 and 31

to the cyclopropyl under either acidic or alkaline conditions also made it a difficult group to handle. In contrast the cyclopropyl ketone is stable to base but can be reconverted readily to a 4-halogenated butyrophenone with trimethylsilyl iodide. The necessary functional group manipulations were then performed on the cyclopropyl compound and the primary halide was regenerated at a later point in the synthesis.

3.2.2.1) Iodobutyrophenone, **30**

The synthesis of 3'-iodobutyrophenone, **30**, is outlined in Scheme 3.4. The anilino cyclopropyl ketone **42** was cleanly iodinated with iodinium nitrate to give 4-amino-3-iodophenyl cyclopropyl ketone, **43**, by a procedure previously published for iodinating aniline.[61] The amino group was then diazotized. The diazonium salt was isolated and dried prior to decomposition to give the aryl fluoride, **44**.[62] The cyclopropyl ketone was ring-opened with trimethylsilyl iodide[63] to give the desired 4-iodobutyrophenone, **30**, in a 80% yield. This reagent was chosen over concentrated hydrochloric acid since it gave good yields and purer product.

3.2.2.2) Iodobutyrophenone, **31**

The paraiodinated butyrophenone, **31** was also successfully synthesized as shown in Scheme 3.4 from anilino cyclopropyl ketone, **42**. Diazotization of **42** followed by in situ reaction with sodium iodide gave 4-iodophenyl cyclopropyl ketone, **45**, in 43% yield. As with **44** the

cyclopropyl ring of **45** was opened to give 4-iodobutyrophenone **31**, in 90% yield by treatment with trimethylsilyl iodide.

3.3) Substituted Aryl Piperidols

In the original synthesis of Haloperidol and its derivatives, the 4-arylpiperidol moiety of the molecule was synthesized as shown in Scheme 3.5.[64] In an attempt to simplify the synthesis of the arylpiperidols, a new synthetic scheme was devised. It is based on the reaction of either an aryl lithium or aryl Grignard with piperidone to give the 4-aryl-hydroxypiperidine.

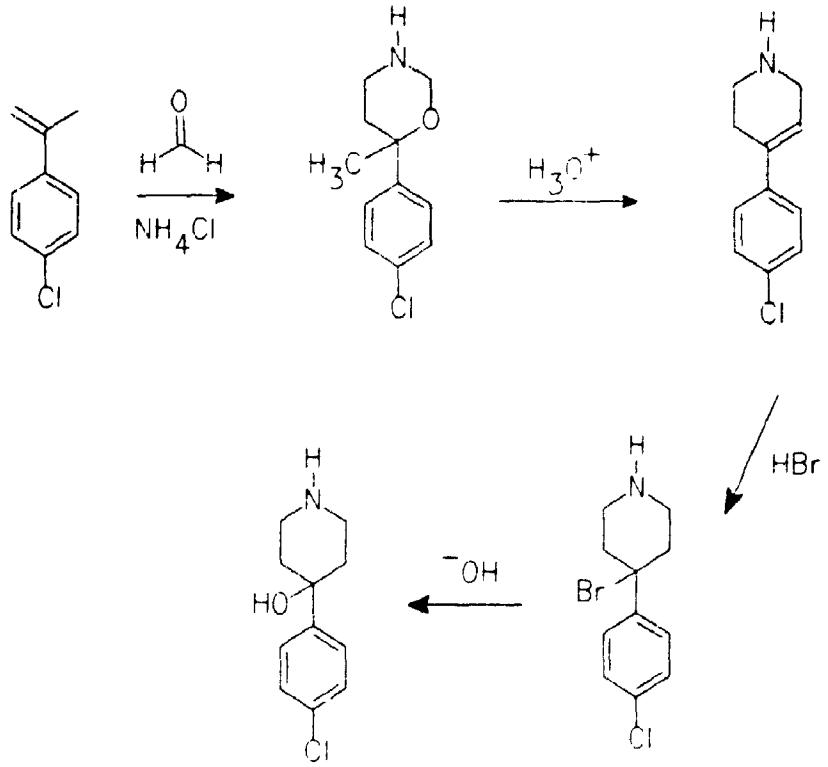

26

Scheme 3.5: Published Synthesis of Aryl Piperidols

3.3.1) Synthesis of an Anilino Derivative

3.3.1.1) Amino Aryl Piperidol, 29

Several attempts were made to synthesize an aryl piperidol, **29**, which is substituted para with an amino group. This would potentially provide access to both "cold" and "hot" iodoperidol, **17**. 4-(4-Chlorophenyl)-4-piperidol, **26**, (Scheme 3.5) could also be synthesized from the anilino derivative via the diazonium salt. Scheme 3.6 shows the purposed synthetic route to the anilino piperidol, **29**.

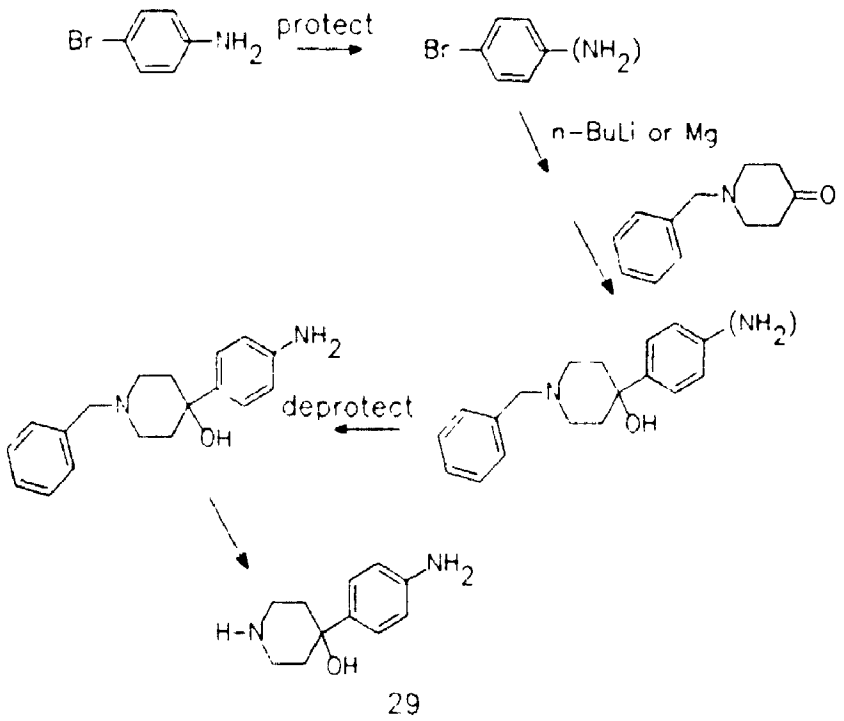

29

Scheme 3.6: Proposed Synthesis of Aryl Piperidol

To synthesize the aryl Grignard or aryl lithium of 4-bromoaniline the amino group would have to be protected. The first method attempted had been successfully employed in the synthesis of aminotamoxifen.[65] An aniline had been protected as the deprotonated trifluoroacetamide before reaction with

an aryl Grignard reagent. In an attempt to adapt this method the acetamide, **46**, was synthesized from bromoaniline and trifluoroacetic anhydride as shown in Scheme 3.7. It was treated with sodium hydride to deprotonate the amide to give **47**. The solution was then added to magnesium in tetrahydrofuran to form the Grignard reagent, **48**. Cyclohexanone was used as a model compound for the piperidone and several attempts were made. However, NMR analysis of the products showed mostly starting materials. The difference between this system and the aminotamoxifen synthesis is that in the later case the sodium salt was part of the ketone and the Grignard reagent was added to it. In this case we attempted to generate a Grignard reagent from the compound containing the sodium salt of the amide.

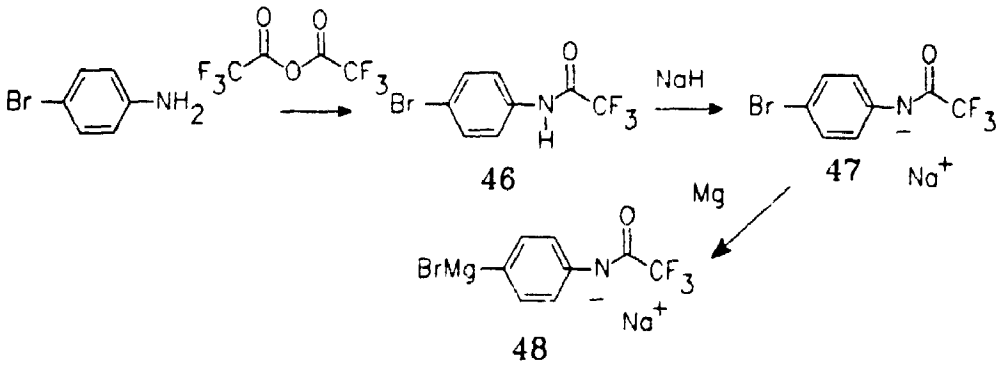

Scheme 3.7: Protection of an Aniline as the Trifluoroacetanilide Sodium Salt

The next approach was to replace the amine protons with trialkylsilyl groups as shown in Scheme 3.8. Trimethylsilyl was the first group tried. Both sodium hydride or n-butyl lithium were employed as bases to deprotonate p-bromoaniline

prior to reaction with trimethylsilyl chloride. The attempt employing sodium hydride gave several products including what appeared to be the mono and disilylated product. The ease in which hexamethyl disilazanes can be cleaved could partially explain this lack of success. The reaction employing n-butyl lithium gave mostly starting material. A published procedure for this reaction was found. By this procedure the first proton is removed with ethyl magnesium bromide and, after reaction with trimethylsilyl chloride, the second proton is removed with n-butyl lithium.[66] This method, however, was not attempted.

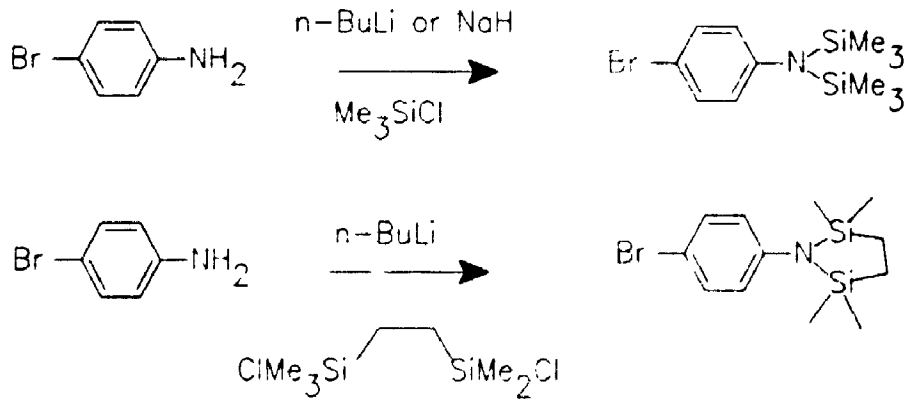

Scheme 3.8: Protection of the Aniline with Alkyl Silyl Groups

Instead 1,2-di(dimethyl)silylethyl group which also had been reported as a protecting group for aniline was tried as

shown in Scheme 3.8. The protected compound is a cyclic disilazane called a Stabase adduct and was reported to be more stable and easier to make than the ditrimethlysilyl adduct.[67] The reported procedure employed n-butyl lithium as base followed by reaction with 1,1,4,4-tetramethyl-1,4-dichlorosilethylene. Several attempts were made employing this procedure with p-bromoaniline. Most resulted in several products which were difficult to separate. Thick layer and column chromatography lead to decomposition of some of the products. Gas chromatography was slightly more successful in partially purifying the desired product. However, in our hands, this procedure did not appear to be of any preparative use so this route was abandoned.

3.3.2) Synthesis of Halogen Substituted Aryl Piperidols

As with the butyrophenone portion of the molecule, the original plan to synthesize anilino arylpiperidol derivatives (Scheme 3.6) was not successful. The alternative strategy was to synthesize the iodo compound by the most convenient route. The most convenient route appeared to be the use of the appropriately halogenated starting material.

3.3.2.1) Synthesis of 4-(4-Chlorophenyl)-4-piperidol, 26

The 4-chlorophenylpiperidol, 26, was synthesized by the route shown in Scheme 3.8. Halolithium exchange of 4-bromochlorobenzene preferentially occurs at the bromine. This aryl lithium was prepared and directly reacted with N-benzylpiperidone, a readily available and inexpensive protected piperidone. The 4-chlorophenylpiperidol, 49, was

purified by vacuum distillation to give a 70% yield.

The next step, N-debenzylation, is most commonly done by medium pressure hydrogenation over a palladium catalyst.[68] However, these conditions could potentially cause dehalogenation of **49**.[69] To avoid this complication attempts were made at hydrogenation using platinum oxide as the catalyst. This catalyst is reported not to dehalogenate but is a less active catalyst for N-debenzylation.

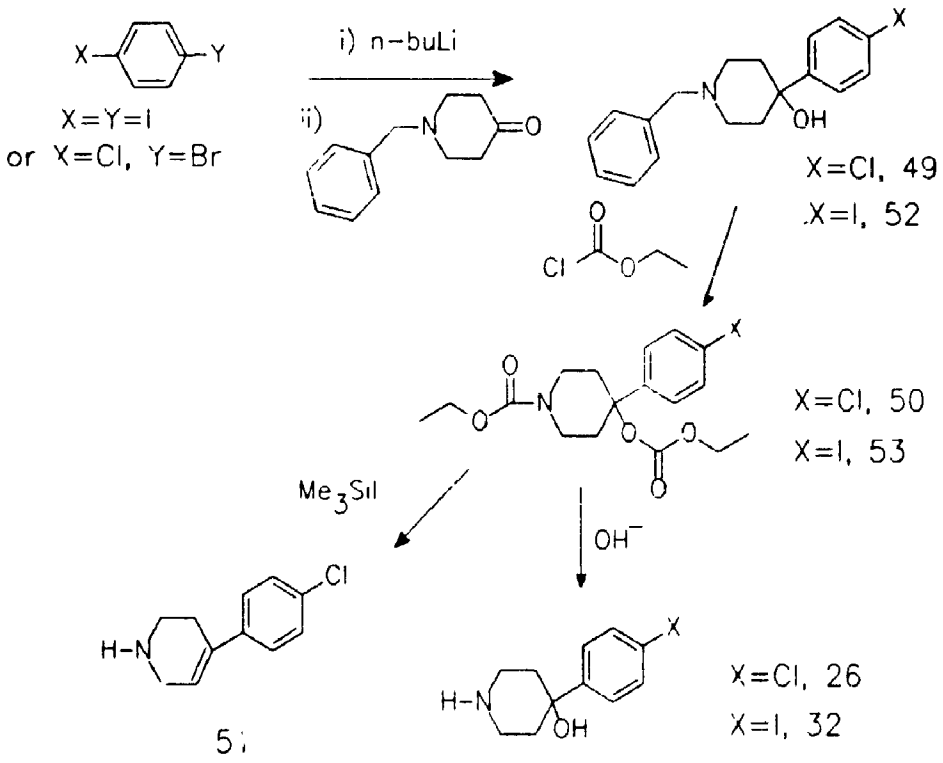

Scheme 3.9: Synthesis of Halogenated Aryl Piperidols

Attempts to debenzylate with this catalyst however were not successful. The reactions were run in a Parr hydrogenator at approximately 40 psi in methanol or methanol

with 1% acetic acid. Acetic acid is reported to help protect catalysts from interacting with basic amines. Even after three days under these conditions, analysis of the product showed mostly starting material. More vigorous conditions were not employed.

An alternative for N-debenzylation by hydrogenation was recently reported.[70] By treating the benzyl amine with ethyl chloroformate, ethyl carbamate and chlorotoluene are formed. When applying this procedure to **49**, it was found that two equivalents of ethylchloroformate and one equivalent of proton sponge were required to successfully debenzylate giving carbamate/carbonate, **50**. Proton sponge is required to remove the proton produced during carbamate formation. If the proton is not removed protonation of the benzyl amine occurs preventing its attack by the ethylcarbonate. The carbonate was formed more quickly than the carbamate. The carbamatepiperidol, **50**, was purified by flash chromatography for product identification only. This resulted in some decomposition of the instable carbonate moiety. To confirm the formation of both the carbamate and carbonate 2-D proton NMR spectra were obtained.

Carbamatepiperidol, **50**, was hydrolysed overnight with 2.5 M sodium hydroxide in water and methanol to give **26**. The melting point compared well with the reported value.[71] Hydrolysis attempts with less concentrated base only hydrolysed the carbonate, not the carbamate. Acid hydrolysis was not attempted in anticipation of dehydration of the

tertiary benzyl alcohol.

Reaction with iodotrimethylsilane followed by treatment with acidic methanol was reported to cleave carbamates.[72] Although the cleavage of carbonates was not mentioned, they are likely cleaved more readily than carbamates. Treatment of **50** with these reagents led to the formation of 4-(4-chlorophenyl)-1,2,3,5,-tetrahydropyridine, **51**. A possible explanation for this product is shown in the mechanism in Scheme 3.10. The intermediates shown are not necessarily real. This scheme is only to show the difference between the reaction of trimethylsilyl iodide and a carbamate and a carbonate. The first step is reversible complexation of the trimethylsilyl group with the carbonyl which upon attack by iodide gives the trimethylsilyl carbamate. The trimethylcarbamate may be cleaved by methanol to give methyl trimethylsilyl ether and the carbamic acid which rapidly decarboxylates to give the amine. In the case of the carbonate, complexation with the trimethylsilyl group, leads to formation of the tertiary benzyl carbocation. This step is followed by elimination. Hydration of the tetrahydropyridine, **51**, was reported to require first hydrobromination of the alkene followed by substitutionof the bromine with hydroxide (Scheme 3.[illegible]).[49] The addition of these two extra step to convert **51** to alcohol, **29**, would likely make this route less efficient than base hydrolysis of **50**. The route using the trimethylsilyl iodide was abandoned.

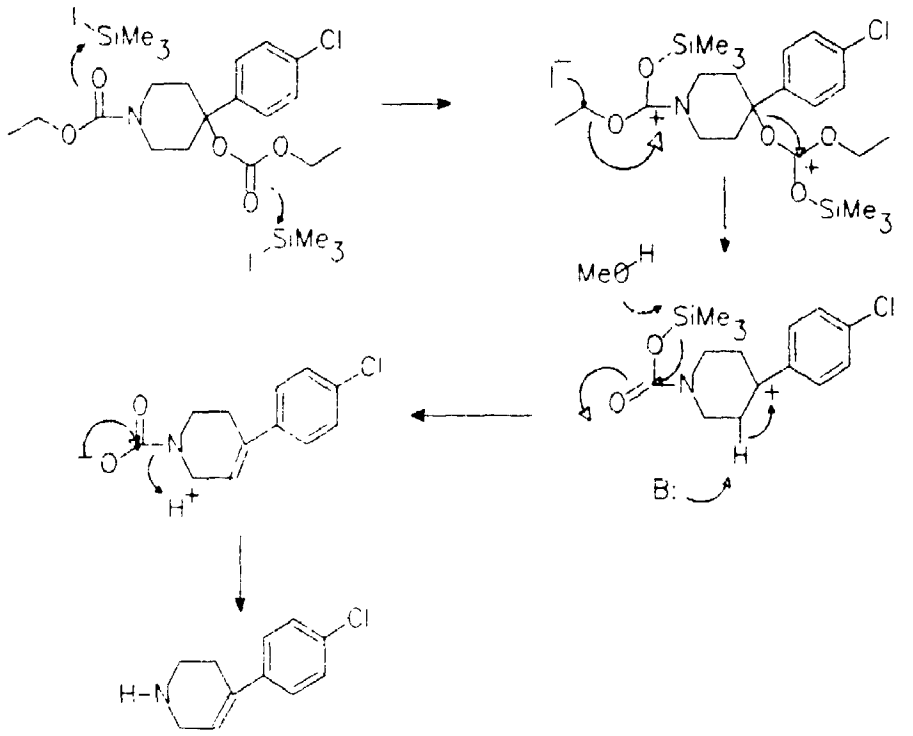

51

Scheme 3.10: Mechanism for the Formation of **51**

3.3.2.2) Synthesis of 4-(4-Iodophenyl)-4-piperidol, **32**

4-(4-Iodophenyl)-4-piperidol, **32**, was synthesised by the same route as 4-(4-chlorophenyl)-4-piperidol, **26** (Scheme 3.9). In the first step of the synthesis, 1,4-diiodobenzene was used in place of 4-chlorobromobenzene. Monolithiation of diiodobenzene and subsequent reaction with N-benzylpiperidone was run in a similar manner as in the synthesis of the 4-chloro compound. 4-Iodophenyl-N-benzyl piperidol, **52** was produced in lower yield than **49**. This was due to the production of coupling product during formation of the aryl lithium compound. Iodophenyl compounds are known

to couple more readily than bromophenyl compound under the reaction conditions.[73] The 4-iodophenylcarbamate, **53**, was synthesized as described for **50**. Compound **53** was hydrolysed with base to give 4-(4-iodophenyl)-4-piperidol, **32**.

3.4) Coupling of the Aryl Piperidol and Butyrophenone Fragments

Prior to substitution of the functionalized butyrophenones with the aryl piperidols, the ketones were protected as ketals to prevented loss of the primary halide leaving group by cyclization during coupling. Thus **31** was reacted with ethylene glycol to give **54**. And by the same procedure **55** was synthesized from **30**. The ketal of 4-fluorobutyrophenone, **56**, was synthesised from 4'-fluoro-4-chlorobutyrophenone,**25**. Scheme 3.11 shows the ketals and aryl piperidols which were combined to give the ketals, **57**, **58** and **59**. In most cases, the ketal of the adduct was not isolated and characterised. Instead it was immediately hydrolysed and the final product was characterised. The procedures for ketalization and substitution were similar to those previously reported for haloperidol.[74] The solvent used for the substitution reaction was dependent on the alkyl halide leaving group. In the case of chlorine, the reaction was refluxed in dimethyl formamide. For the substitution of the alkyliodide the reaction was refluxed in tetrahydrofuran. Compounds **17**, **21** and **22** were characterized by ^{1}H and ^{13}C NMR spectra and exact mass determination by

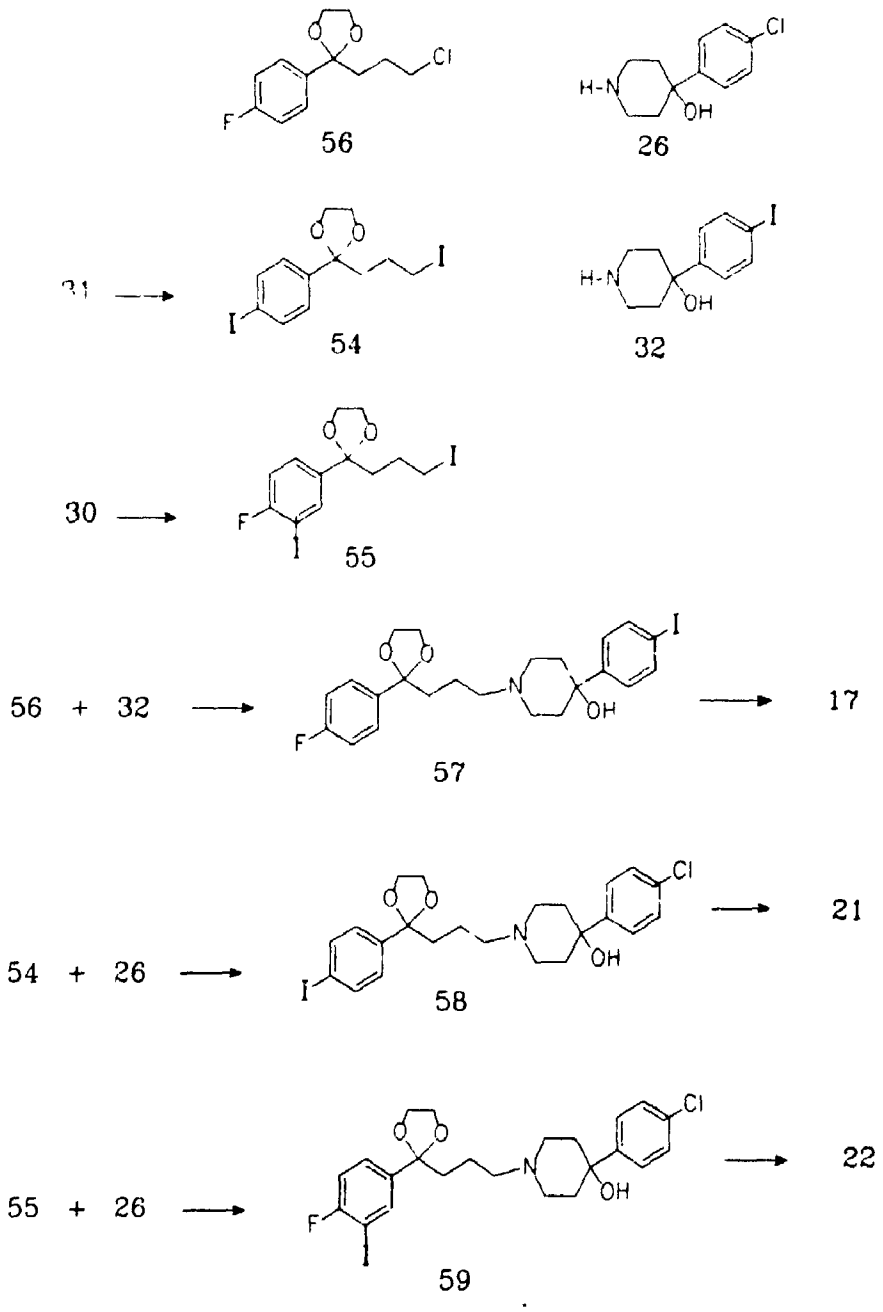

Scheme 3.10: The Aryl Piperidols and Butyrophenones Synthesized and their Coupling to Form 17, 21 and 22

high resolution mass spectrometry. At this stage three of the six possible iodohaloperidols were available for receptor binding assays and for radioiodination through the trialkyltin intermediates.

3.5) Synthesis of Trialkyltin Haloperidol, **61**

To synthesize radioiodinated iodoperidol, **17**, the ^{127}I-iodinated compound had to be converted to a trialkyl tin derivative. The trialkyl tin compounds are known to react with electrophilic radioiodine quite readily to give the aryl radioiodide.[75] The three routes available to convert an aryl halide to a aryl trialklystannane are shown in Scheme 3.12.

Method (i) in Scheme 3.13 which was attempted first involved the treatment of **17** with palladium (0) catalyst and hexabutylditin. This route had been recently employed in the synthesis of a radioiodinated benzamide.[76] Hexabutylditin was synthesised from tributyltin chloride by reaction with magnesium.[77]

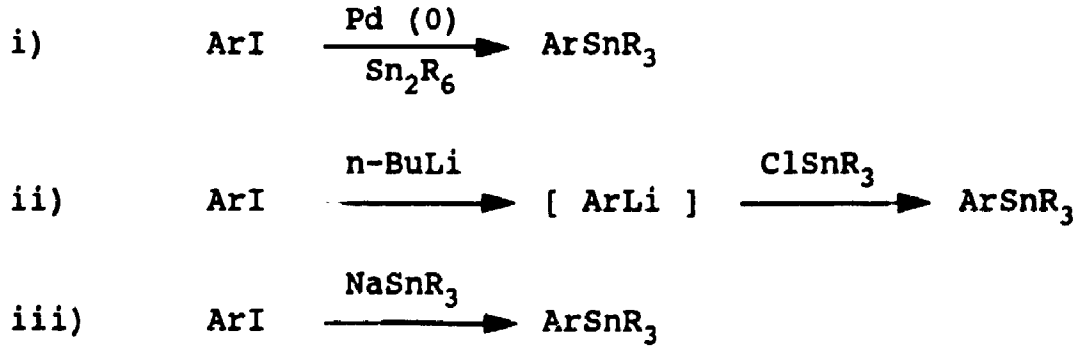

Scheme 3.12: Methods of conversion of Aryliodides to Aryltrialkylstannanes

Tetrakis(triphenylphosphine)palladium (0) was used to catalyse the reaction. It was synthesised from palladium chloride and triphenyl phosphine employing hydrazine as the reducing agent.[78] As with all palladium (0) complexes, it quite easily oxidizes. The product of this synthesis was analysed by ^{31}P NMR at room temperature without taking precautions against oxidation. Several peaks including one at the reported shift for the desired product were present.[79] The literature reported NMR was do at -78 °C. Whether the impurities were present in the catalyst or if they were formed during analysis is not known but both are likely.

The catalytic cycle which has been proposed for palladium (2) catalysts reacting with an aryl halide and hexaalkyldistannanes is given in Scheme 3.13.[80] It has been proposed that the tetrakis(triphenylphosphine)-palladium (0) catalyst dissociates to give di(triphenylphosphine)palladium (0) complex which undergoes oxidative additions and reductive eliminations to give a palladium (2) catalyst prior to undergoing a similar cycle. Several attempts were made to convert **17** to the tributyltin analogue employing this method. Poor solubility of **17** in toluene, the recommended solvent, appeared to hinder formation of the desired products. Increasing the amount of catalyst as well as the amount of hexabutyldistannane did not improve the situation.

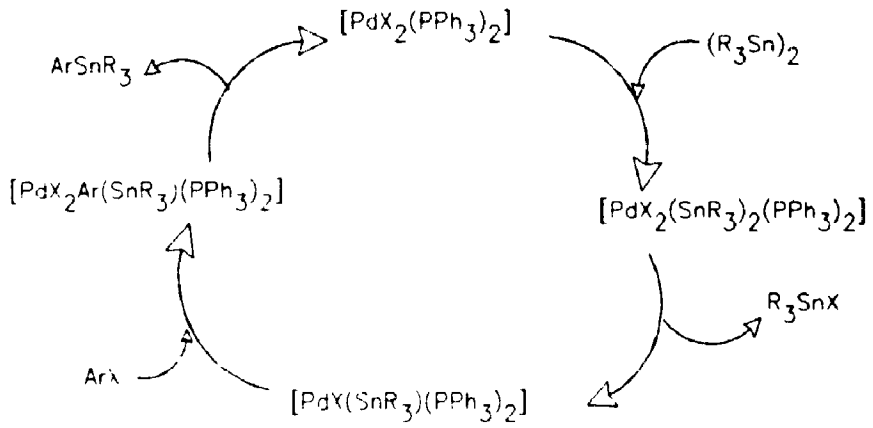

Figure 3.12: Catalytic Cycle for the Reaction of Palladium (II) Catalysts and Hexaalkylditin and Aryl Halide

To ensure that the problem did not lie in the purity of the catalyst, a model compound, 4-chlorobromobenzene, which was completely soluble in the reaction mixture was reacted under the same conditions. By NMR analysis the reaction mixture showed almost complete conversion to 4-chloroaryltributylstannane. In an attempt to partially alleviate the solubility problem, stannylation of **17** was repeated in tetrahydrofuran in which it is partially soluble. However, after two days, during which fresh catalyst was added periodically, there was little evidence for any reaction. This route was abandoned. Perhaps the substrate was too insoluble and possibly the tertiary amine in **17** interfered with the catalyst.

The desired trimethylstannane derivative of Haloperidol, **60**, had been synthesized from Haloperidol **2**,

as a substrate for radiobromination. This reaction is shown in Scheme 3.14[74] and is the third method given in Scheme 3.12. The synthesis of **60** by this route was not initially attempted since the reported procedure used Haloperidol as the substrate for stannylation. After failure of the first method we synthesized **2** and attempted to reproduce this method.

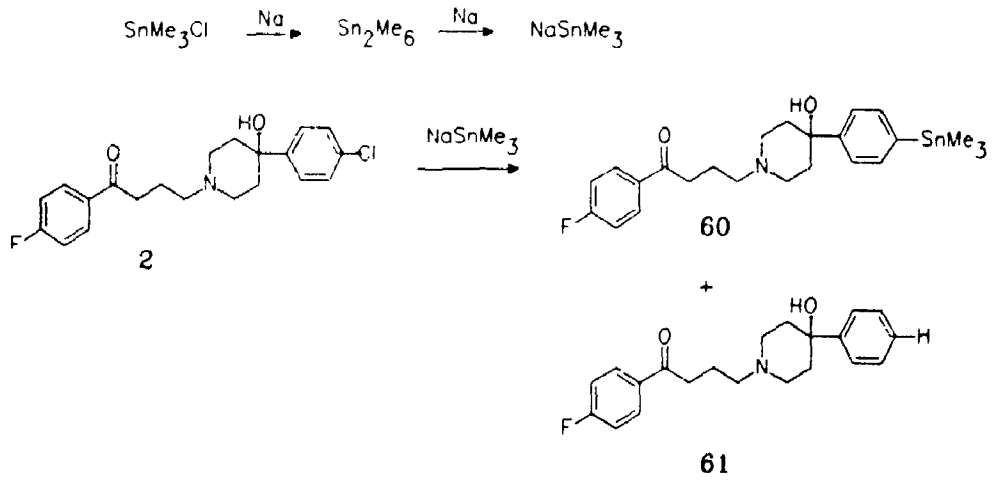

Scheme 3.14: Published Synthesis of **64**

Haloperidol was synthesized from the ketal of 4-chloro-4'-fluorobutyrophenone, **56**, and 4-(4-chlorophenyl)-4-piperidol, **26**. Trimethylstannyl sodium was prepared from hexamethyldistannane which in turn is prepared from trimethylstannyl chloride and sodium metal in liquid ammonia. Hexamethyldistannane was isolated by vacuum distillation before again being treated with sodium in dry glyme. Trimethylstannyl sodium can be prepared directly from trimethylstannyl chloride with an excess of sodium. This method, however, does not allow the separation of the salts

formed by the reaction of the first equivalent of sodium with trimethylstannyl chloride. For practical reasons it is desirable to remove the salts.

The concentration of the trimethylstannyl sodium solution was determined by subtracting the amount of non-trimethylstannyl base from the total base content. The total base concentration was determined by quenching an aliquot of the solution in water and titrating it with standardized acid. The concentration of base not due to trimethylstannyl sodium was determined by quenching an aliquot with an excess of bromopentane, adding water and titrating. This method relies on the fast and complete reaction of trimethylstannyl sodium and alkylbromides.

In our hands, under the conditions (-10 °C, 17h) described by Moerlin and Stocklin,[74] no product was formed. HPLC and NMR analysis showed only starting material. Subsequent variants in which the reaction was allowed to warm to room temperature, the reaction time was extended or a large excess of trimethylstannyl sodium was employed did not appear to produce the desired trimethyl tin compound. Three major products from these attempts were seen by HPLC using a reverse phase column. The middle was identified as starting material by coinjection of the reaction mixture with a sample of **2**. Since starting material was the middle peak, it is likely that one of the other products was more polar and one less polar. The less polar product, may have been the hydrogen substituted haloperidol, **61**. This was

reported to be one of the side products of this reaction.[74] The more polar product was isolated by semipreparative HPLC and analysed by ^1H NMR. Though the structure of this product could not be deduced, it was not the trimethylstannyl compound. This was evident by the lack of a large singlet at 0.2 ppm in the ^1H NMR due to the methyls of the trimethylstannyl group.

The mechanism for the reaction of aryl halides and trimethylstannyl sodium has been studied and the proposed mechanism is given in Scheme 3.15.[81] Investigations into the mechanism were sparked by the observation that bromobenzene and n-butylbromide react with trimethystannyl sodium at approximately the same rate. This result implied that the reaction with bromobenzene probably did not go by nucleophilic aromatic substitution as previously supposed. The formation of benzene in the presence of a proton donor suggested the presence of an aryl anion. These mechanistic studies used bromobenzene, trimethylstannyl sodium and t-butyl alcohol as a proton source.

According to the suggested mechanism the aryl halide undergoes halogen-metal exchange (a) to give the aryl anion and trimethylstannylhalide. If these intermediates stay in a cage the aryl anion will react with the stannylhalide (b) to give the desired trimethylarylstannane and sodium halide. If however they migrate out of the cage (c) the aryl anion would be free to be protonated (e) to give an arene or to react with another molecule of trimethylstannyl halide (d).

In the stannylation of 2 the tertiary alcohol acts as a proton source. It should be noted that trimethylstannyl sodium reacts preferentially with the bromobenzene than witn t-butyl alcohol. This is explained as a preference for attacking a "soft" bromine over a "hard" proton

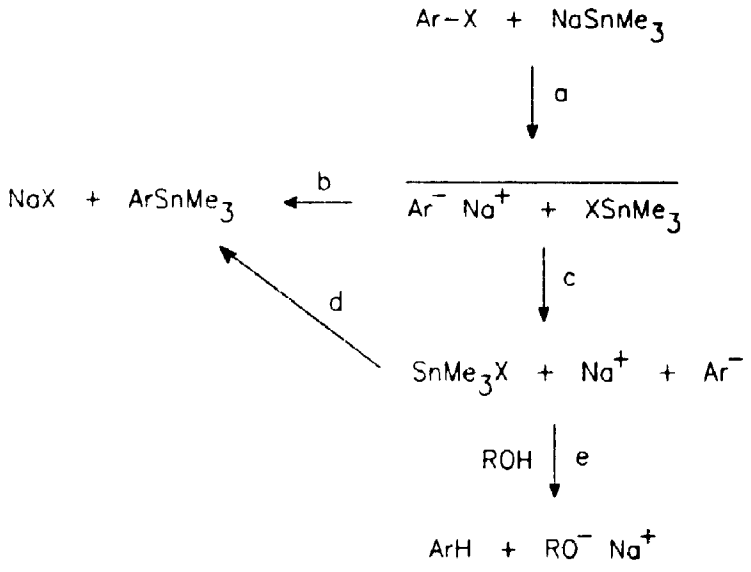

Scheme 3.15: Mechanism for the Reaction of Aryl Halides with $NaSnMe_3$

Further evidence to support this mechanism was the demonstration of an increase in the formation of trimethylaryl stannane compared to arene as the viscoscity of the solvent was increased. If the reaction went by nucleophilic aromatic substitution the viscosity of the solvent would not affect the relative rates of reactions. The effect of solvent viscosity on rate has been demonstrated for free radicals in solvent cages.[82] This

mechanism could explain the formation of **61**. However, the lack of formation of the **60** cannot be explained.

We were not able to reproduce the synthesis of trimethylstannylhaloperidol from haloperidol but in light of this mechanism it seems likely that iodoperidol, **17**, would be a better substrate for the same reaction, since it has been shown that iodobenzenes react much more quickly than chlorobenzene with trimethylstannylsodium.

The synthesis of 4-(4-trimethylstannylphenyl-4-piperidol)-4'-fluorobutyrophenone, **60** was eventually achieved by the reaction of trimethystannyl sodium with iodoperidol, **17**. At icebath temperatures and under the condition used with haloperidol, all starting material was reacted within four hours. HPLC analysis, using the absorbanc at 254 nm, uncalibrated, of the crude reaction mixture showed 63% of hydrogen substituted product, **61**, and 26% to be the desired product, **60**. The trimethylstannyl compound, **60**, was isolated by semi-preparative HPLC. Spectra compared well with those previously reported. The ^{1}H NMR showed the distinctive coupling due to the isotopes of tin. The methyl peak at 0.26 ppm had side bands with a coupling constant of 53.1 Hz due to the tin-proton coupling. In retrospect, the product distribution may have been made more favourable either by protecting the alcohol or by using a more viscous solvent to slow the movement of the phenyl anion and the iodotrimethylstannane out of the cage. These routes, however, were not investigated.

3.6) Radioiodination of Trimethyltinhaloperidol,**60**

No-carrier-added [^{131}I]-**17** was synthesized from the trimethylstannyl compound, **60**, by reaction with [^{131}I]-iodine monochloride produced *in situ*. The proposed mechanism for this reaction involves the ipso attack of iodine monochloride by the phenyl ring to form an α-complex.[75] That is the attack by the carbon substituted with the trimethylstannyl group. This is followed by loss of the trimethylstannyl group. Some support for this mechanism is derived from the increased radiochemical yields for halodemetallation on going from aryltrimethylsilicon to aryltrimethylgermanium to aryltrimethylstannane.

[^{131}I]-**17** was prepared in a 47% radiochemical yield from 1 mCi (37 MBeq) of radioiodide. The reaction was run in 80 µl of acetonitrile and one crystal of N-chlorosuccinimide was used to oxidize the sodium [^{131}I]-iodide to iodine monochloride. The reaction mixture was sonicated for thirty minutes and directly purified by HPLC on a reverse phase analytical column employing UV and radioactivity detectors. Reinjection of the collected fraction showed no side products by UV.

The radiochemical yield for no-carrier-added iododestannylation was reported not to be affected by the amount of water present in the solvent using methanol and acetic acid.[75] Though we have not performed a detailed study on this question, the opposite was observed to be true in

acetonitrile. A radiochemical yield of 47% was obtained with 30% water in the reaction mixture. When the labelling procedure was attempted with greater than 50% water in the reaction mixture, yields fell to less than 10%.

Our reactions were run in a tenth of the solvent and were sonicated instead of stirred. The reaction times and temperatures were the same. Also we employed acetonitrile and N-chlorosuccinimide and in the published study methanol or acetic acid and N,N-dichloramine-T were employed. The difference in oxidizing agent is not likely to have an effect on the yield since both produce iodine monochloride as the electrophilic species. However the difference could possibly be explained by a decrease in solubility of **60** as the amount of water increases. This is an important practical problem since radioiodide is purchased as sodium iodide in an aqueous solution. Though freeze drying can be done, it is desirable to avoid it since iodide easily oxidizes to much more volatile iodine. Freeze drying of radioactive iodide is difficult to do without contaminating the vacuum system and losing some radioactivity.

3.7) Summary

The synthesis of three of the five purposed nonradioactive iodinated Haloperidol derivatives, **21**, **22** and **17** has been completed. Two of these compounds **21** and **22**, to our knowledge, have not previously been reported. Having produced these three radioiodinated compounds allowed us to

have their receptor binding ability determined. The results of these experiments which are discussed in Chapter 4, suggested that we label **17** and further investigate its potential as an imaging agent. We have successfully synthesized the trimethyl tin derivative **60** from **17**. The compound readily labelled to give [^{131}I]-**17**.

Chapter 4: Results and Discussion - Biology

4.1) *In Vitro* Receptor Binding Affinity

The abilities of iodinated Haloperidol derivatives, **17**, **21** and **22** to bind to D-2 receptors was determined *in vitro*. The assay was performed in the laboratories of Prof. P. Seeman, Department of Pharmacology at the University of Toronto. This previously published prccedure[83] involves measuring the ability of the iodinated derivatives to compete with [^{3}H]-spiperone for D-2 receptors. The receptors were in a homogenate of tissue from pig anterior pituitary. This organ has a high concentration of D-2 receptors and low concentration of other receptors.

The K_i values for the iodinated derivatives **17**, **21**, and **22** are given in Table 4.1. The definition of K_i is given in Appendix I. Also presented is the value for 4-(4-chlorophenyl-4-piperidol)-4-fluoro-2-iodobutyrophenone, **13**, and Haloperidol, **2**, which were reported elsewhere.[32]

The K_i values demonstrate the importance of the electronegativity and the size of the atom substituted in the para position of the butyrophenone portion of the molecule. Replacement of the fluorine (K_i = 1.2 nM for **2**) by iodine (K_i = 149 nM for **21**) led to a decrease in the binding affinity by two orders of magnitude. Initial studies of butyrophenone neuroleptics showed hydrogen substitution in this position also greatly reduced neuroleptic potency.[84] The substitution of iodine ortho to the fluorine (K_i = 24 nM

for **22**) reduced its ability to bind by one order of magnitude. Iodine substitution meta to the fluorine (K_i = 27.8 nM for **13**) also has been reported to decrease binding affinity by one order of magnitude. Iodoperidol, **22**, (K_i =1.1 nM) has a binding affinity similar to that of haloperidol (K_i = 1.2 nM). The lack of sensitivity to halogen substitution in the para position of the phenyl piperidol was also seen with Bromperidol, **7** (K_i =1.4 nM).

Table 4.1: Inhibitor Affinity Constants for **2** and the Iodinated Derivatives determine in a Competition Experiment with [^{3}H]-Spiperone

Compound	K_i (nM)
Haloperidol, **2**	1.2[20]
17	1.1
22	24
13	27.8[30]
21	149

Since the new analogues, **21** and **22**, did not have a comparable or improved binding affinity in comparison to **2** we decided not to investigate them further.

4.2) *In Vivo* Biodistribution

The biodistribution of ^{131}I-Iodoperidol, **17**, in rats

has been previously reported at various time points up to eight hours.[37] The relative uptake in the striatum compared to the cerebellum was not mentioned. As stated earlier, we felt that iodoperidol, **17**, deserved further investigation since no receptor selective uptake in the brain had been investigated. Also we wish to investigate its *in vivo* distribution over a longer period of time to determine if receptor bound agent cleared slower than nonreceptor bound. The biodistribution of [^{131}I]-**17** was determined in female rats at various time points up to 48 h. Iodine-131 was used as the label, not iodine-123, for the practical advantage of a longer half life. The animals were sacrificed, organs removed and the activity counted. The results of this experiment are presented in Table 4.2. Before calculating the total injected dose, the amount of radioactivity at the point of injection in the tail was subtracted. The amount of activity in the tail ranged from less than 1 % to 25 % of the counts available. This net total activity provides a measure of the amount of radioactivity which is actually in circulation. The results are reported as percent injected dose per gram of tissue (%ID/g).

The area of greatest D-2 receptor concentration is the striatum of the brain. The cerebellum is known to have virtually no D-2 receptors.[3] For this reason the striatum and cerebellum were separated from the rest of the brain by the dissection over an ice cold plate[85] and counted separately. The ratio of uptake between the striatum and the

cerebellum is considered to be representative of specific uptake over nonspecific uptake.[86] A plot of the uptake in the different regions of the brain is presented in Figure 4.1. In Figure 4.1 and Table 4.2 brain refers to the portion left after removal of the striatum and cerebellum.

The uptake in all parts of the brain peaked at 1h and decreased over time as shown in Figure 4.1. The %ID/g in the brain went from 1.02 ± .06 to 0.29 ± .03 over 48 h. At one hour, the uptake in the striatum was slightly higher than the cerebellum with a ratio of uptake in the striatum over the cerebellum of 1.2. This, however, is not likely a significant difference. Over the forty-eight hours this ratio remained at approximately 1.0. Regrettably this experiment showed no selective clearance between the striatum and cerebellum within this period.

It is interesting to compare the absolute initial uptake in the striatum with other compounds from Table 2.1. The initial uptake is slightly less than that for bromperidol, 7, which was 1.2 %ID/g at 1h and greater than that for haloperidol which is 0.9 %ID/g. This suggests that, of these three, 7 has better characteristics for crossing the blood-brain barrier. High absolute uptake is one of the desired characteristics required for a D-2 imaging agent. This was also mentioned in the previously reported biodistribution of 17.

The level of radioactivity in the blood is extremely low at all time points measured. The highest level is at 1 h

Figure 4.1: Per Cent Injected Dose of [^{131}I]-2 in the Striatum, Cerebellum and the Rest of the Brain over 48h

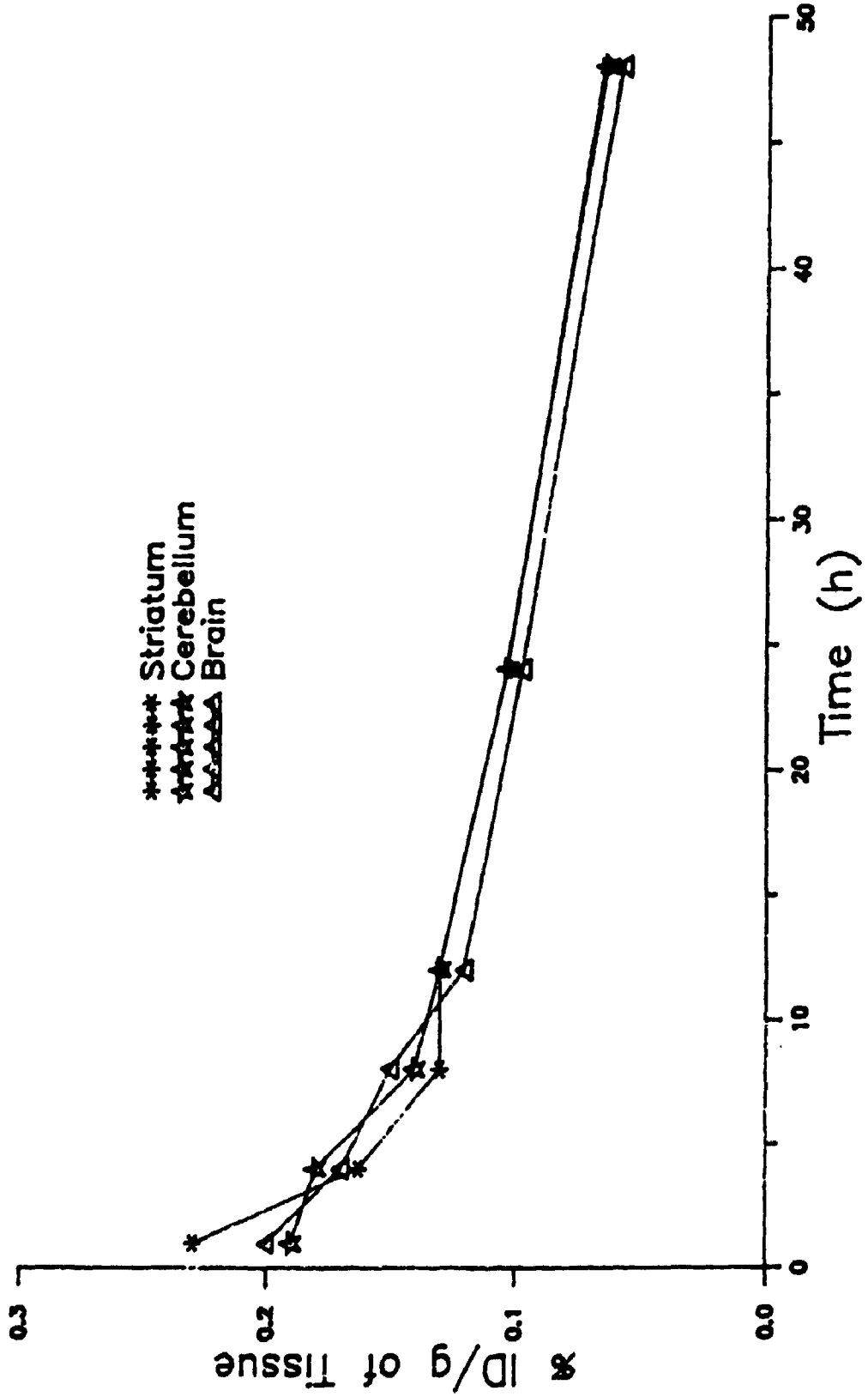
Striatum
Cerebellum
Brain
% ID/g of Tissue
0.0
0.1
0.2
0.3
0
10
20
30
40
50
Time (h)

Table 4.2: Biodistribution Results in Rat with [^{131}I]-17 at Various Time Points

(% injected dose/g of tissue ± SD[a]; 3 rats per time point)

Organ	Time (h) 1	4	8	12	24	48
Blood	.040(.003)	.029(.006)	.017(.003)	.018(.003)	.011(.002)	.015(.008)
Lungs	3.7(.7)	2.4(.2)	1.9(.17)	1.3(.1)	.81(.09)	.49(.04)
Heart	.67(.04)	.49(.04)	.40(.02)	.30(.03)	.215(.003)	.140(.003)
Liver	2.1(.5)	3.7(.47)	5.6(.8)	6.2(.02)	5.3(.6)	5.3(.2)
Pancreas	3.0(.6)	2.1(.91)	3.1(.5)	2.6(.3)	1.0(.3)	.8(.2)
Spleen	2.4(.1)	2.2(.?)	2.01(.06)	1.66(.09)	1.21(.03)	.66(.03)
Kidneys	3.2(.3)	2.3(.2)	2.7(.9)	1.49(.06)	.94(.02)	.49(.02)
Muscle	.19(.07)	.14(.01)	.123(.009)	.0940(.0005)	.0767(.0006)	.040(.001)
Cerebellum	.99(.05)	.93(.03)	.8(.1)	.69(.03)	.53(.01)	.32(.01)
Striatum	1.2(.2)	.85(.08)	.7(.1)	.69(.03)	.5(.1)	.32(.3)
Brain	1.02(.06)	.88(.06)	.78(.2)	.62(.03)	.50(.02)	.29(.03)

a) standard deviation

at 0.040 ± 0.002 %ID/g. The fast extraction out of the blood into the tissue is typical of butyrophenones including Haloperidol, 2.[87] The highest initial uptake at 1 h was in the lungs (3.7 ± 0.7 %ID/g). High lung extraction has been reported for several organic amines.[88] The activity in thelungs is the highest at 1h and decreases to 0.45 ± 0.04 ID%/g by 48 h. High initial uptake is also seen in the spleen, kidney and pancreas. The liver is the only organ in which the uptake does not decrease over time. At 1h, it is slightly greater than 2.2 ± 0.5 %ID/g and by 12 h it has risen to 6.2 ± 0.2 %ID/g. The uptake peaks at this point and begins to clear, though by 48h it is still above 5 %ID/g. The high liver uptake is probably related to 17's lipophilicity. However, high uptake in these organs would not have interfered with a brain imaging. The uptake in the thyroid was never above 1.7 %ID/g over the time course of the experiment. The data from time points 1, 4 and 8 h agree well with that which was previously published.[36]

The biodistribution results are what would be expected for a lipophilic amine. Unfortunately the desired receptor selectivity was not seen. Lipophilicity is an important characteristic in the design of a brain agent. It plays a role in determing diffusion across the blood-brain barrier and partitioning between blood and tissue. For an imaging agent to cross the blood-brain barrier, it must be fairly lipophilic. A log P of between 1.5 and 2.0 has been said to be ideal.[89] For the butyrophenones, this log P must be

determined at a biological pH since protonation of the tertiary amine makes it more polar and therefore more water soluble. Also, lipophilicity plays a role in the nonspecific uptake of a receptor imaging agent. The more lipophilic the compound is, the greater the nonspecific uptake. For a lipophilic receptor imaging agent, one must either have very high initial receptor binding compared to nonspecific binding or, as we have proposed, have selective clearance of the nonspecific binding agent over time.

Lipophilicity can be quantified by measuring a compound's distribution between octanol and water. It is then reported as the log of this value (log P). There are three accepted methods for determining this value. The first and most reliable method is to measure a compounds distribution between water (or a buffer at biological pH) and octanol.[90] The concentration in each layer is usually measured by UV spectroscopy. For radiolabelled compounds, the experiment is simplified by being able to count the activity distributed in each of the two phases. A second method is to use reverse phase HPLC. From the relative retention times between a compound with a know log P and one with a unknown log P a hydrophobicity constant is calculated. This value has been show to correlate well with P values determined by the first method.[91]

The third method is the calculation of Log P values.[92] One of the most commonly employed calculation methods is the fragment method developed by C. Hansch. This method involves

summing the appropriate fragment constants for the structural elements present in the molecule. The total is then modified by a factor which compensates for interactions such hydrogen bonding, dipole-dipole interactions and branching.

Table 4.3 shows the log P for various butyrophenones which have been investigated as D-2 imaging agents. These values were gathered from the literature and have been determined by different methods. For a few compounds, log P values determined by more than one method are given and differences are seen. The largest difference in results is due to the pH of the aqueous solution. For example 7 has a log P of 2.4 when calculated at a pH of 7.4 and a log P of 4.2 when calculated for the neutral molecule. To allow comparison between 17 and other D-2 agents the log P (octanol/water) has been calculated by the fragment method.[93] The compounds are listed from the least lipophilic to the most lipophilic. Also given is the inhibitor affinity constant and the ratio of uptake between the striatum and the cerebellum for each of these compounds.

All compounds in Table 4.3 are quite lipophilic with the lowest calculated value for Spiperone, 3 (log P = 3.21). The compounds are from three different structural groups. There are the haloperidol derivatives, 2, 7, and 17, the spiperone derivatives 3, 12, and 11 and the benzamide derivatives 18, 19 and 20. The log P's range from 3.21 to 4.25. These values are for the unprotonated amine which does

Table 4.3: Lipophilicity Constants, Inhibitor Affinity Constants and Striatum over Cerebellum Uptake Ratios for Selected D-2 Imaging Agents

Agent	Published Log P and Method	Cal'd Log P	K_i (nM)	Ratio of % ID/g striatum/cerebellum
Spiperone, 3	2.67 cal'd[27] 3.37 HPLC[27] 3.37 oct/H_2O[27]	3.21	0.26	4.0
Haloperidol, 2	2.1 cal'd at pH = 7.4[36]	3.52	1.17	1.5
Bromoperidol, 7	4.2 cal'd[27] 2.4 cal'd at pH = 7.4[36]	3.67	1.0	1.0
N-methylspiperone, 12	3.18 cal'd[27] 3.64 HPLC[27] 3.61 oct/H_2O[27]	3.92	0.25	20
Iodohaloperidol, 17	2.6 cal'd at pH = 7.4[36]	3.93	1.0	1.0
Iodobenzamide, 20		3.93	0.56	10.3
Iodopride, 19	2.85 HPLC[42]	3.95	1.2	7.2
Raclopride, 18		4.05	4.0	5.75
N-(3-fluoropropyl)-spiperone, 11	4.03 cal'd 3.73 HPLC	4.25	0.18	9.1

not model the *in vitro* situation very well but does allow acomparison. The corresponding affinity constants range from0.25 to 4.0 nM. The log P for Haloperidol type compounds, **2**, **7** and **17**, increases as one would predict as the halogen on the phenyl piperidol goes from chlorine to iodine. Iodoperidol's, **17**, calculated log P is 3.93.

In Scheme 2.4 of Chapter 2, the three compartment model was presented to explain how we proposed to overcome the nonspecific binding problem. It was proposed that with time the nonspecifically bound compound could act as a reservoir for specifically bound compound and as time passed and as the agent was cleared, receptor selective binding would be observed. The lack of success of this model for Iodoperidol, **17**, could then be attributed to the K_i for receptor binding not being low enough. Again using Figure 2.4 as a model either the rate of association (k_3) was not high enough or the rate of dissociation was (k_4) was coo high. If the rate of dissociation from the receptor is too high, the agent can clear as quickly from the receptor as from the nonspecifically bound site and from the brain.

However it appears that the success of an imaging agent cannot be predicted simply by its lipophilicity and it receptor binding affinity. This is demonstrated most dramatically by raclopride, **18**. This compound, labelled with carbon-11, has been successfully used to image D-2 receptors in humans.[47] It has a binding affinity of 4.0 nM and the log P was calculated to be 4.0. Also, the benzamides appear to

be quite selective even though they are very lipophilic. They also have a tertiary amine like the Haloperidol derivatives which would be protonated *in vitro*. On the other hand the spiperone compounds all have binding affinities less than 0.3 nM. The N-(3-fluoroethyl)-spiperone, **11**, is very lipophilic but still shows good selectivity.

4.3) Summary

The *in vitro* binding affinity was determined for **21**, **22** and **17** and, unfortunately, the affinities of **21** and **22** were weaker than Haloperidol. For that reason these compounds were not radiolabelled. Iodoperidol, **17**, which had been previously reported, was labelled with iodine-131. To determine if a lipophilic compound like **17** could show an increase in the ratio of uptake in the striatum over cerebellum over a 48 h time course biodistribution studies were performed. However, selectivity for D-2 receptors was not observed. The radioactivity decreased from the striatum and the cerebellum at the same rate. Comparison of the lipophilicity and affinity of several successful agents shows that the prediction of *in vivo* biodistribution from *in vitro* results is not very reliable.

Chapter 5: Experimental

5.1) Chemistry

The NMR spectra were run on a Varian Models XL-200 and XL-300 spectrometers using internal TMS. The multiplicities of the ^{13}C spectra were determined by an attached proton test. Infrared Spectra were run on an Beckman Acculab 4 Infrared Spectrometer. Flash chromatography was performed using Terochem silica gel, 20-45 μm. HPLC analysis and separations were performed on a C_{18} reversed phase column (Hibar RT, 250-4 LiChrosorb analytical column and Varian micro-Pak MCH-10 semipreparative column). The Varian (Vista 5500) HPLC used was equipped with a Varian UV-200 detector and a Harshaw sodium iodide flow scintillation detector which were run by a Varian (Vista 402) data system. Mass spectra were run on Varian MAT Model 8230. The melting points are reported uncorrected. Sodium [^{131}I]iodide was donated by Merck Frosst Canada (5 mCi (5 MBq)/0.1 mL of 0.1 NaOH).

4'-Acetamido-4-chlorobutyrophenone, 40

Acetanilide (5.0 g, 37.0 mmol) and 4-chlorobutyryl chloride (26.0 g, 185 mmol) were dissolved in 100 mL of carbon disulphide under argon while being cooled in an ice bath. Aluminum chloride (24.5 g, 185 mmol) was added to the reaction mixture over 30 minutes. After addition was complete, the suspension was slowly heated to reflux which

was maintained for 4.5 h. The solution was then left to separate into two layers while it cooled to room temperature. The upper layer of carbon disulphide was decanted off slowly while maintaining an inert atmosphere. The lower layer, containing the product, was slowly poured over ice producing a yellow precipitate which was filtered and washed several times with water. Recrystallization from diethyl ether yielded 8.86 g (65%) of **40**: mp 158-160 °C; ^{1}H NMR (d_6-acetone) δ 9.5 (1H, s, NH), 7.9 (2H, d, CH), 7.7 (2H, d, CH), 3.6 (2H, t, CH_2Cl), 3.2 (2H, t, $CH_2C{=}O$), 2.1 (2H, quint, CH_2) and (3H, s, CH_3); ^{13}C NMR (d_6-acetone) δ 197.7 (C=O), 169.4 (NHC=O), 144.7 (CNHAc), 132.6 (CC=O), 129.9 (2CH), 119.1 (2CH), 45.3 (CH_2Cl), 35.6 ($CH_2C{=}O$), 27.9 (CH_2), 24.4 (CH_3); mass spectrum m/z calcd. for $C_{12}H_{14}ClNO_2$: 239.071, found: 239.072.

4-Aminophenyl cyclopropyl ketone, **42**

4'-Acetamido-4-chlorobutyrophenone, **40**, (20 g, 84 mmol) was refluxed in 400 mL of 0.7 M aqueous potassium hydroxide and 300 mL methanol for 17 h. Concentration under vacuum precipitated the product which was filtered and washed with water. Recrystallization from chloroform/35-60 petroleum ether yielded 13.5 g (85%) of **42**: mp 108-110 °C; ^{1}H NMR (d_6-acetone) δ 7.7 (2H, d, CH), 6.6 (2H, d, CH), 5.1 (2H, s, NH_2), 2.5 (1H, m, CH), 1.0 (2H, m, CH_2), 0.9 (2H, m, CH_2); ^{13}C NMR (d_6-acetone) δ 197.9 (C=O), 153.1 (CNH_2), 130.5

(2CH), 127.2 (<u>C</u>C=O), 113.4 (2CH), 15.8 (CH), 10.3 ($2CH_2$); mass spectrum m/z calcd. for $C_{10}H_{11}NO$: 161.084, found: 161.084.

4-Iodophenyl cyclopropyl ketone, **45**

To an ice cold solution of 5.0 g (31 mmol) **42** in 200 mL of 0.5 M hydrochloric acid was added 3.2 g (46.5 mmol) of sodium nitrite dissolved in a minimum of water. After 10 min the ice bath was removed and stirring was continued for an additional 40 min. Urea was added until bubbling ceased, and was followed by the addition of 69.0 g (46.5 mmol) of sodium iodide. After 10 min, the reaction mixture was extracted with chloroform and washed with aqueous sodium thiosulphate followed by water. After drying over anhydrous sodium sulphate the chloroform was removed under vacuum leaving a red oil. Vacuum distillation yielded 3.5 g (43%) of a yellow waxy solid, compound **45**: bp 110-112 °C at 0.05 mm Hg; ^1H NMR ($CDCl_3$) δ 7.7 (2H, d, CH,), 7.6 (2H, d, CH), 2.5 (1H, m, CH), 1.0 (2H, m, CH_2), 0.9 (2H, m, CH_2); ^{13}C NMR ($CDCl_3$) δ 199.1 (C=O), 137.4 (2CH), 136.7 (<u>C</u>C=O), 129.1 (2CH), 100.4 (CI), 16.7 (CH), 11.7 ($2CH_2$); mass spectrum m/z calcd. for $C_{10}H_9IO$: 271.965, found: 271.970.

4'-Iodo-4-iodobutyrophenone, **31**

Trimethylsilyl iodide (2.02 g, 10.0 mmol) was added drop-wise to a solution of **45** (2.2 g, 8.0 mmol) in 30 mL of carbon tetrachloride cooled in a ice/salt bath and under

argon. After 1 h, the cold bath was removed and stirring continued for an additional hour. The mixture was then diluted with chloroform and washed with aqueous sodium thiosulphate. After drying over anhydrous sodium sulphate the solvent was removed under vacuum and the remaining residue was crystallized from ethyl acetate to yield 3.2 g (98 %) of **31**: mp 81-82 °C; ^{1}H NMR ($CDCl_3$) δ 7.8 (2H, d, CH), 7.6 (2H, d, CH), 3.2 (2H, t, $CH_2C=O$), 3.0 (2H, t, CH_2I), 2.2 (2H, quint, CH_2); ^{13}C NMR ($CDCl_3$) δ 197.8 (C=O), 137 (2CH), 135.9 ($\underline{C}C=O$), 129.4 (2CH), 101.2 (CI), 38.8 ($\underline{C}H_2C=O$), 27.3 (CH_2), 6.2 (CH_2I); mass spectrum m/z calcd. for $C_{10}H_{10}I_2O$: 399.873, found: 399.888.

1-(4-Iodophenyl)-1,1-(ethylene dioxy)-4-iodobutane, **54**

4'-Iodo-4-iodobutyrophenone, **31**, (1.0 g, 2.5 mmol), ethylene glycol (0.46 g, 7.5 mmol) and p-toluene sulphonic acid (0.005 g, 0.03 mmol) in 15 mL of benzene were refluxed for 12 h employing a Dean-Stark trap. The solution was then diluted with methylene chloride and extracted with diluted sodium hydroxide. After drying over anhydrous sodium sulphate, the solvent was stripped under vacuum to yield 0.8 g (72%) of **54**: ^{1}H NMR ($CDCl_3$) δ 7.6 (2H, d, CH), 7.1 (2H, d, CH), 4.0 (2H, t, CH_2O), 3.7 (2H, t, CH_2O), 3.1 (2H, t, CH_2I), 1.8 (4H, m, CH_2); ^{13}C NMR ($CDCl_3$) δ 142.1 ($\underline{C}C-O$), 137.3 (2CH), 127.7 (2CH), 109.4 ($\underline{C}O_2$), 93.9 (CI), 64.6 ($2CH_2O$), 41.0 (CH_2), 27.8 (CH_2), 6.7 (CH_2I).

N-Benzyl-4-(4-chlorophenyl)-4-piperidol, 49

4-Bromochlorobenzene (5.00 g, 26.0 mmol) in 30 mL of anhydrous ether was cooled in a dry ice/acetone bath under argon. A 2.5 M solution of n-butyl lithium (9.5 mL, 23.4 mmol) was added drop-wise by syringe. The solution was stirred under these conditions for 3.5 h at which time 3.7 mL (21.06 mmol) of N-benzyl-4-piperidone was added and the solution was refluxed for 40 min. After cooling to room temperature, the reaction mixture was washed with 10% sulfuric acid. The aqueous extracts were made alkaline with aqueous sodium hydroxide. The precipitate which formed was extracted into chloroform and washed with water before drying over anhydrous sodium sulfate. Removal of the solvent gave a yellow oil which after vacuum distillation yield 4.56 g (70%) of a waxy solid, 49: bp 120 °C at 0.05 mm of Hg; ^{1}H NMR ($CDCl_3$) δ 7.3 (9H, m, CH), 3.51 (3H, s, $\underline{C}H_2Ph$, OH), 2.7 (2H, m, CH_2), 2.4 (2H, t of d, CH_2), 2.1 (2H, t of d, CH_2), 1.6 (2H, d of d, CH_2); ^{13}C ($CDCl_3$) δ 147.0 ($\underline{C}COH$), 138.2 (C), 132.6 (CCl), 129.2 (2CH), 128.3 (2CH), 128.2 (2CH), 127.0 (CH), 126.1 (2CH), 71.0 (COH), 63.2 ($\underline{C}H_2Ph$), 49.3 ($2CH_2N$), 38.4 ($2CH_2$); mass spectrum m/z calcd. for $C_{18}H_{20}ClNO$: 301.123, found: 301.123.

4-(4-Chlorophenyl)-4-piperidol, 26

N-benzyl-4-(4-chlorophenyl)-4-piperidol, 49, (2 g, 6.46 mmol), ethyl chloroformate (6.6 mL, 68.8 mmol) and "proton

sponge" (1.4 g, 6.54 mmol) were refluxed in 80 mL benzene for 18 h. The protonated proton sponge was then filtered and washed with benzene. The filtrate was extracted with dilute hydrochloric acid and water before drying over anhydrous sodium sulfate. Removal of solvent produced a yellow oil which was purified for product identification by flash chromatography on silica (1:1/diethyl ether/30-65 °C pet. ether). This procedure yielded 1.35 g (54%) of **50**: ^{1}H NMR ($CDCl_3$) δ 7.3 (4H, s, CH), 4.1 (6H, m, CH_2), 3.4 (2H, t, CH_2), 2.5 (2H, d, CH_2), 1.9 (2H, m, CH_2), 1.2 (6H, m, CH_3); ^{13}C NMR ($CDCl_3$) δ 154.9 (C=O), 152.3 (C=O), 141.6 (CCO), 133.2 (CCl), 128.2 (2CH), 125.7 (2CH), 80.5 ($COCO_2$), 63.2 (OCH_2), 60.9 (OCH_2), 39.1 ($2CH_2N$), 34.8 ($2CH_2$), 14.3 (CH_3), 13.8 (CH_3).

The crude **50** from a 33.0 mmol scale synthesis of **49** was refluxed in 250 mL of methanol and 250 mL of 5 M potasium hydroxide for 24 h. The methanol was then removed under vacuum and the remaining solution was extracted with diethyl ether. The ethereal solution was then extracted with dilute hydrochloric acid which was then made alkaline with concentrated aqueous sodium hydroxide. The resulting precipitate was extracted into diethyl ether. After drying over anhydrous sodium sulfate the solvent was remove under vacuum and the product recrystalized from methylene chloride/60-80 petroleum ether to yield 3.50 g (57%) of **26**: mp 138-140 °C; lit.[71] 134.4-136 °C; ^{1}H NMR ($CDCl_3$) δ 7.4

(2H, d, CH), 7.3 (2H, d, CH), 3.0 (2H, t, CH_2), 2.9 (2H, d, CH_2), 1.9 (2H, d of t, CH_2), 1.7 (2H, d, CH_2); ^{13}C NMR ($CDCl_3$) δ 147.8 (C), 132.2 (CCl), 128.2 (2CH), 126.1 (2CH), 70.7 (COH), 42.0 ($2CH_2N$), 38.9 ($2CH_2$); mass spectrum m/z calcd. for $C_{11}H_{14}ClNO$: 211.077, found: 211.077.

4-(4-Chlorophenyl-4-piperidol)-4-iodobutyrophenone, **21**

1-(4-Iodophenyl)-1,1-(ethylene dioxy)-4-iodobutane, **54**, (0.60 g, 1.35 mmol), **26** (0.286 g, 1.35 mmol), and potassium carbonate (1.35 g, 8.17 mmol) in 40 mL of tetrahydrofuran were refluxed for 23 h. After cooling, the suspension was filtered through a celite pad which was washed with methylene chloride. The filtrate was then extracted with water and dried over anhydrous sodium sulfate. The solvent was removed under vacuum and the remaining oil was dissolved in 6 mL of methanol and 6 mL of 1 M hydrochloric acid (6.0 mmol) and was refluxed for 1 h. After cooling, the methanol was removed under vacuum and the precipitate was filtered and recrystalized from chloroform/methanol to yield 0.49 g (69%) of the hydrochloride salt of **21**: mp 270-274°C; ^1H NMR (d_4-acetic acid) δ 7.8 (2H, d, CH), 7.6 (2H, d, CH), 7.4 (2H, d, CH), 7.2 (2H, d, CH), 3.6 (2H, d, CH_2), 3.4-3.0 (6H, m, CH_2), 2.4 (2H, t, CH_2), 2.1 (2H, b, CH_2), 1.9 (2H, d, CH_2); ^{13}C NMR (d_4-acetic acid) δ 199.2 (C=O), 145.9 (CCOH), 138.7 (2CH), 136.5 (CC=O), 133.7 (CCl), 130 (2CH), 129 (2CH), 101.6 (CI), 69.8 (COH), 57.0 (CH_2N), 49.5 ($2CH_2N$),

35.8 ($2CH_2$), 35.6 ($CH_2C=O$), 18.7 (CH2); mass spectrum m/z calcd. for $C_{21}H_{23}ClINO_2$: 483.041, found: 484.045.

4-Amino-3-iodophenyl cyclopropyl ketone, 43

The iodinium nitrate solution was prepared as previously described.[61] To a stirred solution of 25.0 g (147.2 mmol) of silver nitrate dissolved in 200 mL of chloroform and 50 mL of pyridine was added 37.0 g (147.2 mmol) of iodine. After the iodine had dissolved, the silver iodide was isolated by filtration and washed with a mixture 20 mL of chloroform and 20 mL of pyridine.

4-Aminophenyl cyclopropyl ketone, 42, (15.8 g, 98.1 mmol) was added to the filtrate and the solution was stirred for 3 h at room temperature. To precipitate the pyridinium nitrate, 300 mL of ether was added slowly and the resulting precipitate was filtered and washed with chloroform. The volume of the filtrate was reduced to approximately half and washed with an aqueous sodium thiosufate solution. The solvent was removed under vacuum and the solid product was recrystalized from chloroform/35-60 petroleum ether to yield 9.6 g (34%) of 43: mp 116-118 °C; ^1H NMR ($CDCl_3$) δ 8.3 (1H, d, CH), 7.8 (1H, d of d, CH), 6.7 (1H, d, CH), 4.6 (2H, b, NH_2), 2.5 (1H, m, CH), 1.1 (2H, m, CH_2), 0.9 (2H, m, CH_2); ^{13}C NMR ($CDCl_3$) 197.4 (C=O), 150.7 (CNH_2), 139.9 (CH), 129.8 (CH), 129.7 (<u>C</u>C=O), 113.2 (CH), 82.6 (CI), 16.3 (CH), 11.2 ($2CH_2$); mass spectrum m/z calcd. for $C_{10}H_{10}INO$: 286.976, found: 286.980.

4-Fluoro-3-iodophenyl cyclopropyl ketone, 44

Sodium nitrite (3.8 g, 55.1 mmol) dissolved in a minimum of water was added dropwise to 43, (8.0 g, 27.9 mmol) suspended in 100 mL of 40% tetrafluoroboric acid and cooled in an ice bath. After 15 min, the diazonium salt which precipitated was filtered, washed with water and dryed under vacuum. The decomposition of the diazonium salt was initiated by waving a flame across the bottom of the flask. Once the evolution of nitrogen was observed, heating was stopped. When the reaction stopped, heating was resumed to ensure completion. This product was then dissolved in chloroform and washed with dilute sodium hydroxide and water. After drying over anhydrous sodium sulfate, the solvent was removed under vacuum leaving a yellow oil. Purification by vacuum distillation gave 2.33 g (29%) of 44: bp 115 °C at .25 mm Hg; ^{1}H NMR ($CDCl_3$) δ 8.4 (1H, d of d, CH), 7.9 (1H, d of d of d, CH), 7.1 (1H, d of d, CH), 2.5 (1H, m, CH), 1.2 (2H, m, CH_2), 1.0 (2H, m, CH_2); ^{13}C NMR ($CDCl_3$) δ 196.8 (C=O), 164.3 (CF, J_F=252.8 Hz), 139.7 (CH, J_F=2.7 Hz), 135.7 (CC=O, J_F=3.3 Hz), 130.2 (CH, J_F=8.6 Hz), 115.5 (CH, J_F=24.5 Hz), 81.7 (CI, J_F=26.3 Hz), 17.1 (CH), 12.0 ($2CH_2$); mass spectrum m/z calcd. for $C_{10}H_8FIO$: 289.956, found: 289.961.

4'-Fluoro-3'-iodo-4-iodobutyrophenone, 30

The procedure described for the conversion of 45 to 31

was repeated using 650 mg (2.24 mmol) of **44**, and 570 mg (2.8 mmol) trimethylsilyl iodide. Distillation of the product in a Kugelrohr apparatus yielded 650 mg (65%) of **30**: bp 170°C (oven temperature) at 0.2 mm Hg; ^{1}H NMR ($CDCl_3$) δ 8.3 (1H, d of d, CH), 7.9 (1H, d of d of d, CH), 7.1 (1H, d of d, CH), 3.3 (2H, t, CH_2I), 3.0 (2H, t, $CH_2C=O$), 2.2 (2H, quint, CH_2); ^{13}C ($CDCl_3$) δ 195.0 (C=O), 164.6 (CF, J_F=253.8 Hz), 139.9 (CH, J_F=3.0 Hz), 134.6 (CC=O, J_F=3.3 Hz), 130.3 (CH, J_F=8.7 Hz) 116.0 (CH, J_F=24.5 Hz), 81.8 (CI, J_F=26.9 Hz), 38.9 ($CH_2C=O$), 27.3 (CH_2), 6.5 (CH_2I); mass spectrum m/z calcd. for $C_{10}H_9FI_2O$: 417.864, found: 417.872.

1-(4-Fluoro-3-iodophenyl)-1,1-(ethylene dioxy)-4-iodobutane, **55**

The procedure described for the conversion of **31** to **54** was repeated using 2.3 (5.5 mmol) g of **30**, and 1.02 g (16.5 mmol) of ethylene glycol. This yielded 1.96 g (77%) of **55**: ^{1}H NMR ($CDCl_3$) δ 7.8 (1H, d of d, CH), 7.4 (1H, d of d of d, CH), 7.0 (1H, d of d, CH), 4.0 (2H, m, OCH_2), 3.7 (2H, m, OCH_2), 3.2 (2H, t, CH2I), 1.9 (4H, m, $2CH_2$); ^{13}C NMR ($CDCl_3$) δ 161.3 (CF, J_F=245.8 Hz), 140.3 (C-CO_2, J_F=3.5 Hz), 136.5 (CH, J_F=1.7 Hz), 127.5 (CH, J_F=7.5 Hz), 115.2 (CH, J_F=24.1), 108.5 (CO_2), 81.0 (CI, J_F=25.8 Hz), 64.6 (CH_2O), 41.1 (CH_2), 27.6 (CH_2), 6.7 (CH_2I).

4-(4-Chlorophenyl-4-piperidol)-4'-fluoro-3'-

iodobutyrophenone, **22**

The procedure described for the coupling of **54** and **26** to give **58**, followed by its hydrolysis to give **21** was repeated with 380 mg (0.82 mmol) of **55** and 173 mg (0.82 mmol) of **26**. The product from acid hydrolysis, in this case, was made alkaline and the free amine was isolated. Recrystalization from chloroform/60-80 petroleum ether yielded 205 mg (50%) of **22**: mp 144-116 °C; ^{1}H NMR ($CDCl^{3}$) δ 8.4 (1H, d of d, CH), 7.9 (1H, d of d of d, CH), 7.34 (2H, d, CH), 7.29 (2H, d, CH), 7.1 (1H, d of d, CH), 2.9 (2H, t, $CH_2C=O$), 2.7 (2H, m, CH_2N), 2.4 (4H, m, CH_2N), 1.9 (5H, m, CH_2, OH), 1.6 (2H, m, CH_2); ^{13}C NMR ($CDCl_3$) δ 198.3 (C=O), 164.3 (CF, J_F=253.3 Hz), 146.9 (C), 139.8 (CH, J_F=3.9 Hz), 135.2 (C, J_F=3.2 Hz), 132.6 (CCl), 130.2 (CH, J_F=8.4 Hz), 128.3 (2CH), 126.0 (2CH), 115.7 (CH, J_F=24.5 Hz), 81.6 (CI, J_F=26.4), 70.9 (COH), 57.6 (CH_2N), 49.2 ($2CH_2N$), 38.2 ($2CH_2$), 36.2 ($CH_2C=O$), 21.9 (CH_2); mass spectrum m/z calcd. for $C_{21}H_{2}NO_2IFCl$: 501.032, found: 501.034.

1-(4-Fluorophenyl)-1,1-(ethylene dioxy)-4-chlorobutane, **56**

The procedure described for the conversion of **31** to **54** was repeated using 10.0 g (57.1 mmol) of 4'-fluoro-4-chlorobutyrophenone, **25** and 10.6 g (171.0 mmol) of ethylene glycol. This procedure yielded 10.1g (81%) of **56**: ^{1}H NMR ($CDCl_3$) δ 7.4 (2H, d of d, CH), 6.9 (2H, t, CH), 3.9 (2H, m, OCH_2), 3.7 (2H, m, OCH_2), 3.5 (2H, t, CH_2Cl), 2.0 (2H, m,

CH_2CO2) 1.8(2H, m CH_2); ^{13}C NMR ($CDCl_3$) δ 162.4 (CF, J_F=246.8 Hz), 138.2 (C, J_F=3.1 Hz), 127.4 (2CH, J_F=8.2 Hz), 114.9 (2CH, J_F=21.4 Hz), 109.6 (CO_2), 64.5 ($2CH_2O$), 44.9 (CH_2Cl), 37.3 (CH_2CO_2), 26.9 (CH_2).

N-Benzyl-4-(4-iodophenyl)-4-piperidol, **52**

Following a procedure similar to that for the synthesis of **49**, 20.0 g (60.6 mmol) of 1,4-diiodobenzene in 800 mL of anhydrous ether was cooled in a dry ice/chloroform bath (-65°C) under argon. To it was added dropwise 28.0 mL of a 2.6 M solution of n-butyl lithium in hexanes. After 1 h 10.3 g (54.5 mmol) of N-benzyl piperidone was added and the mixture was allowed to warm room temperature and refluxed for 1 h. The work-up described for the synthesis of **49** was repeated. The solid product was recrystalized from methylene chloride and ether to yield 12.1 g (51%) of **52**: mp 118-122 °C ; ^1H NMR ($CDCl_3$) δ 7.5 (2H, d, CH), 7.2 (5H, m, CH), 7.1 (2H, d CH), 3.4 (2H, s, CH_2Ph), 2.6 (2H, d, CH_2), 2.3 (2H, t, CH_2), 2.0 (3H, m, CH_2, OH), 1.5 (2H, d, CH_2); ^{13}C ($CDCl_3$) δ 148.2 ($\underline{C}COH$), 138.2 ($\underline{C}CH_2N$), 137.3 (2CH), 129.2 (2CH), 128.2 (2CH), 127.0 (CH), 126.7 (2CH), 92.4 (CI), 71.0 (C-OH), 63.1 ($\underline{C}H_2Ph$), 49.2 (CH_2N), 38.3 (CH_2); mass spectrum m/z calcd. for $C_{18}H_{20}INO$: 393.054, found: 393.059.

4-(4-Iodophenyl)-4-piperidol, **32**

The procedure described for the debenzylation of **49** to

give **50** followed by its hydrolysis to **26** was repeated with 8.4 g (21.4 mmol) of **52**, 19 mL (198.0 mmol) of ethyl chloroformate and 5.0 g of "proton sponge" (23.9 mmol). The hydrolysed product was recrystalized from methanol/ chloroform to gave 5.2 g (80%) of **32**: ^{1}H NMR (CD_3OD) δ 7.6 (2H, d, CH), 7.2 (2H, d, CH), 4.8 (2H, s, OH, NH) 3.0 (2H, d of t, CH_2), 2.8 (2H, m, CH_2), 1.8 (2H, d of t, CH_2), 1.6 (2H, m, CH_2); ^{13}C NMR ($CDCl_3$) δ 149.6 (CC-OH), 137.8 (2CH), 127.4 (2CH), 92.5 (CI), 71.4 (C-OH), 42.2 (CH_2), 38.8 (CH_2); mass spectrum m/z calcd. for $C_{11}H_{14}INO$: 303.007, found : 303.011.

4-(4-Iodophenyl-4-piperidol)-4'-fluorobutyrophenone, **17**

1-(4-Fluorophenyl)-1,1-(ethylenedioxy)-4-chlorobutane, **56**, (3.96 g, 13.2 mmol), 4.0 g (1.35 mmol) of 4-(4-iodophenyl)-4-piperidol, **32**, and 16.0 g (179.8 mmol) of potassium carbonate, 1.0 g potassium iodide (6.7 mmol) in 300 mL of dimethyl formamide were refluxed for 18 h. After cooling the suspension was filtered through a celite pad which was washed with methylene chloride. The filtrate was extracted with water and then dried over anhydrous sodium sulfate before removing the solvent under vacuum. The oily product was isolated as the hydrochloride salt to give 3.78 g (55%) yield of **57**: mp 165-168 °C; ^{1}H NMR (CD_3OD) 7.1 (2H, d, 2CH), 6.8 (2H,, d of d, 2CH), 6.7 (2H, d, 2CH), 6.4 (2H, d of d, 2 CH), 3.4 (2H, m, CH_2), 3.2 (2H, m, CH_2), 2.7 (4H, m, $2CH_2$), 2.5 (2H, m, CH_2), 2.0 (2H, m, CH_2), 1.4 (4H, m,

$2CH_2$).

The ketal, **57**, was hydrolysed with 40.0 mL of 0.8 M hydrochloric acid (0.32 mmol) as described above. The hydrochloride salt of the product was recrystalized from diethyl ether and methanol to yield 2.02 g (36%) of the hydrochloride salt of **17**: mp 228-234°C; ^{1}H NMR (CD_3OD) δ 8.0 (2H, d of d, CH), 7.7 (2H, d, CH), 7.2 (2H, d, CH), 7.1 (2H, t, CH), 4.8 (1H, s, OH), 3.3-3.0 (8H, m, CH_2), 2.3 (2H, d of t, CH_2), 2.1 (2H, m, CH_2), 1.9 (2H, d, CH_2); ^{13}C NMR (CD_3OD) δ 198.8 (C=O), 165.3 (CF, J_F=254.4 Hz) 147.8 (C), 138.3 (2CH), 134.0 (C, J_F=2.9 Hz), 131.7 (2CH, J_F=9.4 Hz), 127.6 (2CH), 116.5 (CH, J_F=22.1 Hz), 93.3 (CI) 69.5 (C-OH), 57.4 (CH_2N), 49.9 ($2CH_2N$), 36.3 ($2CH_2$), 36.3 ($2CH_2$), 19.7 (CH2); mass spectrum m/z calcd. for $C_{21}H_{23}FINO_2$: 467.071, found: 467.083.

4-(4-Trimethylstannylphenyl-4-piperidol)-4'-fluorobutyrophenone, **60**

Hexamethylditin and the trimethylstannyl sodium solution were synthesized as previously described[74]. Ammonia gas was passed through a sodium hydroxide pellet trap to insure dryness and approximately 80 mL was condensed into a solution of 10.0 g of trimethyl tin chloride (50.0 mmol) dissolved in 17 mL hexanes under argon. To this solution was added 1.15 g of freshly cleaned sodium metal (50.0 mmol) in small pieces. The ammonia was then allowed to evaporate

under a stream of argon. The remaining suspension was then filtered under argon and the precipitate was washed with hexanes. Vacuum distillation gave 4.39 g (54%) of hexamethyl ditin: Bp 90-92 °C at 30 mm Hg, lit. 84-84 at 45 mm Hg;[74] ^1H NMR ($CDCl_3$) δ 0.17 (s, J_{HCSn}=46.5 Hz, J_{HCSnSn}=16.0 Hz).

To a solution of 1.0 g hexamethylditin (3.08 mmol) in 6 mL absolute glyme cooled in an ice bath was added 142 mg of sodium metal (6.2 mmol). After 3 h the sodium was gone. To determine the concentration aliquots of the solution were titrated with 1 M hydrochloric acid after first being quenched with excess water and 1-bromopentane. The concentration of sodium trimethyltin was determined to be 0.96 M.

To 6.0 mL of 0.9 M solution of sodium trimethyltin solution cooled in an ice bath was added 300 mg of **17** (0.64 mmol) while being cooled in an ice bath. After 4h the mixture was quenched with 10 mL of water and diluted with 15 mL of chloroform. The organic solution was separated and washed with water. The solvent was stripped and the residue dissolved in acetonitrile. The insoluble solids were filtered and washed with acetonitrile. The filtrate was concentrated and this procedure repeated. Analysis of the filtrate by HPLC (25/74.25/0.75 of $H_2O/CH_3CN/Et_3N$, semipreparative column) gave two major products 4-phenyl-4-piperidol-4'-fluorobutyrophenone, **61** and 4-(4-trimethyltinphenyl-4-piperidol)-4'-fluorobutyrophenone, **60** in 2.4 to 1 ratio by uncorrected UV (HPLC) (λ = 254 nm)

analysis. Purification by semipreparative HPLC analysis yeilded 35 mg (11%) of the trimethyltin derivative **60**: ^{1}H NMR ($CDCl_3$) δ 8.0 (2H, d of d, CH), 7.4 (4H, m, CH), 7.1 (2H, t, CH), 2.9 (2H, t, CH_2), 2.7 (2H, m, CH_2) 2.5 (4H, m, CH_2), 2.0 (4H, m, CH_2), 1.7 (2H, m, CH_2), 0.26 (9H, s, CH_3); ^{13}C NMR ($CDCl_3$) δ 198.4 (C=O), 165.6 (CF, J_F=254.3 Hz) 148.2 (C), 140.8 (CSn), 135.9 (2CH), 133.5 (CC=O, J_F=2.9 Hz), 130.7 (2CH, J_F=9.14 Hz), 124.1 (2CH), 115.5 (CH, J_F=21.8 Hz), 71.0 (C-OH), 57.7 (CH_2N), 49.3 ($2CH_2N$), 38.0 ($2CH_2$), 36.2 (CH_2C=O), 29.7 (CH2), -9.6 ($3CH_3$, J_{Sn}=180.5 Hz).

4-(4-^{131}Iodophenyl-4-piperidol)-4'-fluorobutyrophenone, [^{131}I]-**17**

To a solution of approximately 0.1 mg of **60** ($0.2x10^{-3}$ mmol) and one crystal of N-chlorosuccinamide in 80 µl of acetonitrile was added 1.0 mCi (37 mBq) of sodium [^{131}I]-iodide in 35 µl of water. The mixture was sonicated for 40 min and directly purified by HPLC (40/59.9/0.1 of $H_2O/CH_3CN/Et_3N$, analytical column) to yield 47% radiochemical yield [^{131}I]**17**.

1-(4-Fluorophenyl)-4-chlorobutanol, **33**

To an ice cold, stirred solution of 1.89 g of sodium borohydride (49.8 mmol) in 30 mL absolute ethanol was added 5 g 4-chloro-4'-fluorobutyrophenone (24.9 mmol) in 10 mL of absolute ethanol dropwise. After 20 min the ice bath was

removed and the reaction mixture allowed to warm to room temperature over 80 min. The reaction mixture was poured into approximately 20 g of ice and stirred until bubbling stopped. The product was then extracted into methylene chloride and dried over sodium sulfate. Removal of the solvent left a clear colourless oil, **33**, in a quantitative yield: bp 80-90 °C (oven temp) at 0.15 mm Hg; ^{1}H NMR ($CDCl_3$) δ 7.1 (2H, d of d, CH), 6.9 (2H, d of d, CH), 4.5 (1H, t, CH), 3.7 (1H, s, OH), 3.4 (2H, t, CH_2), 1.65 (4H, m, CH_2); ^{13}C NMR ($CDCl_3$) δ 161.8 (CF, J_F=245.3 Hz), 139.8 (C,J_F=3.1 Hz), 127.3 (CH, J_F=8.1 Hz), 114.9 (CH, J_F=21.2 Hz), 72.7 (CH), 44.6 (CH_2), 35.8 (CH_2), 28.5 (CH_2); mass spectrum m/z calcd. for $C_{10}H_{12}ClO$: 202.056, found: 202.056.

(4'-Fluoro-3'-nitrophenyl)-4-chloro-1-butylnitrate, **34**

To a stirring suspension of 2.0 g of nitronium tetraflouroborate (15 mmol) in 15 mL dry acetonitrile cooled in a dry ice/acetonitrile bath (-33°C) was added dropwise 1.0 g of **33** (5.0 mmol) in 8 mL of acetonitrile dropwise. After 20 min, the reaction was poured into 20 g of ice. The product was extracted into methylene chloride which was dried over anhydrous sodium sulfate. The solvent was removed to leave 1.37 g (94 % crude yield) of a yellow oil, **34**: ^{1}H NMR ($CDCl_3$) δ 8.0 (1H, d of d, CH), 7.5 (1H, m, CH), 7.3 (1H, t, CH) 5.7 (1H, d of d, CH), 3.4 (2H, d of d, CH_2), 1.95 (4H, m, CH_2); ^{13}C NMR ($CDCl_3$) δ 155.5 (CF, J_F=267.7

Hz), 135.0 (C,J_F=4.3 Hz), 133.3 (CH, J_F=8.9 Hz), 128.0 (CNO_2, J_F=8.1 Hz), 124.3 (CH, J_F=2.4) 119.3 (CH, J_F=21.4) 82.5 ($CONO_2$), 43.8 (CH_2Cl), 31.8 (CH_2), 28.2 (CH_2); IR (nujol): 1641 (ONO_2), 1543 (NO_2), 1352 (NO_2), 1279 (ONO_2), 854 (ONO_2).

(4'-Fluoro-3'-nitrophenyl)-4-chloro-1-butanol-O-acetate, 36

Synthesis of 33 run at room temperature produced the methylester 36: ^1H NMR ($CDCl_3$) δ 8.0 (1H, d of d, CH), 7.7 (1H, m, CH), 7.3 (1H, d of d, CH) 4.9 (1H, m, CH), 3.5 (2H, t, CH_2), 1.9 (3H, s, CH_3) 1.8 (4H, m, CH_2); ^{13}C NMR ($CDCl_3$) δ 169.9 (C=O) 155.5 (CF, J_F=261.0 Hz), 142.2 (C, J_F=4.1 Hz), 139.0 (CNO_2, J_F=8.1 Hz), 135.0 (CH, J_F=8.6 Hz), 124.6 (CH, J_F=2.6) 118.9 (CH, J_F=20.6) 52.5 (COC=O), 45.3 (CH_2Cl), 34.1 (CH_2), 29.8 (CH_2), 22.8 (CH_3): mass spectrum m/z cal'd $C_{12}H_{14}ClFN_2O_3$: 288.068, found: 288.072.

4'-Amino-4-hydroxybutyrophenone, 41

To a solution of 300 mL of methanol and 300 mL of 1.0 M hydrochloric acid was added 8.0 g of 40 (33.4 mmol). The solution was refluxed for 1 h at which time it was made alkaline and extracted into ether. Recrystalization from methylene chloride yield 4.0 g (66%) of 41: mp 112-114 °C; ^1H NMR (d_6-acetone) δ 7.7 (2H, d, CH), 6.7 (2H, d, CH), 5.4 (2H, b, NH_2), 3.6 (2H, t, CH_2OH), 2.9 (2H, t, CH_2C=O), 1.8 (2H, quint, CH_2) and (3H, s, CH_3); ^{13}C NMR (d_6-acetone) δ

200.4 (C=O), 156.4 (CNH_2), 133.5 (2CH), 116.2 (2CH), 64.4 (CH_2OH), 36.? ($CH_2C=O$), 31.0 (CH_2).

4-(4-Chlorophenyl) 1,2,3,5,-tetrahydropryidine, **51**

To a solution of **50** (200 mg, 0.56 mmol) in 1.0 mL of dry chloroform (0.1 % H_2O by Karl Fischer titration) stirred under argon was added 0.30 mL of trimethylsilyl iodide (1.1 mmol) while being stirred under argon. After refluxing for 2 h, methanol (0.2 mL) to which hydrochloric acid had been bubbled through was added. The volatile compounds were removed and the solid was recrystallized from methanol and ether to yield 88 mg (69%) of the hydrochloric salt of **51**: mp 188-190 °C; ^1H NMR (CD_3OD) δ 7.4 (2H, d, CH), 7.3 (2H, d, CH), 6.1 (1H, m, CH) 4.8 (1H, b, NH) 3.9 (2H, m, CH_2N), 3.5 (2H, m, CH_2N), 2.8 (2H, m, CH_2), ^{13}C NMR ($CDCl_3$) δ 138.9 (C, vinyl), 135.7 (C), 134.8 (CCl), 129.0(2CH) 127.7 (2CH), 117.7 (CH, vinyl), 43.4 (CH_2) 42.2 (CH_2), 24.7 (CH_2); mass spectrum m/z calcd. for $C_{11}H_{12}ClN$: 193.065, found : 193.065.

4-(4-Chlorophenyl-4-piperidol)-4'-fluorobutyrophenone, **2**

The procedure described for the synthesis of **17** was repeated using 500 mg of **26** (2.4 mmol) and 587 mg of **56** (2.4 mmol). After formation of the adduct the product was immediately hydrolysed and the free amine of **2** was recrystalized from ethyl acetate to yield 488 mg (54%) of **2**: mp 142-144 °C,lit 146-148 °C[74]; ^1H NMR ($CDCl_3$) δ 8.0 (2H, d

of d, CH), 7.37 (2H, d, CH), 7.28 (2H, d, CH), 7.1 (2H, t, CH), 3.4 (1H, s, OH), 2.9 (2H, t, CH_2), 2.8 (2H, m, CH_2), 2.4 (4H, m, CH_2), 1.9 (4H, m, CH_2); ^{13}C NMR ($CDCl_3$) δ 198.4 (C=O), 165.4 (CF, J_F=254.5 Hz) 146.9 (C), 133.6 (C, J_F=3.0), 132.7 (CCl), 130.6 (2CH J_F=6.7), 128.3 (2CH), 126.1 (2CH) 115.5 (2CH, J_F=21.9) 71.0 (C-OH), 57.8 (CH_2N), 49.3 ($2CH_2N$), 38.3 ($2CH_2$), 36.2 ($2CH_2$), 21.8 (CH2).

5.2) Biology

5.2.1) *In Vitro* Binding Assay

The dopamine (D-2) receptor binding affinity of Iodohaloperidol derivatives **17**, **21** and **22** was assessed by an *in vitro* competition with [^3H]-spiperone using receptors from pig anterior pituitary. This previously reported assay was performed in the laboratory of P. Seeman at the Department of Pharmacology, University of Toronto.[86]

5.2.2)*In Vivo* Biodistribution

The biodistribution of **17** was determined in female Sprague-Dawley rats after tail injection. The [^{131}I]-**17** was dissolved in saline with 2.5% ethanol and 0.00035% Tween 80. The amount of[^{131}I]-**17** in the injection syringe was counted pre and post injection with a counter usually used as a thyroid probe. Residual radioactivity in the tails was subtracted from the total injected dose. Animals (three per time point) were sacrificed at selected times by suffocation

with carbon dioxide followed by cervical dislocation. Blood samples were obtained by cardiac exsanguination. Organ samples were obtained, washed free of blood, patted dry, weighed and counted for activity. The brain was removed for the cranium, the cerebellum and striatum were dissected away. The remaining brain tissue was counted together. The activity was counted in an automated γ-ray well counter. The activity was corrected for decay and difference in efficiency and geometry between the well counter and the thyroid probe by using a standard. The percent of the injected dose was calculated for each tissue sample are expressed in percent of injected dose/gram tissue (%ID/g). Also given is the standard deviation for each value. The uptake in the striatum to cerebellum was reported as representative of selective and nonselective uptake respectively.

References

1. Kebabian, J.W.; Calne, D.B. *Nature* **1979**, *277* 93.

2. Seeman, P. In *Receptor Biochemistry and Methodology, Dopamine Receptors*; Creese, I.; Fraser, C.M., Eds.; Alan R. Liss, Inc.: New York, 1987; pp. 234.

3. Green, A.R. and Costain, D.W. *Pharmacology and Biochemistry of Psychiatric Disorder*; John Wiley & Sons Ltd.; Chichester, 1981; p. 18.

4. Creese, I.; Stewart, K.; Snyder, S.H. *Eur. J. Pharm.* **1979**, *60*, 55.

5. Nogrady, T. In *Medicinal Chemistry*; Oxford University Press: New York, 1985; pp 168.

6. *ibid*, pp. 169-171.

7. Janssen, P.A.J.; Van Bever, W.F. In *Handbook of Psychopharmacology* Iversen, L.L.; Iversen, S.D.; Snyder, S.H., Eds.;Plenum Press: New York, 1978; pp. 1-31.

8. Angrist, B.M. In *The Benzamides Pharmacology, Neurobiology and Clinical Aspects*; Stanley, M.; Rotrosen, J., Ed.; Raven Press: New York, 1982; pp 1-6.

9. Seeman, P. *Pharmacological Reviews* **1981**, *32*, 232-233.

10. Seeman, P.; Lee, T.; Chau-Wong, M.; Wong, K. *Nature* **1976**, *261*, 717.

11. Seeman, P. In *Receptor Biochemistry and Methodology, Dopamine Receptors*; Creese, I.; Fraser, C.M., Eds.; Alan R. Liss, Inc.: New York, 1987; pp 236-242.

12. Eckelman, W.C.; Reba, R.C.; Gibson, R.E.; et al. *J. Nucl. Med.* **1979**, *20*, 350.

13. Green, A.R. and Costain, D.W. *Pharmacology and Biochemistry of Psychiatric Disorder*; John Wiley & Sons Ltd.; Chichester, 1981; pp 144-154.

14. Seeman, P. In *Receptor Biochemistry and Methodology, Dopamine Receptors*; Creese, I.; Fraser, C.M., Eds.; Alan R. Liss, Inc.: New York, 1987; p 237.

15. Green, A.R. and Costain, D.W. *Pharmacology and Biochemistry of Psychiatric Disorder*; John Wiley & Sons Ltd.; Chichester, 1981; pp. 104-105.

16. Seeman, P. *Pharmacological Reviews* **1981**, *32*, p. 233.

17. Seeman, P. In *Receptor Biochemistry and Methodology, Dopamine Receptors*; Creese, I.; Fraser, C.M., Eds.; Alan R. Liss, Inc.: New York, 1987; p. 239.

18. Seeman, P. *Pharmacological Reviews* **1981**, *32*, p 279.

19. Green, A.R. and Costain, D.W. *Pharmacology and Biochemistry of Psychiatric Disorder*; John Wiley & Sons Ltd.; Chichester, 1981; pp. 125-126.

20. Seeman, P. In *Receptor Biochemistry and Methodology, Dopamine Receptors*; Creese, I.; Fraser, C.M., Eds.; Alan R. Liss, Inc.: New York, 1987; p. 241.

21. Green, A.R. and Costain, D.W. *Pharmacology and Biochemistry of Psychiatric Disorder*; John Wiley & Sons Ltd.; Chichester, 1981; pp. 139-143.

22. Seeman, P. In *Receptor Biochemistry and Methodology, Dopamine Receptors*; Creese, I.; Fraser, C.M., Eds.; Alan R. Liss, Inc.: New York, 1987; p. 236.

23. *ibid*, pp. 234-236.

24. Shiue, C.-Y.; Fowler, J.S.; Wolf, A.P.; Walanabe, M.; Arnett, C.D. *J. Nucl. Med.* **1985**, *26*, 181.

25. Arnett, C.D.; Shiue, C.-Y.; Wolf, A.P.; Fowler, J.S.; Logan, J.; Walanabe, M. *J. Neurochem.* **1985**, *44*, 835.

26. Moerlein, S.M.; Laufer, P.; Stocklin, G.; Pawlik, G.; Weiher, K.; Hiess, W.-D. *Eur. J. Nucl. Med.* **1986**. *12*, 211.

27. Welch, M.J.; Katzenellenbogen, J.A.; Mathias, J.W.; Bradlock, J.W.; Carlson, K.E.; Chi, D.Y.; Dence, C.S.; Kilbourn, M.R.; Perlmutter, J.S.; Raichle, M.E.; Ter Pogoss, M.M. *Nucl. Med. Biol.* **1988**, *15*, 83.

28. Coenen, H.H.; Wienhard, K.; Stocklin, G.; Laufer, P.; Hebold, I; Dawlik, G.; Heiss, W.D. *Eur. J. Nucl. Med.* **1988**, *14*, 80.

29. Coenen, H.H.; Laufer, P.; Stocklin, G. *Life Sciences* **1987**, *40*, 81. Shiue, C.-Y.; Bai, L.-Q.; Teng, R.-R. *J. Nucl. Med.* **1987**, *28*, 1164.

30. Burns, H.D.; Dannals, R.F.; Langstrom, B.; Ravert, H.T.; Zemyanse, S.E.; Deilfer, T.; Wong, D.F.; Frost, J.J.; Keihar, M.J.; Wagner, H.N *J. Nucl. Med.* **1984**, *25*, 1222.

31. Hartvig, P.; Eckernas, S.A.; Ekblom, B.; Lindstrom, L.; Lungvist, H.; Axelsson, S.; Faslh, K.J. Gullberg, P.; Langstrom, B. *Acta Neurol. Scand.* **1988**, *77*, 314.

32. Nakatsuka, I.; Saji, H.; Shiba, K.; Shimizu, H.; Okuno, M.; Yoshitake. A.; Torizuka, K.; Yokoyama, A. *Life Sciences* **1987**, *41*, 1989.

33. Saja, H.; Nakatsuka, I.; Shiba, K.; Tokui, T.; Horiuchi, K.; Yoshitake, A.; Torizuka, K.; Yokoyama, A. *Life Sciences* **1987**, *41*, 1999.

34. Gundlach, A.L.; Largent, B.L.; Snyder, S.H. *Life Sciences* **1984**, *35*, 1981.

35. Kilpatrick, G.J.; Jenner, P.; Marsden, C.D. *J. Pharm. Pharmacol.* **1986**, *38*, 406.

36. Moerlein, S.M.; Mathis, C.A.; Brennan, K.M.; Budinger, T.F. *Nucl. Med. Biol.* **1987**, *14*, 91.

37. Wong, D.F.; Gjedde, A.; Wagner, H.N.; Dannals, R.F.; Douglass, K.H.; Links, J.M.; Kuhar, M.J. *J. Cereb. Blood Flow Metab.* **1986**, *6*, 147.

38. Muhr, C.; Bergstrom, M.; Lundberg, P.O.; Bergstrom, K.; Hartzig, P.; Lundquist, H.; Antoni, G.; Langstom, B. *J. Comput. Assist. Tomogr.* **1986**, *10*, 175. Hagglund, J.; Aquilonius, S.-M.; Eckernas, S.-A.; Hartzig, P.; Lundquist, H.;Gullberg, P.; Langstom, B. *Acta Neurol. Scand.* **1987**, *75* 87. Smith, M.; Wolf, A.P.; Brodie, J.D.; Arnett, C.D.; Barouche, F.; Shiue, G.-Y.; Fowler, J.S.; Russell, J.A.G., MacGregor, R.R.; Wolken, A.; Angrist, B.; Rotrosen, J. Peselow, E. *Biol. Psychiatry* **1988**, *23*, 653.

39. Perlmutter, J.S.; Kilbourn, M.R.; Welch, M.J.; Raichle, M.E. *J. Neurosci.* **1989**, *9*, 2344. Volkow, N.D.; Wolf, A.P.; et al. *J. Nucl. Med.* **1989**, *30*, 730.

40. Oldland, S.R.D.; Veall, N. *Appl. Rad. Isot.* **1986**, *37*, 715.

41. Hall, H.; Kohler, C.; Gawell, L.; Farde, L.; Sedvall, G. *Prog. Neuro-Psychopharmacol. & Biol. Psychiat.* **1988**, *12*, 559.

42. Ehrin, E.; Farde, L.; de Paulis, T.; Erifson, L.; Greitz, T.; Johnshon P.; Litton, J.-E.; Nesson, J.L.G.; Sedval, G.; Stone-Elander, S.; Ogren, S.-O. *Int. J. Appl. Radiat. Isot.* **1985**, *36*, 269.

43. de Paulis, T.; Janowsky, A.; Kessler, R.M.; Clanton, J.A.; Smith, H.E. *J. Med. Chem.* **1988**, *31*, 2027.

44. Kung, H.F.; Kasliwal, R.; Pan, S.; Kung M.-P. Mach, R.H.; Guo, Y.Z. *J. Med. Chem.* **1988**, *31*, 1039.

45. Kung, H.F.; Guo, Y.-Z.; Billings, J.; Mach R.H.; Blau, M.; Ackerhalt, R.E. *Nucl. Med. Bio.* **1988**, *15*, 195.

46. Farde, L.; Wiesel, F.-A.; Janssan, P.; Uppfeldt, G.; Wahlen, A.; Sedvall, G. *Psychopharm.* **1988**, *94*, 1. Farde, L.; Wiesel, F.-A.; Halldin, C.; Sedvall, G. *Arch. Gen. Psychiat.* **1988**, *45*, 71.

47. Alavi, M.G.; Velchik, H.F.; Kung, H.F.; Kung, M.P.; Chang, W.; Noto, R.; Pan, S.; Billings, J.; Sorentoni, K.; Rauch, A. Reilley, J. *J. Nucl. Med.* **1989**, *30*, 731. Wong, D.F.; Young, L.T.; Pearlson,G.; Singer, H.; Tune, L.; Ross, C.; Dannals, R.F.; Wilson, A.A.; Ravert, H.T.; Links, J.; Wagner Jr., H.N. Gjedde, A. *ibid.*

48. Seeman, P. *Pharmacological Reviews* **1981**, *32*, p. 244.

49. Seeman, P. In *Receptor Biochemistry and Methodology, Dopamine Receptors*; Creese, I.; Fraser, C.M., Eds.; Alan R. Liss, Inc.: New York, 1987; p. 236.

50. Wong, D.F.; Wagner, H.N.; Tune, L.E.; Dannals, R.F.; Pearleson, G.D.; Links, J.M.; Tanninga, C.A.; Broussolle, E.P.; Ravert, H.T.; Wilson, A.A.; Toung, J.K.T.; Malat, J.; Williams, J.A.; O'Tuama, L.C.; Snyder, S.H.; Kuhar, M.J.; Gjedde, A. *Science* 1986, *234*, **1558**.

51. Janssen, P.A.J.; Van Bever, W.F. In *Handbook of Psychopharmacology* Iversen, L.L.; Iversen, S.D.; Snyder, S.H., Eds.;Plenum Press: New York, 1978; pp. 2-3.

52. Janssen, P.A.J.; Van de Westeringh, C.; Jageneau, A.H.M., *J. Med. Pharm. Chem.* **1959**, *1*, 281.

53. Hodgson, H.H. *Chem. Rev.* **1947**, *40*, 251.

54. Hunter, D.H.; Strickland, L.A. *Appl. Radiat. Isot.* **1986**, *37*, 889.

55. Kabalka, W.G.; Varma, R.S. *Tetrahedron* **1989**, *45*, 6601.

56. Brewster, R.Q.; Williams, B.; Phillips, R. *Org. Syn. Coll.* **1955**, *III*, 337.

57. Olah, A.G.; Narang, S.C.; Olah, J.A.; Lammerstsma, K. *Proc. Natl. Acad. Sci. USA* **1982**, *79* 4491.

58. Zillberman, E.N. *Russ. Chem. Rev.* **1962** *31*, 615.

59. Baker, J.W.; Easty, D.M., *J. Chem. Soc.* **1952**, 1193. Baker, J.W.; Easty, D.M., *ibid.* 1208. Baker, J. W.; Neale, A.J., *ibid.* **1954**, 3225. Baker, J.W.; Heggs, T.G., *ibid.* **1955**, 516. Baker, J.W.; Heggs, T.G., *ibid.* 616.

60. Honeyman, J.; Morgan, J.W.W. In *Advances in Carbohydrate Chemistry*; Wolfrom, M.L. Eds.; Academic Press Inc.: New York, 1957; pp 125-127.

61. Lown, J.W.; Joshua, A. V. *Can. J. Chem.* **1977**, *55*, 122.

62. Rutherford, K.G.; Redmond, W.; Rigamonti, J. *J. Org. Chem.* **1961**, *26*, 5149

63. Miller, R.D.; McKean, D.R. *J. Org. Chem.* **1981**, *46*, 2421.

64. Schmidle, C.J.; Mansfield, R.C. *J. Am. Chem. Soc.* **1956**, *78* 425.

65. Strickland, L.A.; Ponce, Y. Z.; Hunter, D.H.; Zabel, P.; Powe, J.; Morressey, G.; Dreidger, A.A.; Chamberlain, M.J. *Drug Design and Delivery* accepted March 16, **1990** .

66. Vincent, S.H.; Shambhu, M.B.; Digenis, G.A. *J. Med. Chem.* **1980**, *23*, 75.

67.Djuric, S.; Venit, J.; Magnus, P. *Tet. Lett.* **1981**, *22*, 1787.

68. Hudlicky, M., *Reductions in Organic Chemistry*; Halstead Press:New York, 1984, p 93.

69. *ibid*, p. 67.

70. Kapnang, H.; Charles, G. *Tet. Lett.* **1983**, *24*, 3233.

71. Weast, R.C.; Grasselli, J.G. *Handbook of Data on Organic Compounds 2nd Edition*; CRC Press Inc.: Boca Raton, Florida, 1985. HODOC No. 20282.

72. Jung, M.E.; Lyster, M.A., *J. Chem. Soc. Chem. Comm.* **1978**, 315.

73. Wakefield, B.J. *The Chemistry of Organolithium Compounds*; Regamon Press: Oxford, 1974; p 51.

74. Moerlein, S.M.; Stocklin, G. *J. Med. Chem.* **1985**, *28*, 1319.

75. Moerlein, S.M.; Coenen, H.H. *J. Chem. Soc. Perkins Trans. I* **1985**, 1941.

76. de Paulis, T.; Janowsky, A.; Kessler, R.M.; et al. *J. Med. Chem.* **1988**, *31*, 2027.

77. Wursthorn, K.R.; Kuivila, H.G., *J. Organomet. Chem.* **1977**, *140*, 29.

78. Coulson, D.R. *Inorg. Syn.* **1972**, *13*, 121.

79. Man, B.E.; Musco, A. *J. Chem. Soc.* **1975** 1673.

80. Azizian, H.;Eaborn, C.; Pidcock, A., *J. Organomet. Chem.* **1981**, *215*, 49.

81. Wursthorn, K.R.; Kuivila, H.G.; Smith, G.F., *J. Am. Chem. Soc.* **1978**, *100*, 2779.

82. Koenig, T., *J. Am. Chem. Soc.* **1969**, *91*, 2558.

83. Seeman, P.; Watanabe, M.; Grigoriadis, D.; et al, *Mol. Pharmacol.* **1985**, *28*, 391.

84. Seeman, P. In *Receptor Biochemistry and Methodology, Dopamine Receptors*; Creese, I.; Fraser, C.M., Eds.; Alan R. Liss, Inc.: New York, 1987; p 2.

85. Glowinski, T.L.; Iverson, L.L. *J. Neurochem.* **1966**, *13*, 655.

86. List, S.J.; Seeman, P. *Proc. Natl. Acad. Sci. USA* **1981**,*78*, 2620.

87. Lewi, P.J.; Heykants, J.J.P.; Allewijn, F.T.N. *Arzneim.-Forsch.* **1970**, *20*, 943.

88. Chaturved, A.K.; Rao, N.G.S.; Rama Sastry, B.V. *Toxicol. Appl. Pharmacol.* **1980**, *54*,265.

89. Hansch, Corwin In *Residential School of Medicinal Chemistry* Drew University, 1986.

90. Leo, A.; Hansch, C.; Elkins, D., *Chem. Rev.* **1971**, *71*, 525.

91. Minick, D.J.; Frenz, J.H.; Patrick, M.A.; Brent, D.A., *J. Med. Chem.* **1988**, *31*, 1923.

92. Hansch, C.; Leo, A. *Substituents Constants for Correlation Analysis in Chemistry and Biology*; Wiley-Interscience; New York, 1979.

93. The values were calculated on ClogP/3.6, personal communication C. Hansch.

Chapter 6: Introduction to the Estrogen Receptor Imaging Agent Project

The following three chapters describe our work towards an estrogen receptor imaging agent. The purpose of imaging estrogen receptors will be brought out in detail in the following sections of this chapter. However, in short, due to the high concentration of estrogen receptors in some carcinomas, one could potentially locate tumors by imaging the radiopharmaceutical bound to estrogen receptors.

In the first three sections of this chapter, I will give the biological background for the project. The first section is a brief discussion of estrogens and estrogen receptors. In the second section, I have described the relationship between estrogen receptors and cancer. This is followed by a brief description of antiestrogens and their relationship to estrogen receptors and of the therapeutic role of antiestrogens in the treatment of hormone dependent cancers. Section 2 of this chapter is an outline of desired characteristics of estrogen receptor imaging agents and our strategy for developing an antiestrogen imaging agent. The last section of this chapter describes the synthesis of E and Z amino-tamoxifens, **1** as precursors for the synthesis of both radioactive and nonradioactive E and Z Iodotamoxifens, **2**.

6.1) Biological Background

6.1.1) Estrogens and Estrogen Receptors

The estrogens are steroid hormones produced mainly in the ovaries. Hormones are chemical messengers which are secreted from endocrine glands and travel through the bloodstream to target tissues. This form of communication is responsible for the regulation and integration of many of the functions carried out in the body. In the case of estrogens, the endocrine organ is the ovaries and the result of the interaction of estrogen with the target tissues is the control of the female reproductive tract and development of female secondary sex characteristics. Estradiol, 3, whose structure is given in Figure 6.1 is the most important estrogen.

Estrogens elicit a response from the target tissue very quickly and at very low concentrations[1]. This led to the belief that there must be a mechanism for concentrating the hormone in the target tissue. It was not until 1960, after high specific activity [^{3}H]-estradiol was synthesized, that the selective uptake and retention of this steroid in target tissue was actually observed.[2] The concept of an estrogen receptor was then proposed as the mechanism for concentrating the hormone.

Later, the intercellular location of these receptors was investigated. The estrogen receptor was found, prior to treatment with estradiol, mostly in the cytoplasm. After treatment with estradiol, the ligand bound receptor was

Estrogens

Estradiol, 3

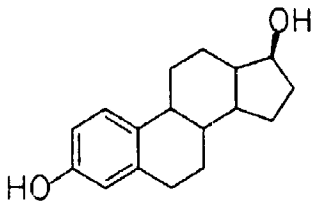

Antiestrogens

Ethamoxytriphetol, 4

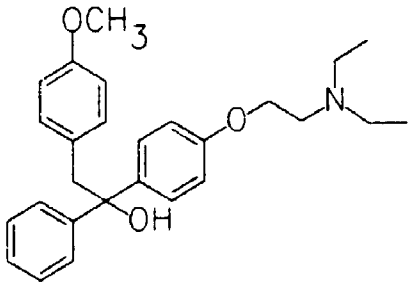

Clomiphene, 5

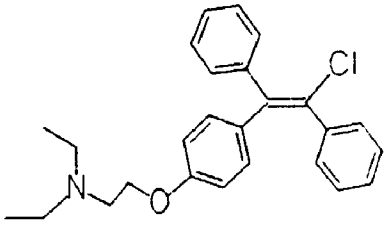

Nafoxidine, 6

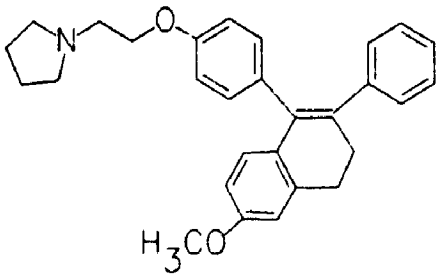

Tamoxifen,7

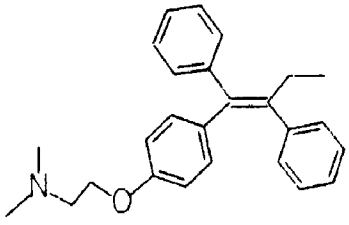

Figure 6.1: Structures of an Estrogen and Some Antiestrogen

found in the nucleus with the concentration of unbound receptor in the cytosol depleted. It has been proposed that when entering the cell, an estrogen forms a complex with the receptor in cytoplasm and translocates into the nucleus. A schematic diagram representing this is given in Figure 6.2. This mechanism is known as the two-step theory of steroid hormone receptor action. Though generally accepted, some evidence has been presented which does not fully support this theory. However, such a discussion goes beyond the realm of this thesis.

6.1.2) Estrogen Receptors and Tumors

Human breast tumor cells, in most cases, contain estrogen receptors. These receptors appear to play an important role in the growth of the tumor. That is, the binding of an estrogen to the receptor is believed, as described above, to aid in the translocation and retention of the receptor into the nucleus. In the nucleus, the estrogens causes a growth response. Studies, as early as 1938, reported that the uterus of estrogen treated animals absorbed fluid containing nutrients and electrolytes and an acceleration of RNA and protein synthesis was observed.[3] This was followed by a wave of DNA synthesis. These actions result in the production of components essential for cell growth and function. This mechanism is responsible for the both the desired growth activity in targic organs as well as the undesired growth in tumors.

6.1.3) Estrogen Receptors and Antiestrogens

Antiestrogens are compounds which block the activity of estrogens. In the laboratory, the activity of an estrogen or antiestrogen is generally determine by measuring the increase or lack of increase in weight of the uterus after treatment. This assay reflects the stimulations of growth activities caused by estrogens and is known as a uterotropic response.[4]

Antiestrogens were first described in the literature in 1954 when it was demonstrated that a weak steroidal estrogen when coadministered with estradiol inhibited the full uterotrophic response observed when estradiol was administered alone.[5] Other nonsteroidal weak estrogens were then tested and also found partially to block the uterotrophic response. A search began for more potent antiestrogens which could potentially be used to treat breast and uterine cancers and menstrual disorders. The first nonsteroidal antiestrogen with full antiestrogenic properties was ethamoxytriphetol, **4**. Figure 6.1. This compound, though originally synthesized as a cardiovascular drug, was able to block totally the uterotrophic effect of estradiol. It was later shown to be a competitive antagonist for the estrogen receptor.

Thus antiestrogen, **4**, was thoroughly investigated in many species including humans. However, central nervous system side effects sparked interest in finding better antiestrogens. Though many different structural types of

antiestrogen have been investigated, the nonsteroidal triarylethylenes are probably the most successful. The remainder of this discussion will be limited to nonsteroidal antiestrogens of this type. The structures of some of these compounds are given in Figure 6.1. The pharmacological action of these compounds has been thoroughly investigated and is quite complex. The extent of the antagonistic or agonistic properties varies depending on the assay or animal model in which the antiestrogen is tested. Several of these antiestrogens including clomiphene, **5**, nafoxidine, **6** and tamoxifen, **7**, have been tested clinically as agents for breast cancer. Of these three, only tamoxifen is presently in widespread clinical use.

Antiestrogens also bind with varying affinity to the antiestrogen binding sites, also called the triphenylethylene binding site. Estrogens, however, do not bind to antiestrogen binding sites. In general, they are inactive binding sites and do not play a role in the regulation of estrogen dependent events.[6] These sites have been found in various tissues throughout the body including the liver and lungs. Many triphenylethylene antiestrogens bind to these sites, saturably and with high affinity.

6.1.4) Antiestrogens and Cancer Treatment

Antiestrogens, like tamoxifen, are capable of binding to the cytoplasm receptor and translocating the estrogen receptor into the nucleus. The antiestrogen bound receptor is thought to block the estrogen bound receptor for binding

to an acceptor site in the nucleus. This site is involved in the growth response. Successfully blocking this site results in the growth of the tumor being impeded.[7]

Treatment of estrogen receptor positive carcinoma is the major use for antiestrogens and tamoxifen, 7, is the most commonly used antiestrogen. In patients with estrogen receptor positive tumors, tamoxifen has a fifty percent success rate as opposed to a thirteen percent success rate in receptor negative tumors. This treatment is often used along with other treatment and has been successful in delaying reoccurrences and prolonging life.

6.2) Estrogen Receptor Imaging Agents

6.2.1) Characteristics Required for an Estrogen Receptor Imaging Agent

Using estrogen receptors for concentrating a radiopharmaceutical to image tumors has two possible applications. The first would be to locate small tumors and reoccurrences in patients which have been previously diagnosed with estrogen receptor positive carcinoma. The second would be to assist in determining if hormone therapy would be appropriate for the treatment of a known malignancy by measuring estrogen receptor concentration. Several labelled estrogens and antiestrogens have been prepared and evaluated for this purpose.

The characteristics required by a radiopharmaceutical to image estrogen receptor positive tumors are listed below.

i) The compound must have a high binding affinity for estrogen receptors. The IC_{50} value (see Appendix I) should be in the nanamolar range.

ii) The compound should not concentrate or, at least, be retained in the organs which would potentially be in the vicinity of the tumor.

iii) The nonspecific binding of the compound should clear relatively quickly. That is, it should clear from the blood or muscle to allow as high as possible target to background ratio. This property is usually dependent on the lipophilicity of the compound.

iv) Also, as described in the Introduction to the thesis, the radiopharmaceutical should be labelled in high specific activity and the iodine should be bonded to an sp^2 carbon for metabolic stability.

A survey of the literature shows compounds investigated as potential radiopharmaceuticals generally are of three different types. Several steroidal estrogens have been labelled and successfully used to image receptors. The structure of some of these and their target to background ratios are given in Table 6.1. Nonsteroidal estrogens and antiestrogens have also been prepared and evaluated for this purpose. They are generally either labelled hexestrol (estrogen) or triarylethylenes (antiestrogen). The structure of some of these are given in Tables 6.2 and 6.3.

6.2.2) Labelled Estrogens as Imaging Agents

The majority of the work has been done on estradiol

Table 6.1: Ratio of Uptake in Uterus to Blood for Selected Steroidal Estrogen Imaging Agents

Agent	Ratio of Uptake in Uterus/Blood
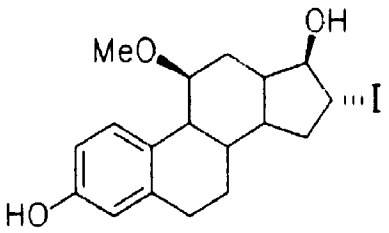 8	37
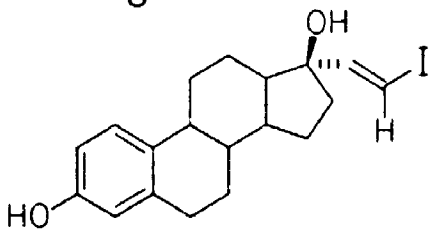 9	E = 3.9 Z = 13.6
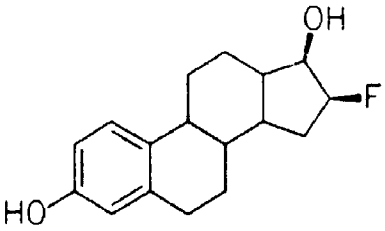 10	20
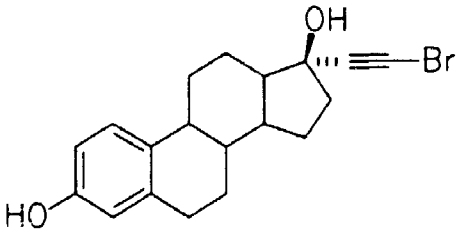 11	12

derivatives. Four examples of halogenated estradiols are given in Table 6.1. The uterus to blood ratio from rat biodistribution studies which are as high as 37 to 1 are also given. Labelled estrogens for both PET and SPECT have been prepared.

Bromoestradiol, **11** was prepared and labelled with 77-bromine.[8] It showed good *in vitro* binding and the uterus to blood ratio was reported to be 12 to 1. 16α-([^{18}F]fluoro)-17β-estradiol, **10** was also synthesized as a PET imaging agent. It was reported to have a 20 to 1 uterus to blood ratio. Two compounds prepared as potential SPECT imaging agent were labelled with iodine. Compound **9** was labelled by adding a vinyl group to the 17α position.[9] Thisallowed the compound to be labelled on an sp^2 carbon without interfering with the A ring. Substitution on the A ring is generally know to lower binding.[10] The E isomer of **9** only gave a 3.9 to 1 ratio in the uterus over the blood while the Z gave 13.6 to 1 ratio. More recently a 16α-iodo compound, **8** was prepared and labelled with 123-iodine.[11] They reported a 37 to 1 ratio of uptake in the uterus over the blood. It is interesting to note that **8** is labelled on a sp^3 carbon and may be susceptible to loss of the iodine, *in vivo*, by nucleophilic substitution.

Several of these compounds have been taken to clinical trials. The most successful agent from this category appears to be fluoroestradiol, **10**. Successful imaging of human breast tumors and *in vivo* quantification of receptor

concentration has been reported.[12] At present it appears that most efforts are focused on these types of compounds.

6.2.3.) Labelled Hexetrols as Estrogen Receptor Imaging Agents

Hexestrols have also been labelled and evaluated as estrogen receptor imaging agents. Hexestrol is an estrogen receptor agonist which binds to estrogen receptor three times more effectively than estradiol.[13] Four examples of halogenated hexestrols are given Table 6.2 along with the uterus to blood ratios which were obtained from rat biodistributions.

Two of the examples shown were labelled with fluorine, compounds **12** and **13**. A ratio of 22 to 1 for uptake in the uterus over blood was obtained by two hours for hexestrol, **12** which was substituted with fluorine on the methyl.[14] Fluorohexestrol, **13**, which was substituted ortho to the hydroxyl group of the phenol, showed a ratio of approximately 50 to 1.[15] The analogous iodinated compound, **15**, had much poorer selectivity for the uterus with ratio of 1.8.[16] Also reported was iodinated hexestrol, **14**.[15] This methyl iodinated compound showed a high ratio of uptake in the uterus over the blood but not as high as **13**. This was attributed to higher nonspecific binding. Again a potential problem **14** might have *in vivo* is displacement of the label. These compounds have not been as successful as the labelled estradiol derivatives in humans and are presently not attracting much attention.

Table 6.2: Ratio of Uptake in Uterus to Blood for Selected Hexetrol Estrogen Receptor Imaging Agents

Agents	Ratio of Uptake in Uterus/Blood
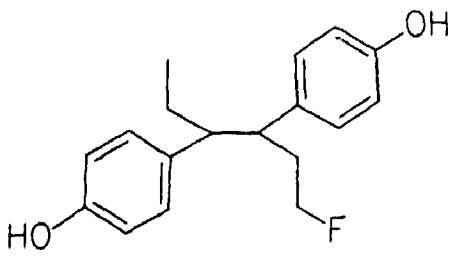 12	22
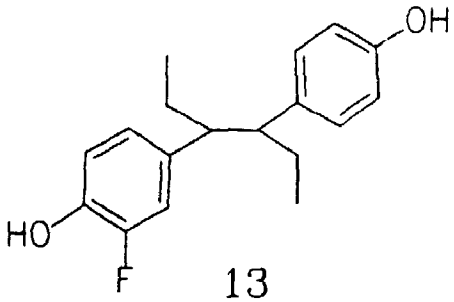 13	50 (approx.)
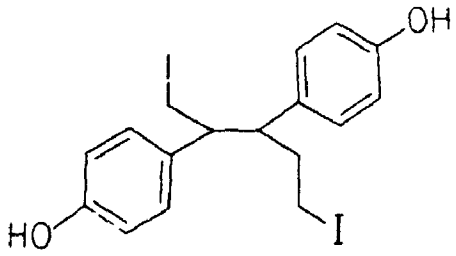 14	30 (approx.)
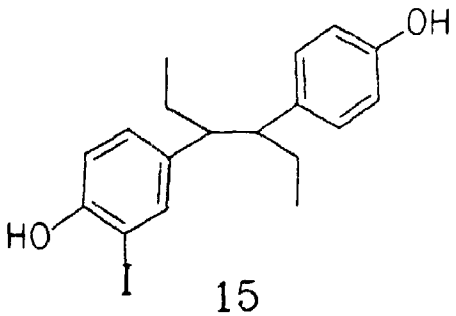 15	1.9

6.2.4) Labelled Triarylethylenes as Estrogen Receptor Imaging Agents

The third type of compound to be prepared is triarylethylene antiestrogen of which tamoxifen, **7**, is one. The structure of these compounds all of which are halogenated derivatives of **7** are given in Table 6.3.

A fluorinated tamoxifen derivative, **16**, has been prepared.[17] Compound **16** has a slightly lower affinity for estrogen receptors than tamoxifen, **7**, when determined *in vitro*. To our knowledge, further biological studies have not been reported. The iodinated tamoxifen derivative, **17**, has also been prepared.[18] From a biodistribution in rats, the uterus over ovaries uptake ratio was determined to be 23 at 6h. Also reported quite recently was the synthesis of E and Z iodotamoxifen, **18**.[19] The Z isomer of **18** had a higher binding affinity than Z-**7** and the E isomer a lower affinity. To date only *in vitro* work has been reported for these compounds and they have not been radiolabelled.

6.3) Strategy for Estrogen Receptor Imaging Agent Design

We have proposed that an iodinated tamoxifen derivative could potentially be used as an estrogen receptor positive carcinoma imaging agent. Tamoxifen, **7**, as described above has been successfully used in the treatment of hormone dependent cancers. The commercially available compound is the citrate salt of the Z isomer.

Tamoxifen is a competitive inhibitor of estradiol for

Table 6.3: Ratio of Uptake in Uterus to Blood for Selected Triarylethylene Estrogen Receptor Imaging Agents

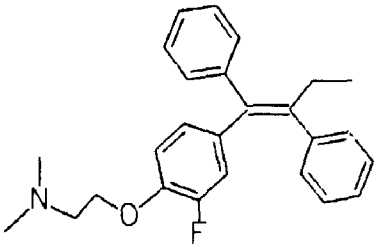

16

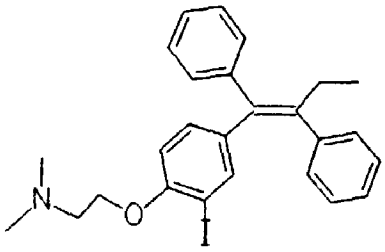

17

Uterus/Blood = 23

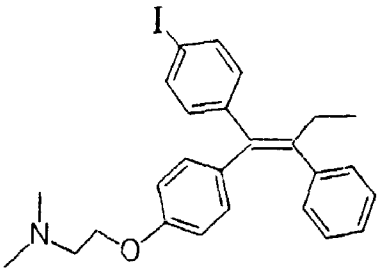

18

Ratio of uptake in uterus to blood has not been determined for 16 and 18.

estrogen receptors obtained from various animals uteri and human endometrium. A wide range of values have been reported for its relative binding affinity which range between 30 and 0.01 percent of estradiol's affinity.[20]

There are a few problems which could potentially arise from employing an iodinated derivative of tamoxifen as an imaging agent. The first is an increase in lipophilicity in the compound. This often increases nonspecific uptake in many tissues. Also tamoxifen binds to antiestrogen binding sites. [^{3}H]-Tamoxifen has been shown to bind to a saturable binding site in many different tissues and in many different species including the immature rat uterus and estrogen receptor positive human breast tissue. Other organs which have antiestrogen binding sites are the liver, some parts of the digestive tract, spleen, kidney and lungs. These organs except for the liver have fairly low concentrations.[21]

The other possible problem could arise if the iodine substitution was to interfere with metabolism. Tamoxifen is almost completely metabolised after administration to both animals and humans. In humans, the excreted metabolites were recovered and identified.[22] Figure 6.3 shows the structure of the isolated metabolites. Metabolite A is the product of hydration of the double bond. Metabolite B, C, D and F all are metabolized on the unsubstituted ring at position one of the butene. Metabolites E and F were formed by changes to the ether side chain. Metabolite G was not excreted but was found to accumulate in the plasma after several doses.

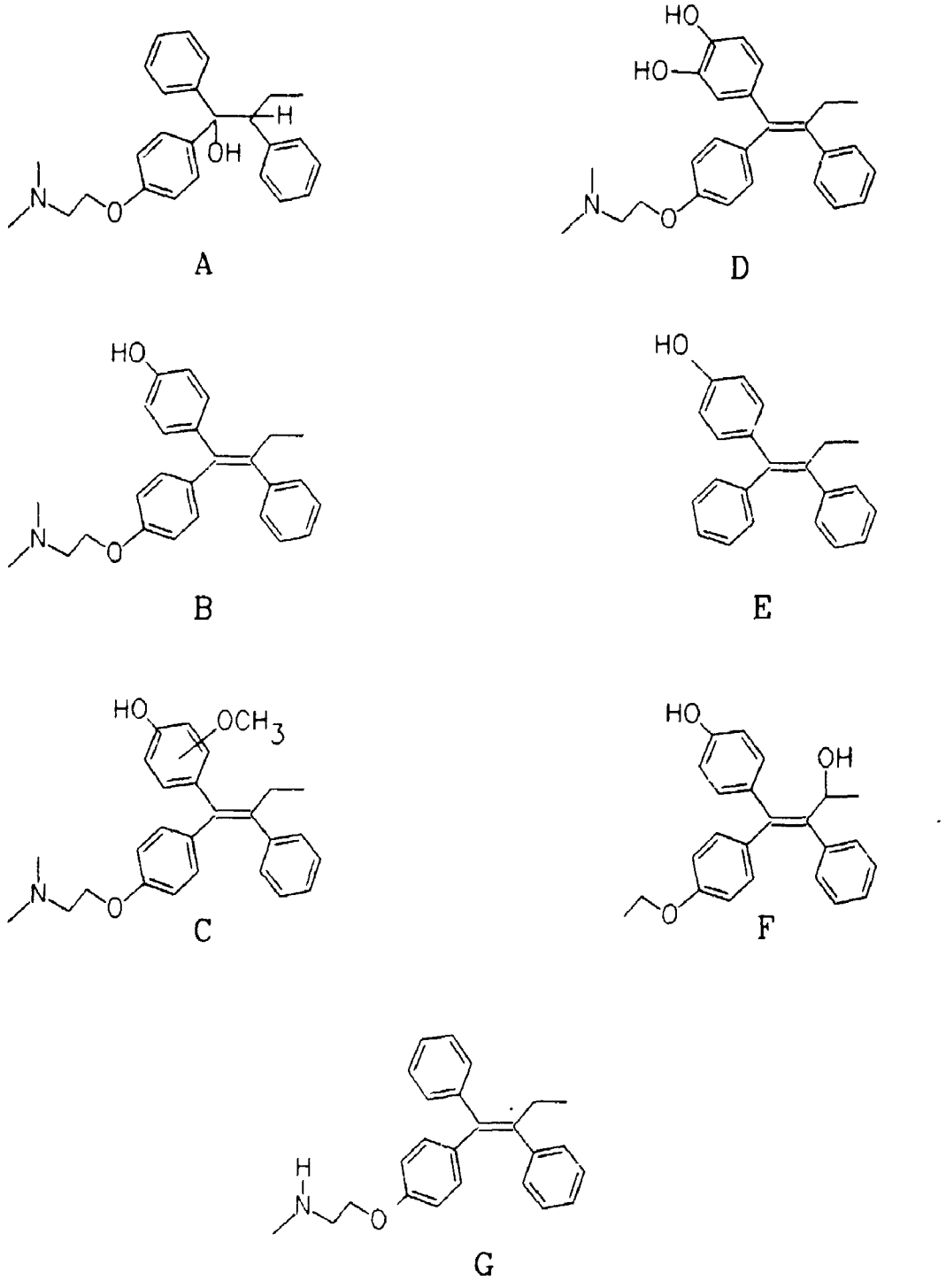

Figure 6.2: Metabolites of Tamoxifen

Metabolite B, 4-hydroxytamoxifen has a binding affinity for estrogen receptors greater than tamoxifen. Metabolite G, N-demethyltamoxifen binds with an affinity similar to tamoxifen to estrogen receptors. Blocking the formation of these two metabolites, in particular, could hinder the uptake of the labelled compound in tumors.

The target molecule was chosen by considering the metabolic pathway of tamoxifen as well as the binding affinity of other derivatives. At the initiation of this project, only one iodinated tamoxifen derivative, **17**, had been synthesized, the structure of which is given in Table 6.3. Substitution of the ring ortho to the side chain was readily accomplished by electrophilic aromatic substitution. However, the presence of an iodine at this position reduced the binding affinity for estrogen receptors to twenty percent of tamoxifen's. Also a dimethyl derivative, **19**, was reported (Figure 6.3). Compound **19**, also showed a reduced binding affinity for estrogen receptors.[23] Considering these findings, we decided to label the phenyl ring at the 2 position of the butene. This ring was unchanged during metabolism. Since the patented synthesis of tamoxifen produced both the E and Z isomer, we set forth to synthesize and evaluate both isomers of **2**.

6.4) Synthesis of Aminotamoxifens, 1

To label **7** at the position chosen requires that a functionalized derivative be prepared. The ring is not

activated therefore direct iodination of tamoxifen would not work. The functionalized derivative synthesized was aminotamoxifen, 1. This allowed the synthesis of the "cold" 2 via the diazonium salt. It was also proposed that a labelling procedure based on the iododediazotization reaction could be employed. This had been previously attempted but with limited success.[24]

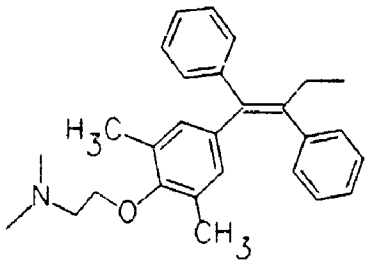

19

Figure 6.3: Structure of Dimethyl Tamoxifen

The aminotamoxifens were synthesized previously in this laboratory by a route analogous to that used to synthesize tamoxifen.[25] The changes made were to allow for the amino functionality. In Scheme 6.1 an outline of the synthesis used is given.[26] The synthesis started with α-(p-nitrophenyl)-acetophenone, 20 which allowed for functionality on the desired position of the ring. Alkylation of 20 with ethyl iodide gave the 21. At this stage the nitro group was reduced to the amino with stannous chloride giving 22. The following step in the original synthesis was a Grignard reaction to add the third phenyl ring. This, however, would not be possible without

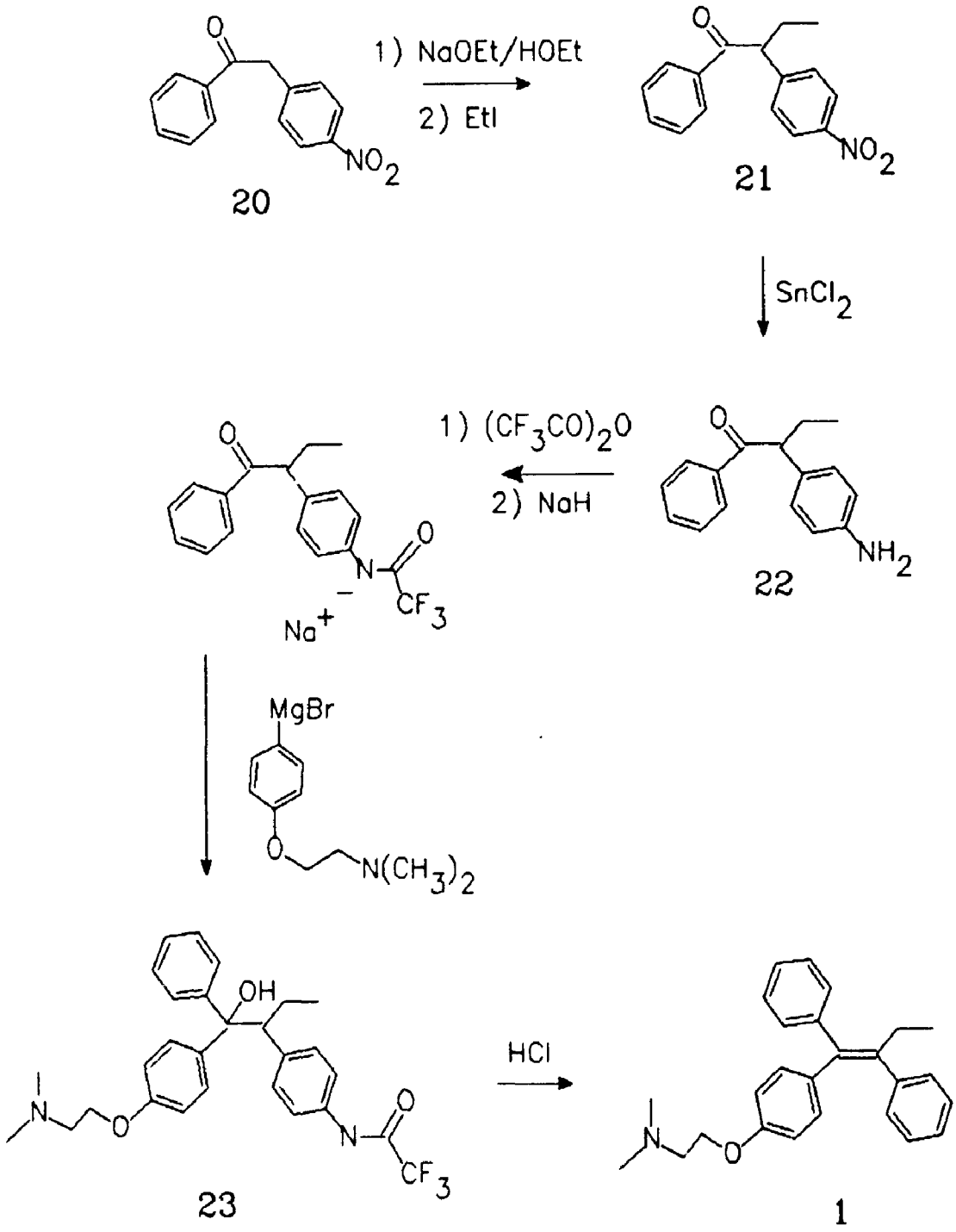

Scheme 6.1: Synthesis of E and Z-1

protecting the amino group from deprotonation by the Grignard reagent. This was done by preparing the trifluoroacetamide and forming the amide salt prior to treatment with the Grignard reagent which resulted in the protected alcohol, **23**. Treatment of **23** with acid both deprotected the amine and dehydrated the alcohol to give the alkene. Both geometric isomers of **1** were produced in similar amounts and were separated by column chromatography.

Reported in the following chapters is the development of a labelling procedure for the synthesis of "no carrier added" iodotamoxifen, **2**. Also given is the biological evaluation of this compound as a estrogen receptor imaging agent. This includes *in vitro* determination of receptor binding affinity for both E and Z isomers of **1** and **2**. Following this is a description of the results of the biodistribution studies performed for both isomers of [^{131}I]-**2**. Also reported are the results of an *in vivo* competition experiment between E and Z [^{131}I]-**2** and estradiol. The final section briefly describes the results of preclinical trial which were preformed on E and Z [^{131}I]-**2** by clinicians of the Radiopharmaceutical Development Group.

Chapter 7: Results and Discussion - Chemistry

The dediazotization of aryl diazonium salts has been applied with limited success in the synthesis of radioiodinated compounds. The radiochemical yields for the "no carrier added" synthesis employing this reaction have been reported to be low. The synthesis of radioastitine and radioiodinated halobenzenes via a diazonium salt were reported to go in 10 to 20 per cent and 6 to 10 percent radiochemical yield respectively.[24]

In the interest of radioiodinating tamoxifen, 7, as well as developing a new "no carrier added" labelling method, studies were performed to investigate improving the yield of this procedure. Iododediazotization goes in a high yield if equimolar or greater amounts of sodium iodide are present. This has been a commonly used route for the synthesis of nonradioactive aryl iodides. Good radiochemical yields have also been reported for dediazotizations of low specific activity compounds.[27] The difficulty appears when less than one equivalent of iodide is present. As discussed in the opening chapter, to image receptors, a high specific activity radiopharmaceutical is required.

7.1) Dediazotization Mechanisms

The low yields described above in the "no carrier added" radioiodination can be explained by considering the mechanism of halodediazotization. Though this reaction has

been known for over one hundred years, it is not until recently that the mechanistic details have been sorted out. The difficulty in defining an acceptable mechanism has likely been due to conflicting reports from different rate and product distribution studies. The two mechanisms are given in Figure 7.1. There is evidence for both the homolytic and heterolytic cleavage of the diazonium group.[28] Heterolytic cleavage of nitrogen forms an aryl cation by a S_N1 type mechanism. Homolytic cleavage of nitrogen occurs after an electron is transfer from a reducing agent to form an aryl radical. It would seem that the formation of a high energy aryl cation would be less likely than the formation of the aryl radical. However, the energetics of the two pathways are not very different since a large part of the driving force for both comes from the release of a molecule of dinitrogen. Of course the latter mechanism requires the prior availability of a reducing agent. The extent to which each mechanism occurs is likely dependent on the conditions of the reaction.

i) Heterolytic Cleavage

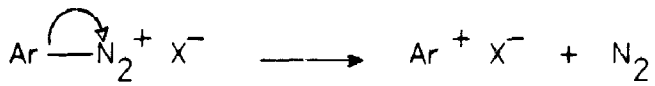

ii) Homolytic Cleavage

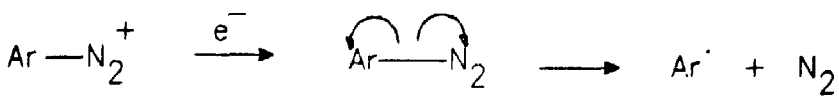

Figure 7.1: Two Possible Mechanisms for Dediazotization

Evidence for both mechanisms have been given. The earliest published report of this reaction was in 1864. It was reported that iodide readily replaced the diazonium group to give aryl iodides while the analogous reaction to form aryl bromides or chlorides required much harsher conditions.[29] T. Sandmeyer later discovered that copper (I) salts catalysed the formation of aryl bromides and chlorides to synthetically useful levels.[30] The Gatterman version of this reaction, which was reported a few years later, extends the catalysis of these reactions to copper (0) powder.[31] There have also been inconsistent claims that copper (II) salts and zinc (II) salts also catalyse the reaction.

The first suggestion that an aryl radical was formed in dediazotization was in 1934 by Greive and Hey.[32] Though it was Waters who first suggested the copper salt acted as a reducing agent.[33] He also attributed the success of cuprous salts to their ideal reduction potential for electron transfer to a aryl diazonium salt. Other metal (II) ions were not successful since they are too weak reducing agent. He also pointed out that iodide may also act as a reducing agent and bromide and chloride likely do not. This explains the difference in the rate of uncatalysed iododediazotization compared to the bromo and chloro reaction.

The mechanism which was initially proposed was the S_N1 type formation of an aryl cation. The formation of phenol as a side product of dediazotization is probably the most

direct evidence for the involvement of this mechanism. To form the phenol from the aryl radical would require a hydroxyl radical. In the aqueous reaction mixture there would not likely be a source of hydroxyl radical. The phenyl radical would be expected to abstract a hydrogen atom. The formation of hydrocarbon side products from dediazotization has also been observed. In Zollinger's book he gives other evidence for this mechanism.[34] He cites several early studies which report dediazotization to be independent of the concentration and nature of the halide. This evidence supports a unimolecular rate determining step. However, contrary results have been used to support the aryl radical mechanism. Substituent effects on decomposition rates are also given in support of heterolytic cleavage.

The role of the catalyst differs depending on the mechanism being considered. For electron transfer, it acts as a reducing agent in that it supplies the aryl diazonium salt with an electron. In the case of a copper (I) or (0) catalyst a cupric salt is formed which then acts to transfer the ligand. For the heterolytic mechanism, the copper catalyst was reported to enhance the reactivity of the halogen towards the attack of the aromatic carbon.[35] This occurs after the rate determining step but would enhance the product distribution towards the formation of the aryl halide.

The evidence for both mechanisms suggests that even though the electron transfer mechanism may be favoured at

present, both must be considered.

In the case of "no carrier added" radioiodination where the iodide concentration is very low, one would likely expect low yields for both mechanisms. Yields for the iodide induced radical formation would be low since it is dependent on the transfer of an electron from the iodide ion which is present in extremely low concentration. In the case of the aryl cation, the rate of formation would be independent of iodide concentration. However, the chances of the high energy cation finding an iodide ion with which to react are poor under "no carrier added" conditions, in particular, if the reaction is run in water.

7.2) Catalysis of Iododediazotization

It was evident that to use a dediazotization in "no carrier added" radioiodination either a catalyst or a method which would reduce side products would have to be implemented. In this section, I describe attempts at using copper (0), (I) and (II) catalysts under various conditions, the results of which are given in Tables 7.1, 7.2 and 7.3.

In general in halodediazotization reactions such as the Sandmeyer reaction, the diazonium salt is formed in an acid solution with sodium nitrite. The mechanism is given in Figure 7.2. The excess nitrite is then destroyed with urea and dediazotization is done immediately. To simplify this study as well as the labelling procedure, we decided to synthesize and isolate the diazonium salt of (E)-tamoxifen,

24.

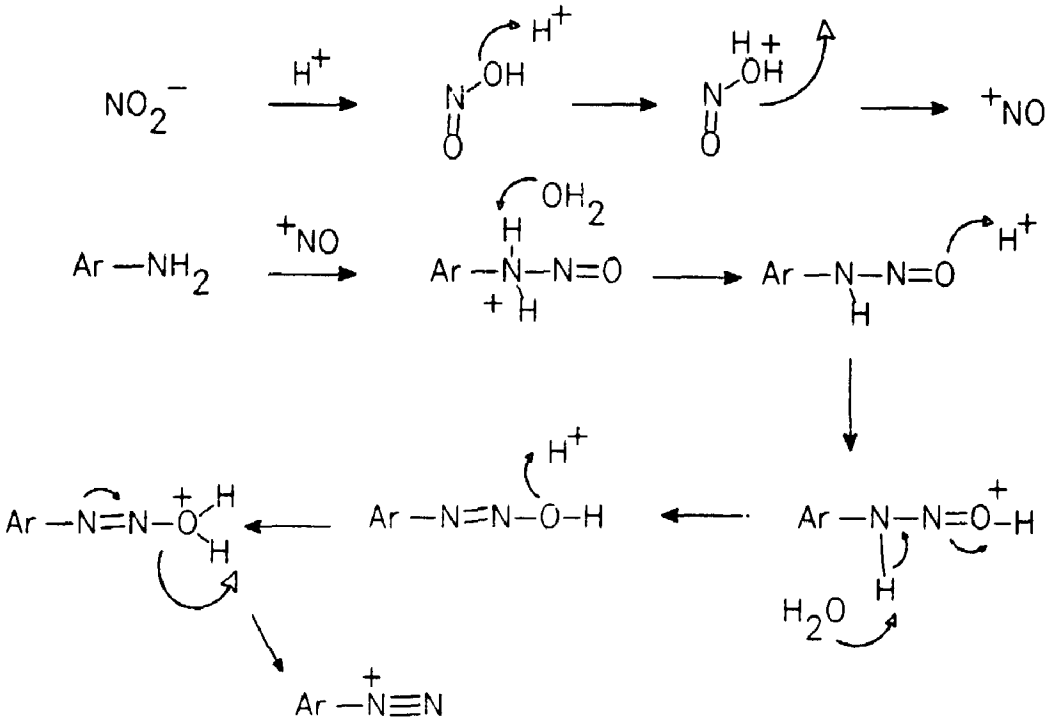

Figure 7.2: Mechanism for Diazonium Salt Formation

The diazonium salts were isolated quite easily and were fairly stable. If properly dried, after being filtered from the aqueous solution, they could be stored for several months in the refrigerator. The decomposition temperatures for the three salts described below were between 65 and 98 °C. The stability was related to the counterion used. The tertiary amine of diazonium salts, 24, is protonated and has the same counter ion as the diazonium salt.

The labelling procedure was developed employing potassium [^{127}I]-iodide. The reactions were run as described in the general procedure in the Experimental employing the conditions described in Tables 7.1, 7.2 and 7.3. The

percentage of iodotamoxifen formed was determined by HPLC on a reverse phase column employing naphthalene as an internal standard. In general they were run on approximately a 2 mg scale of **24**.

7.2.1) Hexafluorophosphate Diazonium Salt

The first series of reactions were performed on the hexafluorophosphate salt of E-**24**-PF_6. The conditions and results are given in Table 7.1. Diazonium salt, **24**, was synthesized from (E)-aminotamoxifen, **1**, and sodium nitrite in aqueous sulphuric acid. A large excessof potassium hexafluorophosphate was added to precipitate the hexafluorophosphate salt of the diazonium ion. After washing away the excess potassium hexafluorophosphate with water, the diazonium salt was isolated and freeze dried. If properly dried and stored in the fridge this diazonium salt was stable for months.

A series of copper catalysts which had been reported to catalyse dediazotizations were tried.[36] Copper bronze was the first catalyst tried since it had been employed in a low specific activity radioiodination.[37] It is an amalgam of tin and copper in approximately a 10 to 90 ratio. Prior to use it was freshly activated by a procedure which involves treating the catalyst with a 2 % solution of iodine in acetone. The catalyst is then washed with hydrochloric acid and acetone. All reactions were run in aqueous solutions. Though "no carrier" iodinations would be run with much less than an equivalent of iodide, the procedure was developed

Table 7.1: Iodinations of E-24-PF_6 Employing Copper Catalyst While Stirred or Sonicated at Room Temperature

Run	Solvent	KI/E-24-PF_6[d]	Catalyst	Procedure	Yield[a] (%)
1	100 µL 10 % H_2SO_4	1	10 mg CuB[b]	stir 1 h	9
2	1.5 mL 3.7% H_2SO_4	1	10 mg CuB	stir 1 h	≤ 4
3	1 mL H_2O +.2 ml acetone	1	10 mg CuB	i) stir 1 h ii) ultrasound[c]	i) ≤ 1 ii) ≤ 4
4	100 µL 10 % H_2SO_4	1	10 mg CuB then add 24 and stir 1 h	stir CuB + KI 1h	9
5	3 mL H_2O	1	20 mg Cu(0) powder	stir 1 h	≤ 1
6	1 mL 10 % H_2SO_4	1	20 mg Cu(0) powder then add 24 and stir 1 h	stir Cu(0) + KI 1h	9

a The yield was determined by HPLC analysis employing an internal standard.
b activated copper bronze catalyst
c ultrasonic cleaner
d based on approximately 2 mg of E-24PF_6

employing one equivalent. These reactions were run on 2.0 mg of the hexafluorophosphate salt of **24**. The product mixtures were analyzed by HPLC for E-**2** employing naphthalene as an internal standard. Yield is based on the amount of E-**24**-PF_6 used.

The first attempts (runs 1 and 2 of Table 7.1) were made with copper bronze as the catalyst and the solvent volume and acid concentration were varied. The main concern was the poor solubility of the hexafluorophosphate salt in water. In 100 µL of 10% sulphuric acid with 10 mg of fresh copper bronze catalyst, only 9 % of the desired E-**2** product was produced (run 1). To demonstrated the sensitivity of this reaction to the potassium iodide concentration, an identical reaction was performed with a large excess of sodium iodide. By HPLC analysis showed 87 % **2** was formed. When the solvent volume was increased 1.5 mL of 3.75 % sulphuric acid the amount of product formed was negligible (run 2). Reaction without acid in 1 mL of water with 0.2 mL of acetone as cosolvent also showed no reaction (run 3). The acetone was added to increase the solubility of the diazonium salt. In an attempt to improve solubility and activate the catalyst, some of the reactions described above were run in an ultrasound bath in place of stirring (run 3). However, this did not improve the yield of iodinated product. An attempt in which the copper bronze catalyst was treated with the potassium iodide prior to adding the diazonium salt did not enhance the yield (run 4).

Copper (0) powder has been reported to catalyze dediazotizations. The test reactions were run under similar conditions to those described for copper bronze. In place of the copper bronze catalyst. 20 mg of freshly prepared copper powder was used (runs 5 and 6). However, yields in the same range were obtained.

It appeared from these reactions that only a 9 % yield of **2** could be obtained from 2 mg of E-**24**-PF_6 and equimolar potassium iodide in a volume of less than 1 mL of acidic water. The acid is likely necessary to prevent the formation of a diazohydroxide species which cannot dediazotize. Catalysis of the formation of the iodocompound did not appear to occur employing either copper bronze or copper powder with hexafluorophosphate diazonium salt.

The solubility of the diazonium salt could be a problem. One method of overcoming this could be by changing the counter ion on the diazonium salt. This also would effect the stability of the salt which could affect the reaction either favourably or unfavourably.

7.2.2) Tetraphenylborate Diazonium Salt

The tetraphenylborate salt of **24** was synthesized in a similar fashion to that described for the hexafluorophosphate salt. An excess of sodium tetraphenylborate was used to precipitate the desired salt. Obtaining a clean NMR spectrum was difficult since the salt decomposed in solution as was evident by a slow darkening of the solution. However, a nujol mull of the compound was

stable enough to obtain an infrared spectrum. This salt showed the characteristic band at 2240 cm^{-1} for the nitrogen-nitrogen stretch. The tetraphenylborate salt of **24** had a lower decomposition temperature than the hexafluorophosphate salt.

Experiments employing copper bronze and copper powder as catalysts were repeated with this salt and the results are given in Table 7.2. These experiments used a larger volume of solvent with an excess of potassium iodide. To increase the solubility of the salt, reactions employing tetrahydrofuran as a cosolvent were attempted. Employing a 5 fold excess of potassium iodide and 10 mg of copper bronze catalyst in 1 mL of 1 % sulfuric acid with 10 µl of THF as cosolvent produced 9 % iodotamoxifen (run 1 i). Under the same conditions if 10 equivalents of potassium iodide was used 22 % of the desired compound was formed (run 1 ii). Employing copper powder as the catalyst and four equivalents of potassium iodide only formed 3 % of the desired product (run 2).

Though mechanistically it is not obvious why a copper (II) salt would have a catalytic effect on this reaction they have been reported to do so.[29] Under similar conditions as employed previously copper sulphate was tried (run 3 i). This reaction however only produced 5 % of the desired product. This reaction was repeated employing phosphoric acid in place of sulphuric acid (run 3 ii). The yield rose to 12 % under these conditions. Cuprous oxide was also tried

Table 7.2: Iodinations of E-24-BPh_4 with Copper Catalysts While Stirred or Ultrasound at Room Temperature

Run	Solvent	KI/E-24-BPh_4	Catalyst	Procedure	Yield[a] (%)
1	100 mL 1 % H_2SO_4	i) 5 ii) 10	10 mg CuB[b]	stir 1 h	9 22
2	1 mL 1 % H_2SO_4	4	20 mg Cu(0) powder	stir 45 min	3
3	i) 1 mL .1 % H_2SO_4 ii) 1 mL .26 % H_3PO_4	4	10 mg $CuSO_4$	stir 1 h	i) 5 ii) 12
4	2 mL .1 % H_2SO_4	4	10 mg Cu(0) powder	stir 1h	6
5	2 mL 1 % H_2SO_4	4	10 mg Cu(0) powder	15 sec ultrasonic probe[c] on med	6
6	2 mL .1 % H_2SO_4	4	no	5 sec ultrasonic probe on high	10
7	2 mL .01 % H_2SO_4	4	10 mg CuB	5 sec ultrasonic probe on high	≤ 1
8	2 mL .1 % H_2SO_4	4	10 mg CuB	5 sec ultrasonic probe on high	8
9	2 mL H_2O	4	10 mg CuB	5 sec ultrasonic probe on high	≤ 1

a The yield was determined by HPLC analysis employing an internal standard
b activated copper bronze catalyst
c ultrasonic disintegrator

as a catalyst, however the results were similar to that for the other catalysts. These results suggest no catalytic activity was demonstrated by these catalysts with the tetraphenyl borate salt. The dependence of the reaction on iodide concentration was again seen.

In an attempt to overcome the solubility problems and increase the activity of the catalysts, a high powered ultrasonic probe was used. The reactions were run in 2 mL of solvent with 4 equivalents of potassium iodide. A reaction run with no catalyst resulted in 10 % yield of **2** (run 6). An analogous test employing copper bronze catalyst only produced an 8 % yield of **2** (run 8). Runs 1 and 8 used 0.1 % sulphuric acid. When runs were done with 0.01 % sulphuric acid and with no acid employing copper bronze catalyst, no product was observed for either attempt (run 7 and 9). This again, demonstrates the dependence on acid for dediazotization. Copper powder also failed to catalyse the dediazotization of this salt with a yield of 6 % (run 5).

7.2.3) ß-Naphthyl Sulphonate Diazonium Salt

The third diazonium salt of tamoxifen prepared was the ß-naphthyl sulphonate, E-**24**-ß-nap. Again difficulties in obtaining NMR spectra occurred due to the instability of the salt in solution. This salt appeared to be slightly more stable than the tetrafluoroborate salt but less stable than the hexafluorophosphate salt. Analysis by infrared spectroscopy did show the characteristic nitrogen-nitrogen peak. This salt of **24** showed some water solubility which

permitted the reactions to be in 0.1 mL of 0.1 % sulphuric acid. The results of these attempts are given in Table 7.3. The yields of iodo compound obtained from reactions with and without a catalyst were again less than 10 %. For example when stirred for one hour with and without copper bronze the yields were 6 and 4 per cent respectively (runs 2 and 1). Again if a large excess of potassium iodide was used a 90 % yield was obtained (run 3). The use of copper powder and cuprous oxide also failed to catalyse the reaction even when stirred for 1h (runs 4 and 5). From these results it appeared that the β-naphthyl sulphonate salt was no more susceptible to catalysis than the other salts.

Attempts were made to synthesize both the methanesulphonate and the p-toluenesulphonate salts however they were less stable and could not be isolated.

7.2.4) Surface Analysis of Activated Copper Bronze

The goal of this work was to develop a labelling procedure for the synthesis of no carrier added [^{131}I]-**2**. This implies that no [^{127}I]-iodide is to be added. Copper bronze catalyst was activated prior to use by a procedure employing iodine. Even though copper bronze had failed in our hands to catalyse the dediazotization of **24** we were curious to know if the activated catalyst could potentially be a source of carrier.

To investigate this possibility we had X-ray photoelectron spectrometry (XPS) done on a sample of freshly activated copper bronze. This analytical technique allows

Table 7.3: Iodinations of E-24-βNap Employing Copper Catalysts While Stirred at Room Temperature

Run	Solvent	KI/E-24-βNap	Catalyst	Procedure	Yield[a] (%)
1	100 μL .1 % H_2SO_4	6	none	stir 1 h	4
2	100 μL .1 % H_2SO_4	6	10 mg CuB[b]	stir 1 h	6
3	100 μL .1 % H_2SO_4	large excess	10 mg CuB	stir 2 h	90
4	100 μL .1 % H_2SO_4	6	10 mg Cu(0) powder	stir 1 h	6
5	100 μL .1 % H_2SO_4	6	Cu_2O	stir 1 h	2

a The yield was determined by HPLC analysis employing an internal standard
b activated copper bronze catalyst

Figure 7.3: XPS Spectrum of Freshly Activated Copper Catalyst

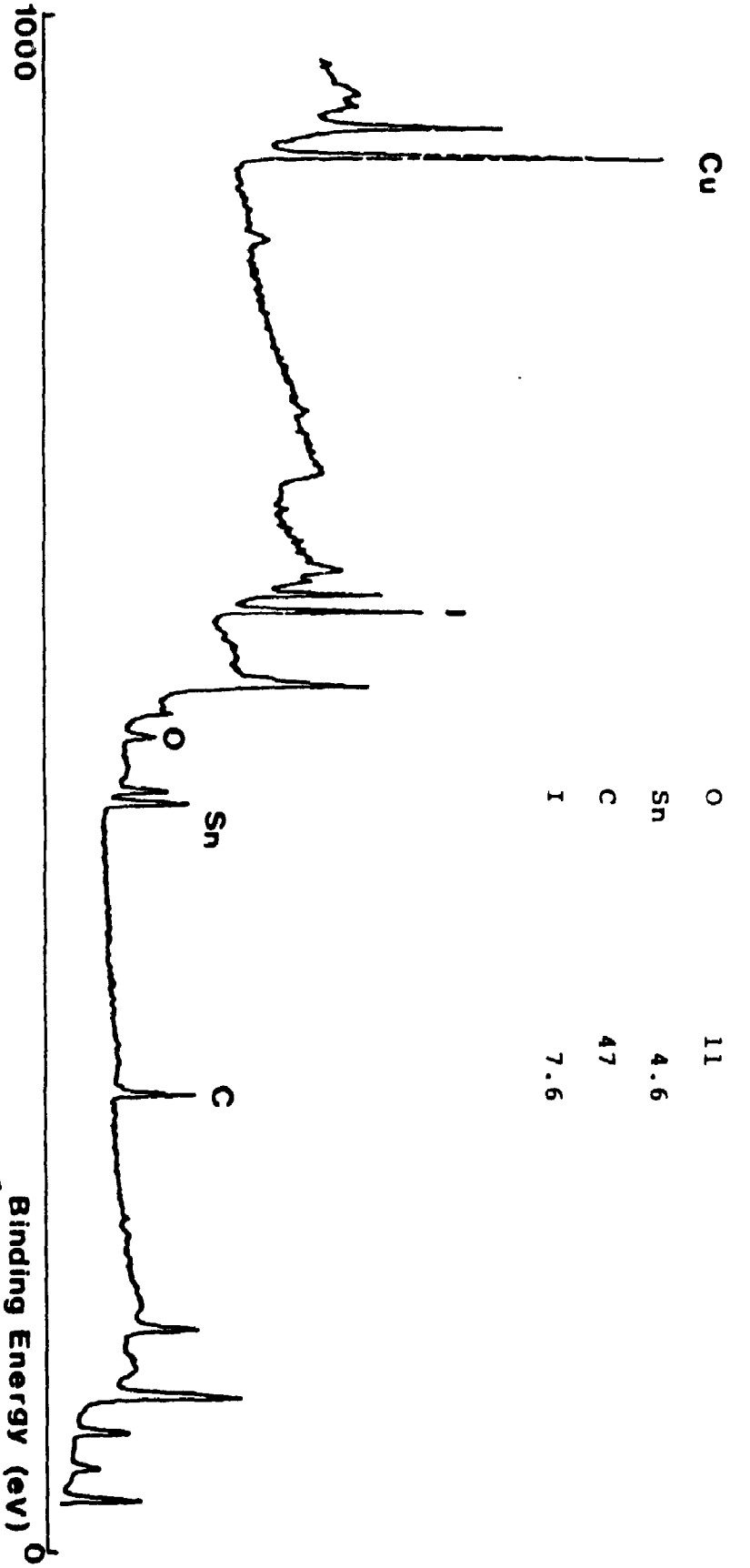

Element	Atom %
Cu	30
O	11
Sn	4.6
C	47
I	7.6

the determination of the species on a surface by measuring the binding energy of the electrons which are released after bombardment with X-rays. The relative number of electrons which are emitted can be determined by the size of the peaks on the spectrum.

The spectrum obtained as well as the atom per cent determined from the spectrum are given in Figure 7.1. The analysis definitely shows that iodide is present in 7 atom % as can be seen by the peak at 619 eV. Also present is copper (0) and tin in 30 % and 5 % respectively. The remainder of the surface is made up of carbon and oxygen. The presence of iodide definitely eliminates copper bronze activated by this method as a catalyst for no carrier radioiodinations.

7.3) Non-Aqueous Solvents or No Solvents

It appeared that catalysis of the dediazotization of the diazonium salt of tamoxifen would not be possible, at least, with the diazonium salts and the catalysts tried. Since catalysis of the reaction with equimolar or greater potassium iodide was not possible, it would likely not be occur under "no carrier added" conditions.

The second strategy was to try to decrease the formation of side products. For instance, in aqueous solutions phenols are potential side products formed from the attack of the aryl cation on water. This section describes reactions employing no solvent or non-nucleophilic polar solvents. The results are given in Table

7.4.

It was hoped that under these conditions the phenol production would be reduced which would allow more opportunities for the aryl cation to couple with the iodide ion. In the case of the electron transfer mechanism, product formation may be enhanced by increasing diazonium salt solubility and decreasing solvent volume, therefore increasing the concentration which would increase the rate of reaction.

A dediazotization without solvent was attempted first. These reactions were run with 0.1 equivalent of potassium iodide which had been freeze-dried with some sodium thiosulphate in a V-shaped vial. The sodium thiosulphate was added to prevent oxidation of the iodide to volatile iodine during freeze drying. These condition were used to simulate those conditions used with sodium 131-iodide which is only commercially available in an aqueous solution and therefore would require freeze drying. Reducing the loss of volatile radioiodine is also important for safety reasons.

The three (E)-diazonium tamoxifen salts described above were tried in dry decompositions. After they were added to the vial, it was heated in an oil bath (110 °C) for 5 minutes. Product analysis by HPLC showed no iodotamoxifen in all three attempts (runs 1, 2 and 3).

Non-nucleophilic polar solvents were also tried. The solvents were chosen by their ability to dissolve one of the three diazonium salts which had been prepared. The

Table 7.4: Iodinations using Organic Solvents or No Solvent

Run	Salt of 24	Solvent	KI/24	Procedure	Yield[a] (%)
1	PF_6^-	none	0.1	110 °C, 5 min	≤ 1
2	BPh_4^-	none	0.1	110 °C, 5 min	≤ 1
3	β-Naphthyl sulphonate	none	0.1	110 °C, 5 min	≤ 1
4	PF_6^-	20 μL CH_3CN	0.18	reflux for 5 min	34
5	BPh_4^-	20 μL CH_3COOH	0.1	reflux for 5 min	≤ 1
6	BPh_4^-	20 μL DMF	0.12	reflux for 5 min	≤ 1

a The yield was determined by HPLC analysis employing an internal standard

hexafluorophosphate salt was in a five fold excess to the potassium iodide and it was refluxed in 20 μL of acetonitrile. The yield was 34 % based on the limiting reagent, potassium iodide (run 4). The other attempts used the tetraphenyl borate diazonium salt in acetic acid and dimethyl formamide. Neither of these attempt produced any iodotamoxifen, **2** (runs 5 and 6).

The reaction of **24**-PF_6 in acetonitrile was the first attempt in which a yield above 10 % was obtained. This was encouraging particularly since less than equimolar iodide was used.

7.4) Radioiodination of Diazonium Salt **24**

7.4.1) Small Scale [^{131}I]-Iododediazotizations

The success described above prompted us to attempt a radioiodination by this method. The first attempt was successful and the procedure was used for future iodinations virtually unmodified. The sodium 131-iodide was freeze dried with a small amount of sodium thiosulphate prior to use. By refluxing approximately 100 μCi (3.7 MBq) of sodium 131-iodide with 1.0 mg of the diazonium salt in 15 μL of dry acetonitrile for 10 minutes we could obtain a 40 to 60 % radiochemical yield of [^{131}I]-**2**. Since this is actually a very small amount of radioiodinated tamoxifen, a gamma detector was necessary to detect the compound. The HPLC used was equipped with a UV and a gamma detector connected in series with very small bore tubing so the peaks appeared at

essentially the same retention time. To separate [^{131}I]-**2** the desired peak had to be collected and reinjected several times.

A sample of nonradioactive **2** was recrystallized in the presence of a sample of radioactive **2** until a constant specific activity was obtained to ensure that the radioactive compound collected was the desired product. This compound injected into the HPLC showed simultaneously run UV and radiotraces with peaks at the same retention time.

A few experiments were performed to optimise the conditions for the radiolabelling. The results, however, were not necessarily conclusive. This is likely due to the difficulties in reproducing results when performing microscale synthetic reactions. Though these experiments did show that 1 to 2 mg of **24**-PF_6 gave a better yield than 7 mg of the diazonium salt. An experiment with 7.3 mg of the **24**-PF_6 only gave a fourteen percent radiochemical yield.

The success of this procedure appears to be due to the removal of the water. This would suggest that phenol formation might be a major problem when run in aqueous solutions. Acetonitrile could also be the ideal solvent since its boiling point is close to the decomposition temperature of the hexafluorophosphate diazonium salt. The Z hexafluorophosphate salt, of Z-**24**, was synthesized by the same procedure used for the E isomer. The labelling also was done by the same procedures and similar yields were obtained. By this procedure we were able to prepare 100 to

200 μCi (3.7 to 7.4 MBq) amounts of both isomer of **2** which allowed biodistribution studies in mice.

7.4.2) Large Scale [^{131}I]-Iododediazotizations

For preclinical trials it was estimated that 1.5 to 2.0 mCi (55.5 to 74 MBq) of the [^{131}I]-**2** would be required. Since the radioiodide is the limiting reagent it was expected these quantities could be produced by simply increasing the amount of sodium 131-iodide. This, however, was not the case. By the procedure described above, a 30 to 40 % radiochemical yield was obtained for up to approximately 200 μCi (7.4 MBq). When the amount of sodium 131-iodide was increased to 5 mCi (185 MBq) or greater, only 300 μCi (11.1 MBq) was produced. It appeared that by this procedure 300 μCi (11.1 MBq) was the upper limit which could be produced and the yield was independent of the amount of sodium 131-iodide used.

Surprisingly this problem was solved by increasing the volume of solvent. By using 1.5 to 2.0 mL of acetonitrile and refluxing for an hour, a 50 % radiochemical yield was obtained. This product was purified and analyzed by the same method described above. An increase in radiochemical yield obtained by increasing the volume is contrary to what would be expected when considering either dediazotization mechanism. A decrease in concentration of iodide ion would decrease the rate of the reaction by electron transfer. The formation of the aryl cation should not be effected by the iodide concentration. However, a lower iodide concentration

would likely change the product distribution decreasing the yield of 2.

A possible explanation which would be consistent with these results would be the solubility of sodium iodide in acetonitrile. By increasing the volume you are actually increasing the amount of iodide present. This, however, is unlikely since sodium iodide is fairly soluble in acetonitrile.

7.5) Summary

This work allowed us to prepare "no carrier added" E and Z iodotamoxifen for animal and human trials. It also has provide a new labelling technique for high specific activity radioiodinated compounds from the anilino group in acceptable yields. During the development of the labelling procedure we isolated three, quite stable, diazonium salts. Also investigated was the use of several copper ctalyst including copper bronze, cuprous oxide, copper powder and copper sulphate. In our hands these catalysts did not enhance the yield of the dediazotization reaction. The copper bronze catalyst was shown to have iodide incorporated in its surface from the activation procedure. A successful labelling procedure was developed by refluxing the diazonium salt in a small amount of acetonitrile without a catalyst.

3.1) Receptor Binding Affinity

The ability E and Z-2, to bind to estrogen receptors was initially determined *in vitro* with a receptor binding assay. The affinity of the E and Z-1, for estradiol receptors was also determined in the interest of uncovering a novel antiestrogen of potential therapeutic use. The binding affinities of the commercially available Z-tamoxifen and 17ß-estradiol were also determined. This provided internal comparison with our compounds.

The inhibition constants (IC_{50}) for these compounds were determined by measuring their ability to compete for estrogen receptors with estradiol. See Appendix I for a detailed explanation of the IC_{50} value determination. The cytosol containing estrogen receptor was prepared for us from rat uteri.[38] The competitor, [^{3}H]-estradiol, and the receptor preparation were incubated at 37 °C for 30 min.

Initially, we attempted the assay in TE-buffer without an organic cosolvent. These results were not reproducible for the iodotamoxifens, 2, and in particular for the Z isomer. The problems appeared to be due to the poor solubility of Z-2 even at low concentrations. Employing N,N-dimethyl formamide as a cosolvent has been reported to alleviate this problem when used in low concentrations.[39] However, our attempts with this solvent were unsuccessful. The receptors did not appear to survive. Even when the assay

was run overnight at ice bath temperatures, the results indicated that the receptor had been changed by the cosolvent. This was evident by the inability of even [^{3}H]-estradiol to bind. Both methanol and ethanol were tried as cosolvents, and similar results were obtained. A solution of 10 % (volume) of glycerol in TE buffer dissolved **2** and gave realistic displacement crves.

In Table 8.1, the IC_{50} values derived from this assay have been made relative to estradiol (set to 100) and relative to Z-7 (set to 100). Also reported are the relative binding affinities (RBA) for the dimethylated tamoxifen, **19**, the ortho iodotamoxifen, **17**, and (E) and (Z) 4-iodotamoxifen, **18**, which were previously reported.

We found Z-7 to have a relative binding affinity of 0.2 when estradiol binding affinity is set to 100. Literature values for Z-7 are reported vary from 30 to 0.1.[20] These variations have been attributed to assay conditions, source and species of receptor, length of time and temperature of incubation and concentration of protein employed. In our hands, the relative value varied from 0.16 to 10 depending on the assay conditions.

Z-Iodotamoxifen, **2**, was found to have a 16 times greater affinity for estrogenic sites than Z-7. E-iodotamoxifen, **2**, has a weaker affinity than Z-7. The difference between the E and Z isomers of **2** (RBA = 50 and 1600) is analogous to the difference between E and Z-7 (RBA = 12 and 100). In both cases the Z isomer has a higher

Table 8.1: Relative Binding Affinities of Tamoxifens and Substituted Tamoxifens for Rat Uterine Estrogen Receptors

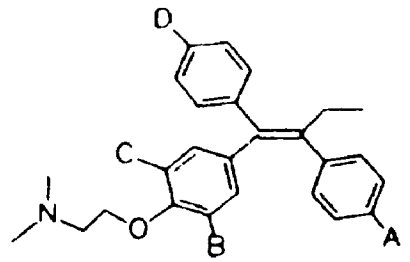

Compound	A	B	C	D	Relative Binding Affinity (IC_{50}) Estradiol = 100	Z-7 = 100
Z-7	H	H	H	H	0.2	100
E-2	H	H	H	H		12^{10}
Z-2	I	H	H	H	3.3	1600
E-2	I	H	H	H	0.1	50
Z-1	NH_2	H	H	H	1.0	500
E-1	NH_2	H	H	H	0.9	45
Z-17	H	H	I	H		20^{19}
Z-19	H	CH_3	CH_3	H		18^{15}
E-18	H	H	H	I		24^{20}
Z-18	H	H	H	I		500^{20}

binding affinity. The E and Z aminotamoxifens, **1**, both have similarly high affinity for the binding site. It appears that substitution in the para position of this ring with either an iodine or an amino group does not adversely effect its binding affinity. This ring appears to be much less sensitive than the ether substituted ring. Dimethytamoxifen, **Z-19**, and iodo derivative, Z-17, both have reduced binding compared to Tamoxifen. More recently, the binding affinities of E and Z-**18** (RBA = 24 and 50) have been reported. Again the Z isomer had a higher affinity.

We were encouraged by our results and felt that both E and Z-**2** deserved *in vivo* investigation.

8.2) Biodistribution in Tumor-Bearing Mice

The biodistributions of E and Z [^{131}I]-**2** were determined in female mice bearing estrogen receptor positive tumors. The estrogen receptor levels in tumors samples were determined for us and were found to contain between 28 and 45 fmol of receptors per g of protein.[40] A human tumor is considered to be estrogen receptor positive and will likely respond to hormone therapy if it contains greater than 0.25 fmol/g.[15]

The mice were inoculated with mouse mammary carcinoma tumor cells. After a several days, when the tumors were palpable, the mice were injected with the [^{131}I]-**2**. Experiments were run simultaneously for both E and Z isomers. Four mice per time point were sacrificed at various

times up to 92 hours. The organs were removed and the activity and weight of each obtained. This allowed the calculation of percent injected dose per gram (%ID/g). The results of the biodistribution of the Z and E-2 are given in Table 8.2 and 8.3 respectively.

The tissues which normally contain the largest concentration of estrogen receptors are the uterus and the tumor. For [^{131}I]-E-2, the activity in the uterus rose steadily from 2.9 to 8 at 92 h. The Z-2 uptake rose from 2.0 at 1 h to 4.1 at 12 h and then began to clear. In the tumor, E-2 showed a trend in uptake similar to the uterus. However it only reached 2.6 %ID/g by 92 h. The same is true for the Z isomer. The activity increased in the tumor to 1.3 %ID/g at 12 h as it did in the uterus and then began to clear. The higher in uptake in the uterus compared to the tumor might be explained by the poor circulation often found in necrotic tumors. This is a major problem with imaging fair sized tumors. Delivery of the agent is hindered by the poor vasculature in the tumor.

It is important to measure the uptake in organs which could potentially be in the vicinity of a tumor and add to the background activity. The liver showed high uptake of both isomers, though the uptake and clearance rates appear to be quite different. The E isomer of 2 shows a steady increase (Table 8.3) in until 24 h, at which time it levelled off and began to slowly clear. At the highest point, 44 %ID/g was found in the liver. The Z isomer showed

Table 8.2: Biodistribution Results in Tumor-Bearing Mice with [^{131}I]-Z-2 at Various Times (% injected dose/g of tissue ± s_m11[a]; 4 mice per time point)

Organ	1	2	3	6	12	24	48	72	92
Blood	2(2)	.51(.08)	.5(.2)	.9(.5)	.29(.09)	.5(.1)	.19(.05)	.17(.05)	.09(.04)
Liver	34(40	28(5)	33.6(.8)	35(5)	36(3)	29.5(.9)	29(3)	23(2)	9(2)
Lung	14(3)	10(1)	12.9(.2)	12(2)	13(2)	6.4(.7)	4.8(.7)	3.0(.3)	2.5(.4)
Muscle	2.1(.1)	1.5(.3)	1.7(.1)	1.5(.3)	1.1(.1)	.76(.04)	.4(.1)	.37(.04)	.24(.07)
Tumor	1.8(.4)	1.4(.4)	1.7(.1)	1.7(.3)	1.8(.2)	1.38[b]	1.0(.1)	.74(.07)	.28(.06)
Uterus	2(.6)	2.1(.4)	2.2(.4)	2.6(.9)	4.1(.4)	3.3(.4)	2.2(.4)	2.2(.6)	0.8(.2)

a) mean of the standard deviation

Table 8.3: Biodistribution Results in Tumor-Bearing Mice with [^{131}I]-E-2 at Various Times

(% injected dose/g of tissue ± s_m[a]; 4 mice per time point)

Organ	1	2	3	6	12	24	48	72	92
Blood	2.4(.4)	1.5(.1)	1.33(.05)	.80(.03)	.20(.02)	.56(.05) .8(.4)	.34(.03) .5(.2)	.24(.02)	.3(.1)
Liver	21(6)	28(4)	36(5)	28(3)	44(4)	41(2) 40(5)	31(3) 44(3)	33(4)	36(4)
Lung					8(2)	7.1(.5)	6.9(.4)	6(1)	6.7(.4)
Muscle	1.7(.4)	1.8(.4)	2.0(.5)	1.2(.1)	.9(.2)	1.5(.1) .07(.1)	.0(.1) 1.0(.1)	.8(.1)	1.27(.02)
Tumor	.8(.2)	2.7(.4)	3.6(.3)	2.3(.3)	2(1)	4.4(.2) 2.15(.06)	5(2) 2.4(.2)	2.2(.4)	2.6(1.1)
Uterus	2.9(.7)	2.7(.4)	3.6(.3)	2.3(.3)	2(1)	4.4(.2)	5(2) 5.5(.8)	6(1)	8(1)

a) mean of the standard deviation

initially higher uptake than the E isomer (Table 8.2). It increased from 34 %ID/g at 1 h to 36 %ID/g at 12 hours. The E isomer only showed 16 %ID/g at 1 h. With the Z isomer, clearance after 12 h is much quicker with only 9 %ID/g left at 92 h.

The high uptake in the liver may be attributed to several mechanisms. Firstly, lipophilic compounds are metabolized and cleared though the liver.[41] The liver also has a high concentration of antiestrogen binding sites.[21] The reason for an increase in uptake over time, in particular with the E isomer, could be due to enterhepatic recirculation of metabolites which have retained their label.

The lungs also show a high uptake from both E and Z isomer, though not as high as the liver. For the E-2, the uptake is only reported from 12 h on. At this point the E-2 was clearing from 8 to 6 %ID/g. The lung uptake for Z-2 was reported for all time points. The uptake peaked at 14 %ID/g which was observed at 1h and slowly cleared to 2.5 at 92 h. Though the lungs do contain a measurable amount of antiestrogen receptors,[10,42] it is likely not high enough to account for the total uptake. There is however a nonspecific mechanism which increases uptake of organic amines in the lungs.[42]

Table 8.3 shows two sets of data for the 24 and 48 h time points. The initial biodistribution was only done to 48 h. To investigate the later time points another experiment

was done repeating two time points.

Neither isomer appears to linger in either the blood or muscle. Good clearance from these organs is essential for imaging. Less than 1 %ID/g was observed in both organs by 6h.

For imaging purposes, it is important to have good target to background ratios. That is, the uptake ratio in either the uterus or tumor over both the blood or muscle. A plot of these values is given in Figure 8.1. for E and Z-2. The upper plot is the results of the biodistribution on the E isomer and the lower is that for the Z isomer. The largest target to background ratio is seen for E-2 in uterus to blood. By seventy hours, the ratio hit 28 to 1. For the Z isomer, the same ratio peaked at 72 h at 13 to 1. Both of these values are acceptable for imaging. Due to the slightly higher uptake in the muscle, the ratio of uterus to muscle uptake is not as high for either isomer. As well, the ratios using the tumor as the target organ are lower due to the lower total tumor uptake.

The difference in clearance between the two isomer has also been reported for the E and Z isomers of 7.[43] One of the major metabolic pathways of tamoxifen is hydroxylation to give hydroxymetabolite, B, in Scheme 6.2. However the Z isomer is metabolized much more readily than the E isomer. The hydroxymetabolite has lower nonspecific binding due to lower lipophilicity as well as lower affinity to antiestrogen receptors. If the iodotamoxifens are

Figure 8.1: Ratio of Uptake in Both Tumor and Uterus Over Both Blood and Muscle

Upper: Results from the Biodistribution Studies on E-2

Lower: Results from the Biodistribution Studies on Z-2

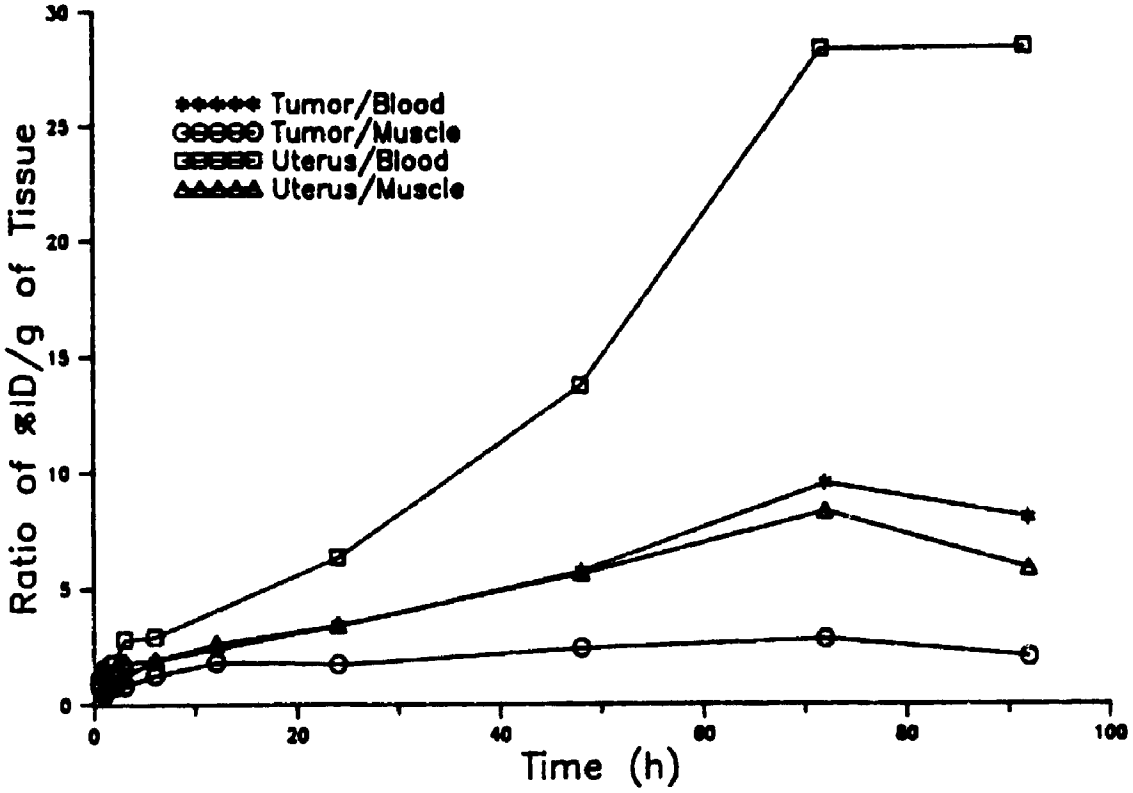
Tumor/Blood
Tumor/Muscle
Uterus/Blood
Uterus/Muscle
Ratio of %ID/g of Tissue
Time (h)
0
5
10
15
20
25
30
0
20
40
60
80
100

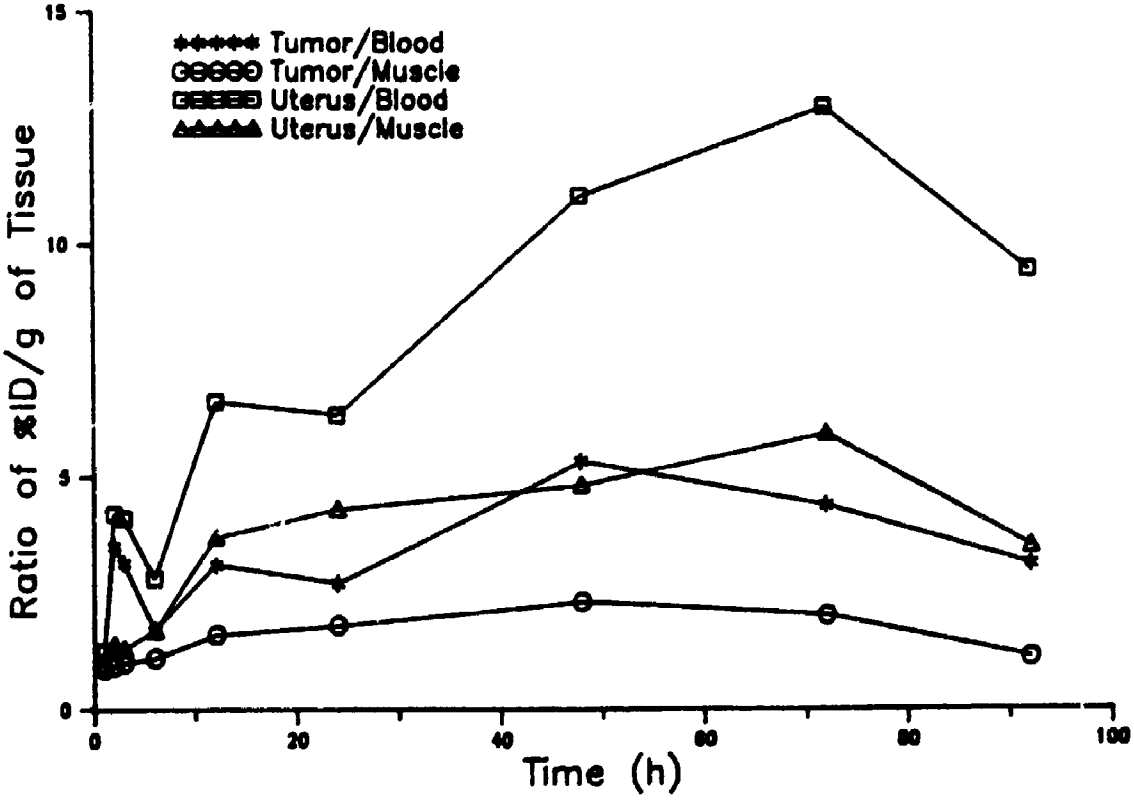
Tumor/Blood
Tumor/Muscle
Uterus/Blood
Uterus/Muscle
Ratio of %ID/g of Tissue
Time (h)
0
5
10
15
0
20
40
60
80
100

metabolized though this same route generally faster clearance of the Z iodo compound would be explained. The hydroxylated metabolite of the E isomer of **7** has a stronger affinity for estrogen receptors than E-**7**. If this is true for E-**2** then this would help to explain the slowly increasing uptake in the target tissues. It also should be noted that the thyroid uptake was low indicating that the iodine remained attached even after likely metabolism.

8.3) *In Vivo* Washout Studies

To discover whether the concentration of the E and Z [^{131}I]-**2** in target organs was due to receptor binding, a washout experiment was performed. If the [^{131}I]-**2** were binding to estrogen receptors, they should be selectively displaced by large dose of estradiol. However, nonspecific uptake is not saturable and should not be effected.

A washout experiment was performed using immature female mice to eliminate the complications due to high levels of endogenous estrogens. The mice were injected with either [^{131}I]-E or Z-**2**. Two early time points were used to assure that the results were similar to those found in earlier mouse biodistribution experiment. After 26 h half of the remaining mice were inoculated with 17ß-estradiol. Animals in the control experiment were sacrificed at 26, 30 and 36 hours. The animals which had received estradiol were sacrificed at 30 and 36 hours. In Figure 8.1 the results of

Figure 8.1: Ratio of Uptake in Both Tumor and Uterus Over Both Blood and Muscle

Upper: Results from the Biodistribution Studies on E-2

Lower: Results from the Biodistribution Studies on Z-2

---------- Uptake in organs after estradiol treatment.

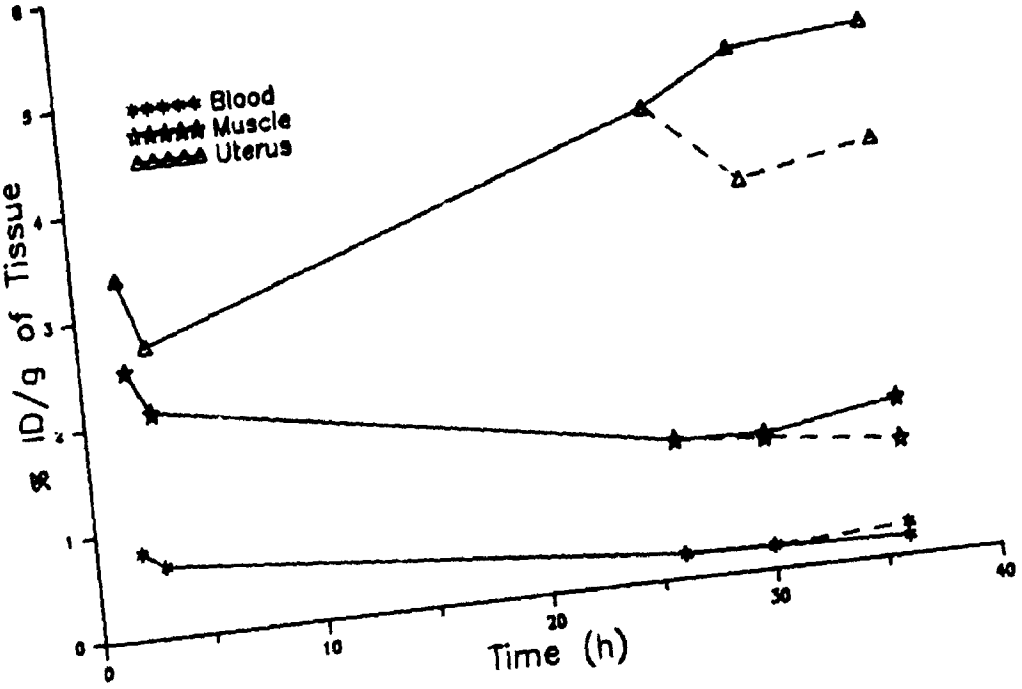
Blood
Muscle
Uterus
% ID/g of Tissue
Time (h)
0
10
20
30
40
1
2
3
4
5
6

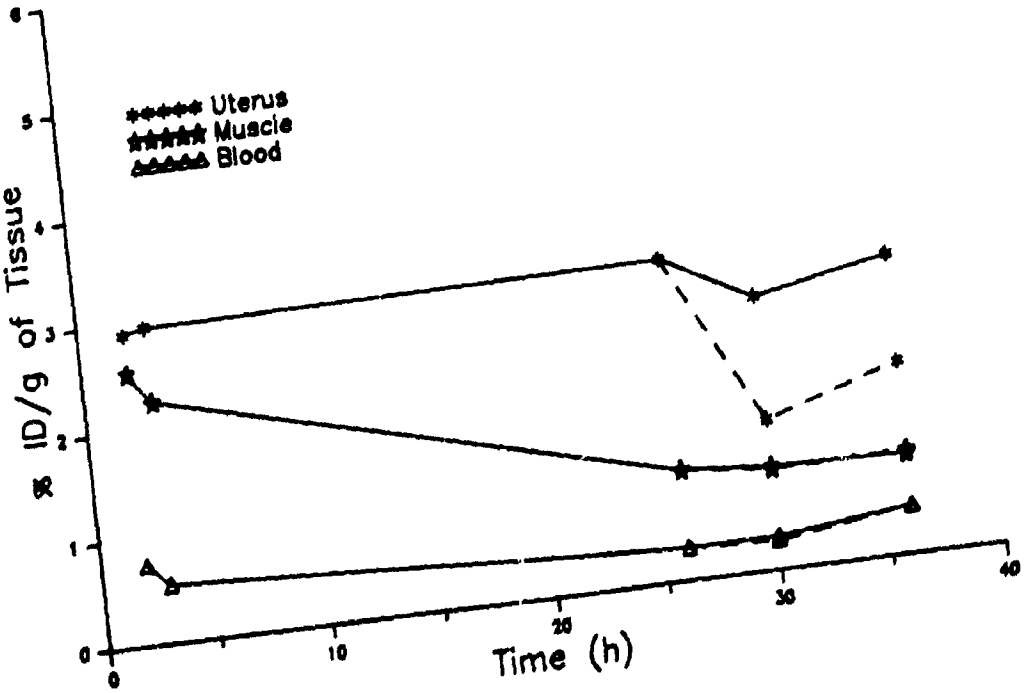
Uterus
Muscle
Blood
% ID/g of Tissue
Time (h)
0
10
20
30
40
1
2
3
4
5
6

these experiments have been plotted for the E and Z isomer (upper and lower respectively).

The samples of blood, muscle and the liver showed no significant difference in uptake from either the E or Z isomer after treatment with estradiol. However, the uptake in the uterus dropped after treatment with estradiol. The administration of estradiol blocked 20% of the activity from [^{131}I]-E-**2** and 50 % from [^{131}I]-Z-**2**. This is direct evidence that at least some of the uptake is due to estrogen receptor binding.

A possible reason for the washout not being complete could be different pharmacokinetics of the estradiol and **2**. Estradiol has a much shorter biological half-life than tamoxifen, **7**. Also E and Z-**2** can bind to antiestrogen binding sites where estradiol can not. On the other hand, part of the uptake in these organs may be nonspecific since **2** is quite lipophilic. More complete washout would have possibly been seen if Z-tamoxifen had been used as the blocking agent. It has similar pharmacokinetics and would also block antiestrogen binding sites.

8.4) Human Biodistribution Studies

The uptake of E and Z-**2** observed in the uterus and tumors of mice was promising and a human study was proposed on these grounds. The study was performed in the Department of Nuclear Medicine at Victoria Hospital by Dr. John Powe with the help of the Victoria Hospital Cancer Clinic. The

details of this study have been reported.[26]

In brief, seven patient received either E or Z [^{131}I]-2 and were imaged with a gamma camera at various time points. The images showed fast clearance from the blood. However in none of the patients could any significant uptake be observed in any of the known metastatic lesions. In one case the lesions in the pelvic bone were demonstrated with [^{99}Tc]-methylene diphosphate, a bone imaging agent. These were not visible with 2. The uptake in the liver was very high and for 50 % of the activity in the torso. A difference in kinetics between the E and Z isomer was observed.

8.5) Summary

The evaluation of E and Z-2 as potential estrogen receptor imaging agent has been performed. The ability of both E and Z isomers of 1 and 2 to bind *in vitro* to estrogen receptors was determined. These studies showed that E and Z-2 bound quite effectively to estrogen receptors. The biodistribution of E and Z [^{131}I]-2 was determined in tumor bearing mice. Concentration in the estrogen receptor positive tumors and in the uterus was demonstrated. The ability of large doses of estradiol to partially block the uptake of E and Z [^{131}I]-2 in mouse uteri was also demonstrated. However, localization of either E or Z [^{131}I]-2 in humans with known estrogen receptor positive tumors was not observed.

Chapter 9: Experimental

9.1) Chemistry

E and Z Aminotamoxifen, **1**, were previously synthesized by Dr. Y. Zea Ponce in our laboratory. The copper bronze catalyst,[44] copper oxide[45] and precipitated copper powder[46] was prepared by standard, previously reported procedures. Sodium 131-iodide was initially purchased from Dupont Canada Co.-NEN Division and later donated by Merck-Frosst Canada. (5 mCi (185 MBq) in 0.1 mL of 0.1 M NaOH). HPLC analyses and separations were performed on a C_{18} reverse-phase column (Varian Micro-Pak MCH-10). The Varian (Vista 5500) HPLC was equipped with a Varian UV-200 detector and a Harshaw sodium iodide flow scintillation detector which was run by a Varian (Vista 402) data system in dual channel mode. A Branson 2000 ultrasonic cleaner (bath) and a MES 150 watt ultrasonic disintegrator (probe) was used in the dediazotization attempts. Surface analyses were performed with an x-ray photoelectron spectrometer (XPS) at Surface Science Laboratory SSX-100 by Dr. Margaret Hyland.

E and Z-127-Iodotamoxifen, 2

E and Z-**2** were prepared as previously reported from E and Z aminotamoxifen, **1**, by diazotization followed by the in situ iodination with a ten fold excess of sodium iodide.[47] Spectra compared well with those which had been reported.

E and Z-Diazoniumtamoxifen Dihexafluorophosphate Salt, 24-PF_6

To a solution of 1.0 g (2.6 mmol) of either E or Z-1 and 0.575 mL (26 mmol) of sulfuric acid in 5 mL of water at ice bath temperatures was added 0.179 g (2.6 mmol) of sodium nitrite. After stirring for 15 min, 15 mL of a saturated solution of potassium hexafluorophosphate was added and the stirring was continued for 10 min. The orange precipitate which formed was filtered and washed with water. Freeze drying yielded approximately 1.6 g (90 %) of either isomer.

E-24-PF_6: mp = 92-94 °C (dec); ^{1}H NMR (d_6-acetone) δ 8.56 (2H, d, CH), 7.83 (2H, d, CH), 7.27 (2H, d, CH), 7.14 (2H, m, CH), 7.05 (2H, d, CH), 6.97 (2H, m, CH), 4.57 (2H, t, CH_2), 3.91 (2H, t, CH_2), 3.27 (6H, s, CH_3), 2.67 (2H, q, CH_2), 0.97 (3H, t, CH_3); ^{13}C NMR (d_6-acetone) δ 158.6 (C), 158.1 (C), 144.5 (C), 142.6 (C), 140.4 (C), 136.2 (C), 133.7 (2CH), 133.1 (2CH), 131.5 (2CH), 131.2 (2CH), 128.8 (2CH), 128.0 (CH), 115.3 (2CH), 111.9 (C), 62.7 (CH_2), 57.6 (CH_2), 44.2 ($2CH_3$), 28.9 (CH_2), 13.5 (CH_3).

Z-24-PF_6: mp = 94-98 °C (dec); ^{1}H NMR (d_6-acetone) δ 8.61 (2H, d, CH), 7.86 (2H, d, CH), 7.42 (3H, m, CH), 7.32 (2H, d, CH), 6.90 (2H, d, CH), 6.77 (2H, d, CH), 4.40 (2H, t, CH_2), 3.80 (2H, t, CH_2), 3.27 (6H, s, CH_3), 2.61 (2H, q, CH_2), 0.94 (3H, t, CH_3); ^{13}C NMR (d_6-acetone) δ 158.7 (C), 157.7 (C), 144.6 (C), 143.0 (C), 140.1 (C), 135.7 (C), 133.8 (2CH), 133.2 (2CH), 133.0 (2CH), 129.8 (2CH), 129.2 (2CH),

128.5 (CH), 115.1 (2CH), 111.9 (C), 62.5 (CH_2), 57.6 (CH_2), 44.3 ($2CH_3$), 28.9 (CH_2), 13.5 (CH_3); IR (nujol mull) 2270cm^{-1} (NN stretch).

E-Diazoniumtamoxifen Tetraphenylborate Salt, E-24-BPh_4

The tetraphenylborate salt of the diazonium of tamoxifen was prepared as described for the hexafluorophosphate salt except sodium tetraphenylborate was used to precipitate the diazonium salt. A yield of 65% was obtained for E-24-BPh_4 salt: mp = 65-67 °C (dec); IR (nujol mull) 2240 cm^{-1} (NN stretch).

E-Diazoniumtamoxifen β-Naphthylsulphonate Salt, E-24-β-Nap

The β-naphthylsulphonate salt was prepared as described for the hexafluorophosphate salt except the sodium salt of β-naphthylsulphonate was used to precipitate the diazonium salt in a 35% yield of E-24-β-Nap. IR (nujol mull) 2210 cm^{-1} (NN stretch).

General Procedure for Iododediazotizations Employing Copper Catalysts

To a suspension of 2 mg E-24 in aqueous solvent was added potassium iodide. The catalyst was then added and the reaction was run under the conditions described in Tables 7.1, 7.2 and 7.3. The solution was then made basic and extracted with 1.0 mL of ether containing 2.0 mg of naphthalene (internal standard). The mixture was analyzed by

HPLC with a UV detector. The relative size of the UV absorbance from **2** compared to that from naphthalene was measured. The absolute amount was determined by multiplying it by a factor which related the extinction coefficients of these two compounds. The results of these experiments are given in Table 7.1, 7.2 and 7.3.

General Procedure for Iododediazotizations in either Dry or Organic Solvents

From stock aqueous solutions, potassium iodide and sodium thiosulphate were put in a V-shaped 2 mL vial and were freeze dried. To each was added approximately but accurately 2.0 mg of **24**, 2.0 mg of naphthalene (internal standard) and if solvent was used, 20 μL of solvent. The potassium iodide and the sodium thiosulphate were 0.1 and 0.02 equivalents of the diazonium salt respectively. The reactions were run under the conditions described in Table 7.4. Samples were prepared for HPLC analysis by first removing the solvent (if necessary) and adding 1.0 mL of 0.1 M sodium hydroxide. The organic material was then extracted into 1.0 mL of ether. The ether layer was analyzed by HPLC. The results are given in table 7.4.

Small Scale [^{131}I]-Iododediazotization of E or Z Diazoniumtamoxifen Hexafluorophosphate Salt

To a 2 mL V-shaped vial was added 2 μL of sodium 131-iodide (0.13 mCi, 4.8 MBq) and 5 mg of sodium thiosulphate

(20 μmol). After freeze drying 15 μL of acetonitrile and 2 mg of 24-PF_6 (2.9 mmol) was added. The mixture was heated to reflux for 1 min. After cooling it was made basic with 0.5 mL of aqueous sodium hydroxide and extracted into methylene chloride. The desired product was purified by HPLC employing both a UV and a radioactivity detector (100:1:0.01 for the Z isomer and 100:0.5:0.005 for the E isomer of acetonitrile: tetrahydrofuran: triethylamine). The radioactivity trace, which was plotted simultaneously with the UV, was monitored for the desired compound and that fraction was collected. To remove impurities visible on the UV trace which were in this fraction it was reinjected into the HPLC. This purification procedure was usually repeated at least once. The overall radiochemical yield ranged between 40 and 60 %.

Large Scale [^{131}I]-Iododediazotization of E or Z Diazoniumtamoxifen Hexafluorophosphate Salt

To a 2 mL V-shaped vial was added 0.1 mL of sodium 131-iodide (5 mCi, 185 MBq) and 50 μl of a 0.06 M solution of sodium thiosulphate and the contents were freeze-dried. The vial was fitted with a small reflux condenser and 2 mL of acetonitrile was added and refluxed for 5 min, when about 3 mg of either E or Z-diazoniumtamoxifen salt was added followed by further reflux for 1 h. After cooling, the solvent was evaporated under a slow stream of air. Aqueous sodium hydroxide (1 mL) was added and extracted with methylene chloride. The methylene chloride solution was

taken to dryness and the residue was taken up in two 100 µl portions of acetonitrile. The desired product was purified by HPLC as described above. The overall radiochemical yield varied between 40 and 60 %.

9.2) Biology

9.2.1) Receptor Binding Affinities

The estrogen receptor cytosol was prepared from the uterus of Sprague-Dawley rats by Mr. K Barr of John P. Wiebe's Hormonal Regulatory Mechanism Laboratory by their previously reported procedure.[38]

Relative receptor binding affinities were determined for both E and Z-1, Z-7 and both E and Z 2. All compounds were assayed concurrently using the same uteri preparation. The assay mixture consisted of 100 µl of the receptor cytosol, 90 µl of tris buffer (10 mM Tris, 1.5 mM EDTA, pH 7.9 at 4 °C), 10 µl of glycerol and 30,000 dpm of [^{3}H]-17-β-estradiol (2,000 MBq/mmol) with or without competitor at various concentrations. A duplicate of each assay was prepared. They were incubated at 30 °C for 30 min at which time they were chilled and 500 µl of charcoal/dextran (0.5/0.05 % w/v) was added to each tube. After 15 min, the charcoal was pelleted by centrifuging at 1800xg and the supernatant decanted into vials. The radioactivity was measured with a Philips PW 4700 liquid scintillation counter using a xylene-PPO-POPOP cocktail.

The radioactivity (cpm) which remained in the

supernatant was plotted against the log [competitor]. From this plot the concentration of the competitor which displaced 50% of the [^{3}H]-estradiol was determined and the relative binding affinities were then calculated and are reported in Table 8.1.

9.2.2) Biodistribution in Tumor-Bearing Mice

The biodistribution of [^{131}I]-E and Z-2 were determine in female C3H/H5J (Jackson Labs, Bar Harbour, MA) bearing in-house induced estrogen receptor positive tumors. The tumors were produced by inoculation intramuscularly in the right hind leg with 10^{5}/0.1 mL Bittner Agent mouse mammary carcinoma tumor cells. The cells were obtained from the Ontario Cancer Foundation, London, Ontario and the inoculations were performed by Mr. G. Morrissey of the Radiopharmaceutical Development Group. Random samples of tumor tissue from each biodistribution experiment were subsequently sent for estrogen receptor content assay.[40] All tumor samples tested positive for estrogen receptors.

The labelled compounds were dissolved in saline with 5% ethanol and 0.0004% Tween 80 and injected in the tail vein of the mice. The amount of radioactivity in the injection syringe was measured pre and post injection. The radioactivity in the tail was subtracted from the amount injected. Four animals per time point were sacrifice by cervical dislocation at selected time points. Blood samples were immediately taken by cardiac exsanguination. The desired organs were then obtained, washed free of blood,

patted dry, weighed and counted for activity. The results are given as per cent injected dose per gram of tissue (%ID/g) in Tables 8.2 and 8.3. Also given is the target to tissue ratio calculated from the %ID/g in the tumor or uterus over that in muscle or blood.

9.2.3) *In Vivo* Washout Studies

A similar biodistribution as described above was repeated with immature (3 to 4 week old) female Swiss white mice. They were injected with either [^{131}I]-E or Z **2** in the same manner as described. At 26 h half the mice were injected i.p. with 10µg/100 µl 17-ß-estradiol dissolved in sesame oil with 2.5% ethanol. Three animals per time point were sacrificed by cervical dislocation at 30 and 36 h (4 and 10 h post estradiol injection for both control and washout. The distribution was measured and the data handled as described above.

9.2.4) Human Biodistribution Studies

A preclinical trial was performed by Dr. John E. Powe of the Department of Nuclear Medicine at Victoria Hospital in cooperation with the Cancer Clinic. Seven women (age 49 to 80) were given 0.46 to 1.2 mCi (17 to 44 MBq) either E or Z [^{131}I]-**2**. Three were given the Z isomer and four the E isomer. These women had previously pathologically confirmed carcinoma of the breast. Multiple images were taken of the different views of whole body using a large field gamma camera with a medium energy collimator. As well as film images computer digitized images were obtained and relative

activity in the chest, liver and abdomen were determined. The study followed a protocol which was approved by the Review Board for Health Sciences Research in Human Subjects. The details of this study have been published.[26]

References

1. Mueller, G.C. In *Estrogen/Antiestrogen Action and Breast Cancer Therapy*; Jordan, V.C., Ed.; The University of Wisconsin Press; Wisconsin, 1986; pp 3-17.

2. *ibid*, p. 5.

3. *ibid*, p. 4.

4. Jordan, V.C. *Pharmacol. Rev.* **1984**, *36*, 245.

5. Lerner, L.J. In *Non-Steroidal Antiestrogens* Sutherland, R.L and Jordan, V.C., Eds.; Academic Press: Australia, 1981; pp 1-16.

6. Jordan, V.C. *Pharmacol. Rev.* **1984**, *36*, pp. 260-261.

7. Nicholson, R.I.; Borthwick, N.M.; Daniel, C.P.; Syne, J.S.; Davies P. In *Non-Steroidal Antiestrogens*; Sutherland, R.L. and Jordan, V.C., Eds.; Academic Press: Australia, 1981; p 281-301.

8. Gibson, R.E.; Eckelman, W.C., Francis, B., O'Brien, H.A.; Mayaeles, J.K.; Wibur, S.; Reba, R.C. *Int. J. Nucl. Med.* **1982**, *9*, 245.

9. Rousseau, H.A.; Ghaffari, M.A.; van Lier, J.E. *J. Med. Chem.* **1988**, *31*, 1946.

10. Kazenellenbogen, J.A.; Heiman, D.F.; Senderoff, S.G.,; In *Applications of Nuclear and Radiochemistry*; Lambrecht, R.M. and Morcos, N., Eds.; Permagon Press: New York, 1982, 311-323.

11. Zielinski, J.E.; Larner, J.M.; Hoffer, P.B. Hochberg, R.B. *J. Nucl. Med.* **1989**, *30*, 209.

12. Mintun, M.A.; Welch, M.J.; Seigel, B.A.; Mathias, C.J.; Bradack, J.W.; McGuire, A.H., Katzenellenbogen, J.A.; *Radiology* **1988**, *169*, 45.

13. Kazenellenboger, J.A.; Heiman, D.F.; Senderoff, S.G.,; In *Applications of Nuclear and Radiochemistry*; Lambrecht, R.M. and Morcos, N., Eds.; Permagon Press: New York, 1982, p 316.

14. Kiesewetter, D.O.; Kilbourn, M.R.; Landvatter, S.W.; Heimer, D.F.; Katzenellenbogen, J.A.; Welch, M.; Goswanmi, R. *J. Nucl. Med.* **1984**, *25*, 1212.

15. Katzenellenbogen, J.A.;.Carlson, K.E.; Helman, D.F *J. Nucl. Med.* **1980**, *21*, 550.

16. Komai, T.; Eckelman, W.C.; Johnsonbaugh, R.E *J. Nucl. Med.* **1977**, *18*, 360.

17. Shani, J.; Gazit, A. Livshitz, T.; Biran, S. *J. Med. Chem.* **1985**, *28*, 1504.

18. Bloomer, W.D.; McLaughlan, W.H.; Weichselbaum, R.R. Tonnesen, G.L.; Hellman, S.; Seitz, D.E.; Hanson, R.N.; Adelstein, S.J.; Rosen, A.L.; Burstein, N.A.; Nore, J.J.; Little, J.B. *J. Radiat. Biol.* **1980**, *38*, 197. Hanson, R.N.; Seitz, D.E. *Int. J. of Nucl. Biol.* **1982**, *9*, 105.

19. McCague, R.; Leclercq, G.; Legros, N.; Goodman, J.; Blackburn, G.M.; Jarman, M. *J. Med. Chem.* **1989**, *32*, 2527.

20. Furr, B.J.A.; Jordan, V.C. *Pharmac. Ther.* **1984**, *25*, 127.

21. Faye, J.C.; Fargin, A.; Valette, A.; Bayard, F.;*Hormone Res.* **1987**, *28*, 202.

22. Adam, H.K. In *Non-Steroidal Antiestrogens*; Sutherland, R.L. and Jordan, V.C., Academic Press: Australia, 1981, 69.

23. Abbott, A.C.; Clark, E.R.; Jordan, V.C. *J. Endocr.* **1976** *69*, 445.

24. Meyer, G.-J.; Rossler, K.; Stocklin, G. *J. Am. Chem. Soc.* **1979**, *101*, 3121.

25. Harper, M.J.K.; Richardson, D.N.; Walpole, A.L. U.K. Patent No. 1,013,801 (1965). Harper, M.J.K.; Richardson, D.N.; Walpole, A.L. U.K. Patent No. 1,064,629 (1967).

26. Strickland, L.A.; Zea Ponce, Y.; Hunter, D.H.; Zabel, P.; Powe, J.; Morressey, G.; Dreidger, A.A.; Chamerlain, M.J. *Drug Design and Delivery* accepted March 16, 1990.

27. Jenssen, J.A. and Pearce, G.W. *J. Am. Chem. Soc.* **1949, 74, 2436.**

28. Galli, C. *Chem. Rev.* **1988**, *88* 765.

29. Griess, P.J. *Philos. Trans. R. Soc. London* **1864**, *164*, 693.

30. Sandmeyer, T. *Chem. Ber.* **1884**, *17*, 1633, 2650.

31. Gattermann, L. *Chem. Ber.* **1890**, *23*, 1218.

32. Greive, W.S.M,; Hey, D.H. *J. Chem. Soc.* **1934**, 1797.

33. Waters, W.A. *J. Chem. Soc.* **1942**, 266.

34. Zollinger, H. *Azo and Diazo Chemistry Aliphatic and Aromatic Compounds*; Interscience Publishers, Inc.; New York, 1961; pp 138-139.

35. Kazenellenbogen, J.A.; Heiman, D.F.; Senderoff, S.G.,; In *Applications of Nuclear and Radiochemistry*; Lambrecht, R.M. and Morcos, N., Eds.; Permagon Press: New York, 1982, p. 167.

36. Hodgson, H.H. *Chem. Rev.* **1947**, *40*, 251.

37. Woodcock, E.A.; Bobik, A.; Funder, J.W.; Johnston, C.I. *Eur. J. Pharm.* **1978**, *49*, 73.

38. Wiebe, J.P.; Barr, K.J. *J. Toxicol. Environ. Health* **1988**, *24*, 451.

39. Katzenellenbogan, J.A.; Johnson, H.J.; Myers, H.N. *Biochemistry* **1973**, *12*, 4085.

40. ref for estrogen receptor assay to determine estrogen receptor concentration

41. Katzenellenbogen, J.A.; Carlson, K.E.; Helman, D.F.; et al *J.Nucl.Med.* **1980**, *21*, 550.

42. Chaturved, A.K.; Rao, N.G.S.; Rama Sastry, B.V. *Toxicol. Appl. Pharmacol.* **1980**, *54*, 265.

43. Robertson, D.W.; Katzenellenbogan, J.A.; Long, D.J.; Rorke, E.A.; Katzenellenbogan, B.J. *J. Steroid. Biochem.* **1982**, *16*, 1.

44. Fuson, R.C.; Cleveland, E.A. *Org. Syn. Coll.* **1943**, *III*, 339.

45. Wittliff, J.L.; Lewko, W.M.; Park, D.; Kute, T.E.; Balter, D.T.; Kane, L.N. In *Hormones, Receptors, Breast Cancer*; McGuire, W.L., Ed.; Ravin Press: New York, 1978, 325-359.

46. Brewster, R.Q.; Groening, T. *Org. Syn. Coll.* **1946**, *II*, 446.

47. Hunter, D.H.; Payne, N.C.; Rahman, A.; Richardson, J.F.; Zea Ponce, Y. *Can. J. Chem.* **1983**, *61*, 421.

Appendix I

A) *In vitro* Competition Assay to Determine Binding Affinities for Receptors

An *in vitro* competition assay was used to determine the binding affinity of a prospective radiopharmaceutical for the receptor. In this assay one measures the ability of a competitor ("cold" radiopharmaceutical) at different concentrations to displace a radiolabelled "gold standard" (ligand). We employed this assay to measure the ability of the amino and iodotamoxifens, **1** and **2** respectively, to bind to estrogen receptors. The details of this method are given in Chapter 9. A similar assay was run for us to determine the affinity of iodohaloperidol derivatives, **21**, **22** and **17** for D-2 receptors.

Data Analysis

This assay relates the amount of [^{3}H]-compound displaced from the receptor by various amounts of competitor. The measured activity which is bound to the receptor is plotted as a logarithmic function of the concentration of competitor. The concentration of competitor which is required to displace fifty per cent of the ligand is determined. This value (IC_{50}) is often reported relative to the "gold standard" set at 100. These results can also be reported as the inhibitor affinity constant (K_i) by employing the following relationship.

$$K_i = \frac{IC_{50}}{(1 + \frac{L}{K_D})}$$

Where L is the concentration of [^{3}H]-ligand used and K_D is the dissociation constant of the [^{3}H]-ligand for that receptor. Below is plotted an example of the raw data obtain from the competiton experiment for estrogen receptors. The log of the concentration of Z-iodotamoxifen is plotted against the amount of [^{3}H]-estradiol bound to the receptor measured in counts per minute.

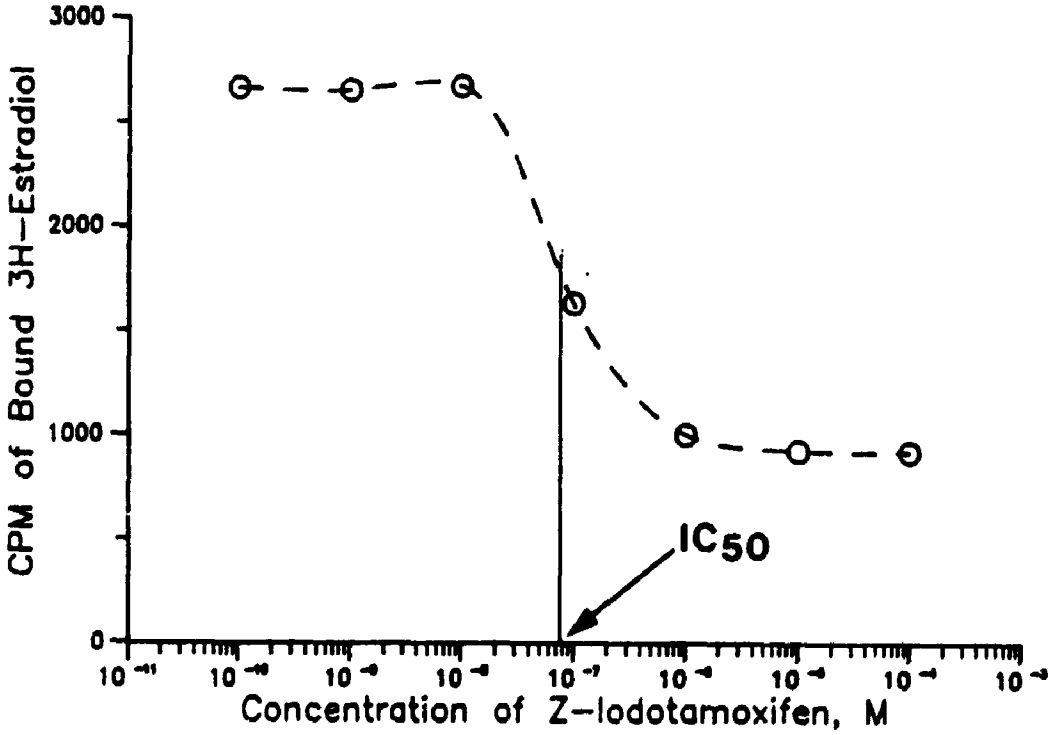

B) *In Vitro* Binding Assay to Determine Receptor Concentration

The concentration of receptors in a tissue sample or a cytosol prepared from a tissue sample can be determined by a receptor binding assay. In this assay the amount of a

labelled compound (ligand) which is specifically bound to the receptor is measured at different concentrations of ligand. This method is referred to several times in Chapter 2 during discussions of measurement of the concentration of D-2 receptors in post-mortem brain tissue from different diseases. A similar assay was also performed for us to determine estrogen receptor concentration in mouse tumors used in the biodistribution of tamoxifen.

The assay is similar to that described in Part A except that no competitor is used and the specific activity of the labelled "gold standard" is decreased by increasing the amount of "cold" compound until saturation of the receptor is achieved. For determining D-2 receptor levels usually [^{3}H]-spiperone is used and for estrogen receptors [^{3}H]-17β-estradiol is used.

By counting the activity bound to the receptor, the concentration of bound ligand can be calculated. One can also determine nonspecific binding by running an identical assay using a large excess of unlabelled ligand. By subtracting the amount of activity which is nonspecifically bound from the total activity bound to the cytosol, the concentration of specifically bound ligand is calculated. The concentration of unbound ligand is approximately equal to the amount of ligand used in the assay. This assumption works since the concentration of receptors is very low and only two to three percent of the ligand is bound.

Data Analysis

The following equilibrium represents the binding of a drug with a single population of receptors.

$$L + R \rightleftharpoons LR \quad (1)$$

Where L is the ligand, R is the receptor and LR is the receptor drug complex. Therefore

$$K_D = \frac{[L][R]}{[LR]} \quad (2)$$

and if v is the fraction of occupied receptors

$$v = \frac{[LR]}{[R] + [LR]} \quad (3)$$

By substituting (2) into (3)

$$v = \frac{[L]}{K_D + [L]} \quad (4)$$

The most commonly used method to treat the data obtained from this experiment is with a Scatchard plot. Equation (4) can be rearranged to give

$$\frac{v}{[L]} = \frac{1}{K_D} - \frac{v}{K_D} \quad (5)$$

By plotting v/[L] against v a straight line is obtained if only a single population of binding sites is being measured. The x-intercept is the number of binding sites. An easier way of handling the data which gives the same results is to plot the $[L]_{bound}/[L]_{free}$ against $[L]_{bound}$. The concentration of L_{bound} is determined as described above and the concentration of L_{free} is equal to the amount of ligand used. These values are usually reported in pmol per gram of tissue.